2016

Calcium (II) catalyzed nitrone additions

Elizabeth A. Congdon
University of Richmond

Calcium(II) Catalyzed Nitrone Additions

by

Elizabeth A. Congdon

Honors Thesis

in

Program in Biochemistry and Molecular Biology
University of Richmond
Richmond, VA

Spring 2016

Advisor: Kristine A. Nolin

This thesis has been accepted as part of the honors requirements
in the Program in Biochemistry and Molecular Biology

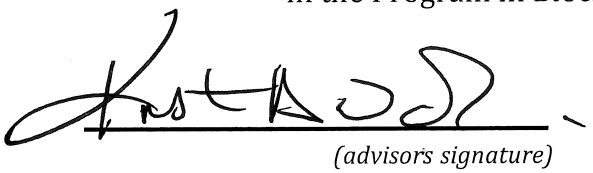

(advisors signature)

4/22/16
(date)

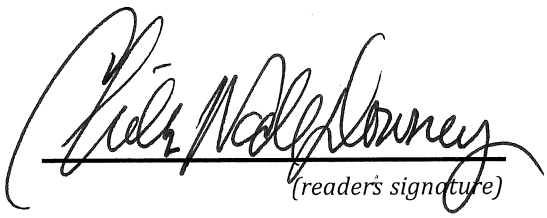

(readers signature)

4/22/16
(date)

Table of Contents

Acknowledgements

I would like to thank Dr. Nolin, my advisor and mentor for the past three years. Thank you for guiding and supporting me over the past few years. I have learned so much from you, both inside and outside the lab. Thank you for keeping me laughing and putting up with my clumsiness in the lab; these last three years have been an incredible experience and I have enjoyed every part of being a member of your lab. Having you as a mentor and friend has meant the world to me. Also, I would like to thank the members of the Nolin lab, for the good times and assistance during my summers with you. In particular, I would like to thank Caroline Braun for convincing Dr. Nolin to let me join the lab, and for taking me under your wing in my first summer. Lastly, I would like to thank my parents for supporting me over through my research, and giving me the opportunity to pursue my dreams at the University of Richmond.

Abstract

Calcium(II) complexes have be shown to be successful catalysts for nitrone reactions. The addition of n-methyl and n-phenyl nitrones to donor-acceptor cyclopropanes was achieved with calcium triflate (Ca(OTf). Differentially substituted tetrahydro-1,2-oxazines were synthesized in good to excellent yields. Calcium triflate was also found to catalyze the addition of silyl enol ethers to n-phenyl nitrones along the Mukaiyama-Mannich addition pathway. B-amino carbonyls were synthesized from a variety of substituted nitrones. Bulky and cyclic silyl enol ethers were also found to be reactive, the products of which were isolated in good to excellent yields.

I. Introduction

For many years, organic chemists have relied on the use of transition metal catalysts to drive a wide variety of reactions, and their use has been beneficial in the synthesis of pharmaceuticals and other aspects of the chemical industry. However, transition metal catalysis is not a sustainable method due to high cost and the limited quantities of many catalytic metals on the earth. Furthermore, transition metal catalysis is not favorable due to the high toxicity of metals and reaction waste. Throughout the past few years, there has been a push to explore alternative, environmentally benign catalytic complexes. Methods employing calcium complexes have been very promising.

Calcium is a promising catalytic species because it is electropositive and has a large atomic radius that allows for a number of coordination sites.[1] Additionally, calcium is the fifth most abundant and easily accessible element on the earth, and, therefore, would be a sustainable option for catalysis.[2] Calcium complexes have been successful in catalyzing a number of desirable reactions including ring opening polymerizations and 4π–electrocyclizations.[3] Their Lewis-acidic nature suggests a potential for a wide range of applications.[4]

In an effort to synthesize nitrogen-containing biologically active compounds, the reactivity of the nitrone (Figure 1) has been applied to a variety of reactions and has been found to be a very valuable reagent.[5] These carbonyl-derivative compounds are easily synthesized and, therefore, are an accessible starting material for the production of common motifs. Nitrones have a 1,3-dipole and an internal iminium species that makes them highly reactive electrophiles.[6] Nitrones have been substrates in a number of reactions, including [3+2] cycloadditions.[6,7] Nitrones have been shown to coordinate with

Lewis acids, therefore making them a candidates for calcium catalysis.[8] The following is a summary of our exploration of the use of calcium for nitrone reactions. To our knowledge, these are the first reports of calcium-catalyzed nitrone reactions.

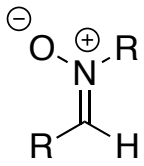

Figure 1. Nitrone

II. 1,3-Dipolar Cycloaddition

Cycloaddition reactions have been widely studied and utilized by organic chemists due to their transition state predictability, which allows for selective additions in molecule synthesis.[8] A 1,3-dipolar cycloaddition reaction utilizes the 1,3-dipole, or three-atom structure with positive and negative charges on either terminus, of a molecule to form five-membered heterocycles.[9] Cyclopropanes have been shown to be successful substrates for this reaction. In particular, their cycloaddition to nitrones has been found to be an excellent method for the synthesis of heterocyclic ring systems and carbon skeleton construction (eq. 1).[8,10]

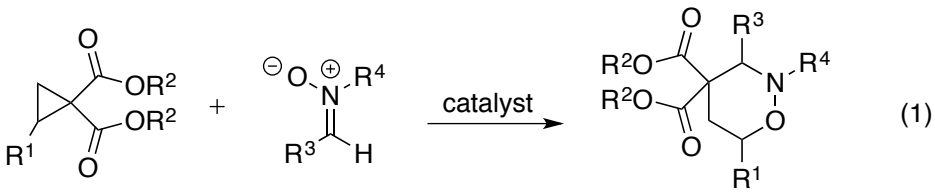

(1)

Cyclopropanes are excellent substrates for 1,3-dipolar cycloadditions because the cyclopropyl ring (Figure 2) has significant ring strain, and the relief of this ring strain is a major thermodynamic driving force.[10] Furthermore, the single bonds of the cyclopropane act similarly to carbon-carbon π-bonds and are susceptible to nucleophillic attack in the

presence of electron-withdrawing groups.[10] Donor-acceptor cyclopropanes contain both an electron-withdrawing and an electron-donating group and, therefore, make excellent electrophiles in the 1,3-dipolar cycloaddition reaction. The use of cyclopropanes can be advantageous due to the ability for cyclopropanes to act as a "synthetic wedge tool," allowing for formation of a one carbon homologue of the product acquired from alkenes.[10] Weakening of the cyclopropyl bonds has been achieved by Lewis Acids, and our lab has been successful in the activation of donor-acceptor (DA) cyclopropanes with calcium complexes.[8,11]

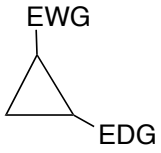

Figure 2. Donor-Acceptor Cyclopropane

The products of this reaction, tetrahydro-1,2-oxazines, are desirable biologically active compounds with potential applications in the pharmaceutical industry. The desirability of this product and our lab's success with calcium catalysis in cyclopropane reactions prompted us to explore the use of calcium for the addition of nitrones to DA cyclopropanes (equation 2). We began by testing a variety of commercially available calcium (II) complexes. Calcium iodide (CaI_2) was initially shown to be reactive with cyclopropane **1** and nitrone **2**, and the products was found to have a 1:4 cis-trans diastereomeric ratio. Further optimization with nitrone **4** (Figure 3) resulted in the ability

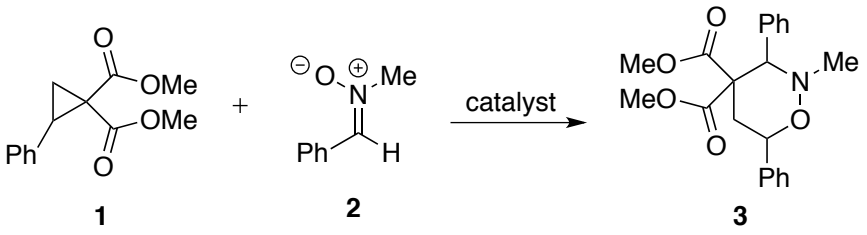

to decrease catalyst loading, nitrone equivalents, and reaction temperature while increasing the diastereomeric ratio to >99:1. Subsequently, the reaction scope was explored for variations of cyclopropane **1** as well as nitrones **2** and **4**.

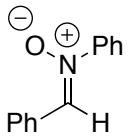

4

Figure 3. N-*phenyl* Nitrone

1. Results and Discussion

1.1 Reaction Optimization

The addition of DA cyclopropanes to nitrones was initially probed with a variety of commercially available calcium(II) complexes using N-*methyl* nitrone **2** and cyclopropane **1** in toluene (Table 1, entries 1-6). $Ca(acac)_2$, $Ca(OMe)_2$, and $Ca(OAc)_2$ were found to be unreactive. Trace reactivity was seen with CaI_2, while $Ca(neodec)_2$ and $Ca(OTf)_2$ were found to be catalytically active with 11% and 100% conversion, respectively. When 10 mol% of $Ca(OTf)_2$ was used, 100% conversion could be achieved at 70 °C after 22 hours. This reaction was found to have a 5:1 diastereomeric ratio in favor of the cis isomer. Nitrone equivalents were reduced from 1.5 to 1.2 due to solubility constraints, causing an 83% conversion and 6:1 cis-to-trans diasteriomeric ratio (entry 7). A solvent screen was performed at 70 °C, and 100% conversion was achieved in acetonitrile (entries 8-12). Due to a decrease in conversion (79%) when the temperature was decreased to 50 °C (entry 13), the reaction temperature for the N-*methyl* nitrone was maintained at 70 °C with the

slight increase in conversion (88%) at this temperature when catalyst loading was

Table 1. N-*methyl* Nitrone Reaction Optimization

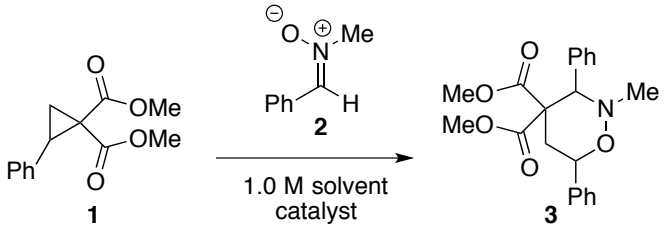

entry	solvent	equiv of **2**[a]	catalyst	catalyst loading (mol%)	Time (h)	temp (°C)	conversion (%)[b]	Cis:Trans[c]
1	toluene	1.5	$Ca(acac)_2$	10	43	90	0	n/a
2	toluene	1.5	$Ca(OMe)_2$	10	43	90	0	n/a
3	toluene	1.5	$Ca(OAc)_2$	10	43	90	0	n/a
4	toluene	1.5	CaI_2	10	43	90	trace	4:1
5	toluene	1.5	$Ca(neodec)_2$	10	22	70	11	>99:1
6	toluene	1.5	$Ca(OTf)_2$	10	22	70	100	5:1
7	toluene	1.2	$Ca(OTf)_2$	10	19	70	83	6:1
8	DCE	1.2	$Ca(OTf)_2$	10	19	70	86	5:1
9	CPME	1.2	$Ca(OTf)_2$	10	22.5	70	87	6:1
10	2-MeTHF	1.2	$Ca(OTf)_2$	10	29	70	86	5:1
11	BuOAc	1.2	$Ca(OTf)_2$	10	29	70	69	5:1
12	MeCN	1.2	$Ca(OTf)_2$	10	18.5	70	100	3:1
13	MeCN	1.2	$Ca(OTf)_2$	10	47	50	79	n/a
14	MeCN	1.2	$Ca(OTf)_2$	2	47	50	88	n/a

a Reactions were run with 0.3 mmol of 1 and 0.33 in dry solvents for 19-24 h.
b Conversions were determined by 1H NMR.
c Diastereomeric ratios determined by 1H NMR

increased to 2 mol% (entry 14).

The reactivity of N-*phenyl* nitrone **4** was also explored during reaction optimization, as seen in Table 2. Tetrahydro-1,2-oxazine **5** was formed with 100% conversion at 70 °C and 50 °C from nitrone **4** and cyclopropane **1** (entries 1 and 2). Complete diastereoselectivity for the cis product was achieved at both temperatures (>99:1) and when catalyst loading was decreased to 5% and 2% (entries 3 and 4). Complete conversion

to product was maintained at 5% $Ca(OTf)_2$, and decreased slightly (95%) at 2% $Ca(OTf)_2$. Since catalyst loading, and reaction temperature could be decreased while diastereoselectivity increased with the N-*phenyl* nitrone, it was used in the place of the N-*methyl* nitrone in the reaction optimization condiitions . As determined by these studies, the reaction conditions for the addition of N-*phenyl* nitrone **4** to cyclopropane **1** were 1.0 equivalents of cyclopropane and 1.2 equivalents of nitrone in the presence of 2 mol% $Ca(OTf)_2$ in 1.0 M CH_3CN at 50 °C. Under these conditions, an isolated yield of 94% was

Table 2. N-*phenyl Nitrone Reaction Optimization*

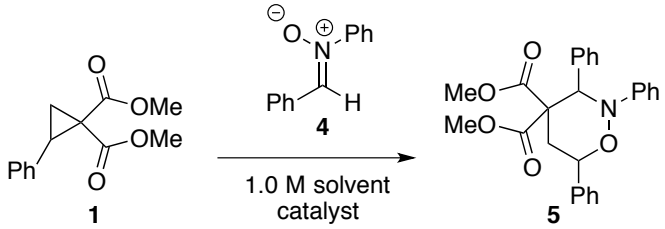

entry	solvent	equiv of **2**a	catalyst	catalyst loading (mol%)	Time (h)	temp (°C)	conversion (%)[b]	Cis:Trans[c]
1	MeCN	1.2	$Ca(OTf)_2$	10	18.5	70	100	>99:1
2	MeCN	1.2	$Ca(OTf)_2$	10	16	50	100	>99:1
3	MeCN	1.2	$Ca(OTf)_2$	5	16	50	100	>99:1
4	MeCN	1.2	$Ca(OTf)_2$	2	16	50	95	>99:1

a Reactions were run with 0.3 mmol of 1 and 0.33 in dry solvents for 19-24 h.
b Conversions were determined by 1H NMR.
c Diastereomeric ratios were determined by 1H NMR

obtained for product **5** with a 66:1 cis to trans diastereomeric ratio.

1.2 Cyclopropane Scope

To begin investigating the scope of the 1,3-dipolar cycloaddition reaction, nitrone **4** was added to cyclopropanes **6a-j** bearing a variety of substituents under optimized reaction conditions. The results of which can be found in Table 3. The resulting tetrahydra-1,2-oxazines were isolated in good yields for electron rich cyclopropanes **6b** and **6c** in 85%

and 87% yields, respectively. Cycloaddition products **7e** and **7f** from electron-deficient cyclopropanes **6e** and **6f** were isolated in slightly higher yields (91% and 93%, respectively) than electron-rich cyclopropanes as expected due to increased electrophillicity of the cyclopropane. Surprisingly, cyclopropane **6g** was less reactive than other electron-deficient species and tetrahydro-1,2-oxazine **7g** was isolated in a 78% yield despite increasing catalyst loading to 5 mol%. Electron rich cyclopropane **6b** showed increased diastereoselectivity (>99:1) towards the cis product while all other electron rich and electron deficient cyclopropanes showed a decrease in diastereoselectivity (27-29:1),

Table 3. Cyclopropane Scope

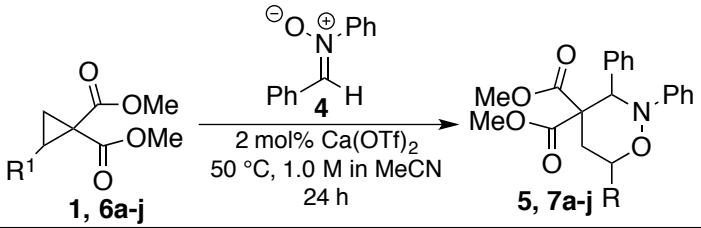

Entry	R^1		Yield	Cis:Trans[a]	
1	Ph	**1**	94	66:1	**5**
2	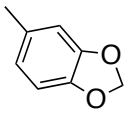	**6a**	99	17:1	**7a**
3	4-OMePh	**6b**	85	>99:1	**7b**
4	4-MePh	**6c**	87	27:1	**7c**
5	2-MePh	**6d**	85	29:1	**7d**
6	4-FPh	**6e**	91	28:1	**7e**
7	4-ClPh	**6f**	93	28:1	**7f**
8	4-BrPh	**6g**	78	29:1	**7g**
9	3-(N-Ts)-indolyl	**6h**	91	>99:1	**7h**
10	2-Thiophenyl	**6i**	86	52:1	**7i**
11	5-Methyl-2-furanyl	**6j**	95	>99:1	**7j**

a Diastereomeric ratios were determined by 1H NMR

which still favored the cis product. Substitution at the ortho position as opposed to the para position showed no effect on the yield or diastereoselectivity (entry 5). Substitutions of heterocyclic groups on the cyclopropane were also found to be reactive and products **7a,h-j** for cyclopropanes **6a,h-j** were isolated in excellent yields (86%-99%) with increased selectivity for the cis product (52->99:1).

1.3 Nitrone Scope

The scope of the 1,3-dipolar cycloaddition reaction of cyclopropanes and nitrones was further expanded to explore the effect of variation in the groups on nitrone **4**. Aryl nitrones with electron donating, electron withdrawing, and heteroaromatic substituents (**8a-d)** were reacted with cyclopropane **1** under optimized conditions, the results of which are shown in Table 4. All three types of nitrones were found to be reactive and tetrahydro-1,2-oxazine products **9a-d** were isolated in good to excellent yields (74%-95%). No significant variation was seen between electron rich (**9a** and **9b**, 88% and 95% yield, respectively) and electron deficient nitrones (entry **9c**, 88% yield). Greater selectivity for the cis product was seen with the electron-deficient nitrone (43:1) than the electron-rich

Table 4. N-*phenyl* Nitrone Scope

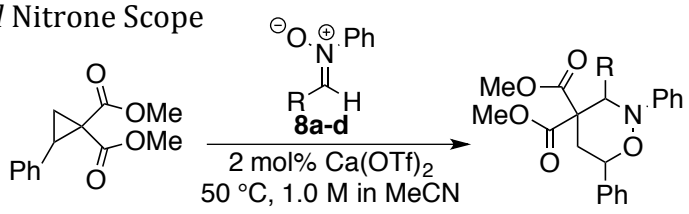

Entry	R		Yield	Cis:Trans[a]	
1	4-OMePh	**8a**	88	17:1	**9a**
2	4-MePh	**8b**	95	20:1	**9b**
3	4-ClPh	**8c**	88	43:1	**9c**
4	3-(N-Ts)-indolyl	**8d**	74	>99:1	**9d**

a Diastereomeric ratios were determined by 1H NMR

nitrones (17-20:1). Substituting the N-*phenyl* nitrone with a heteroaromatic group produced product **9d** in a lower yield (74%) but with increased diastereoselectivity in favor of the cis product (>99:1).

Reactivity and diastereoselectivity were also explored for the addition of various N-*methyl* nitrones to cyclopropane **1,** seen in Table 5. Nitrones with electron-donating, electron-withdrawing, and heterocyclic substituents underwent cycloadditon with the model DA cyclopropane to produce tetrahydro-1,2-oxazine products **11a-c** in excellent yields (83-92%). All N-*methyl* nitrones in our scope displayed the same slight selectivity for the cis product (3:1) as the reaction with nitrone **2** and cyclopropane **1**.

Table 5. N-*methyl* Nitrone Scope

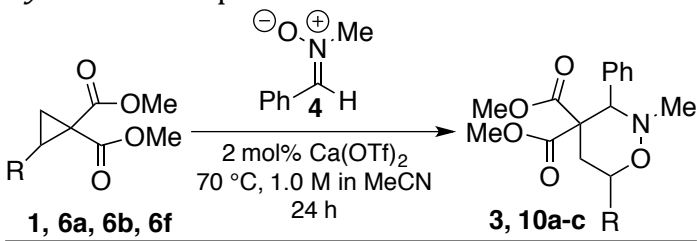

entry	R		yield (%)	*cis*:*trans*[a]	
1	Ph	**1**	94	3:1	**3**
2	4-OMePh	**6b**	86	3:1	**10a**
3	4-ClPh	**6f**	83	3:1	**10b**
4	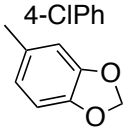	**6a**	92	3:1	**10c**

a Diastereomeric ratios were determined by 1H NMR

2. Conclusion

The results of the addition of nitrones to DA cyclopropanes provide a convenient and effective method for the preparation of diastereoselective tetrahydro-1,2-oxazines. The synthesis of this product is highly valuable because tetrahydro-1,2-oxazines have been used for a number of natural product syntheses, including the total synthesis of (+)-

phyllantidine and (+)-nakadormarin.[8,12] Furthermore, tetrahydro-1,2-oxazines have been critical for the synthesis of FR900482, an antitumor antibiotic.[8] Our method provides an inexpensive and environmentally benign process for the synthesis of this product, and further demonstrates the effectiveness of Ca(II) complexes as Lewis acid catalysts.

III. Mukaiyama-Mannich Reaction

The Mannich reaction, the nucleophillic attack of an iminium ion by an enolized carbonyl compound has been extensively studied and successfully utilized to form carbon–carbon bonds.[13] When the enolized carbonyl compound is replaced with a silyl enol ether, this reaction comes to be known as the Mukaiyama-Mannich reaction. Silyl enol ethers are beneficial substrates because they are highly regio- and stereoselective.[14] This reaction has a wide variety of applications, including the synthesis of a precursor to an analogue of naturally occuring (+)-goniofurfurone and the efficient entry into the core of alkaloids from *Martinella* snails.[15,16]

The internal iminium species of the nitrone allows it to be utilized as an electrophile for the Mukaiyama-Mannich reaction (eq 3). Its use is advantageous due to the presence of a highly reactive carbon-nitrogen bond within the 1,3-dipole as well its ability to be activated by Lewis Acids, which are a requirement for Mannich reactions.[17] Domingo et al. found that the coordination of a Lewis acid to the nitrone increases its electrophillicity to 1.82 eV, making it a strong electrophile and highly succeptable for nucleophillic attack.[18] Studies of the reaction of nitrones with silyl enol ethers and similar silyl ketene esters have

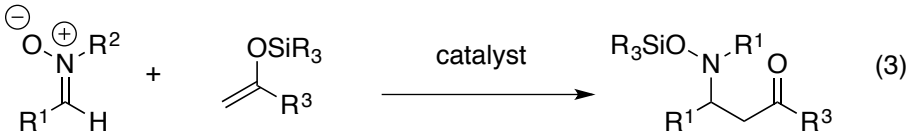

(3)

shown the successful catalysis of 1,3-dipolar cycloadditions with Lewis Acid catalysts to form isoxoladines (Scheme 1, pathway 1).[5,18]However, the synthesis of β-amino carbonyl compounds can also be achieved from these substrates through the Mukaiyama-Mannich addition pathway (pathway 2).[13,19] This pathway is desirable due the biologically active nature of β-amino alcohols, a β-amino carbonyl derivative.[20]

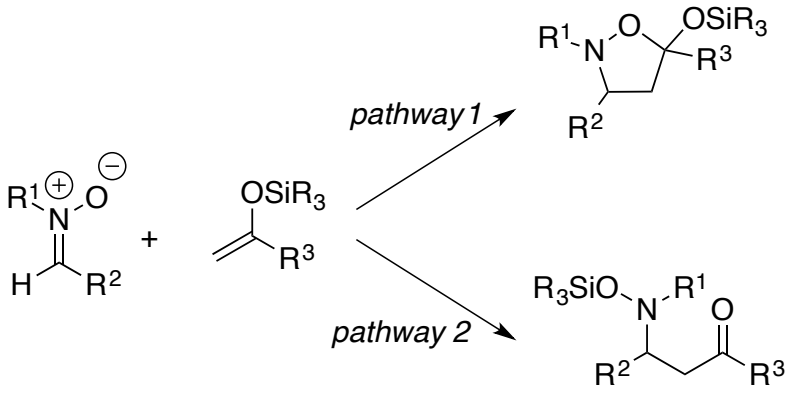

Scheme 1. Possible Reaction Pathways

Due to the success with Lewis acid activation in the Mukaiyama-Mannich reaction and our past findings with calcium catalyzed nitrone reactions, we decided to investigate the application of calcium in the addition of silyl enol ethers to nitrones (equation 4). We began by probing the reaction with various Ca(II) catalysts. Nitrone **4** was found to be reactive with silyl enol ether **12** in the presence of $Ca(OTf)_2$ and reacted along pathway 2 (Scheme 1) to form β-amino carbonyl **13** . After determining optimal conditions, the scope of the reaction was explored. The results of this study are summarized below.

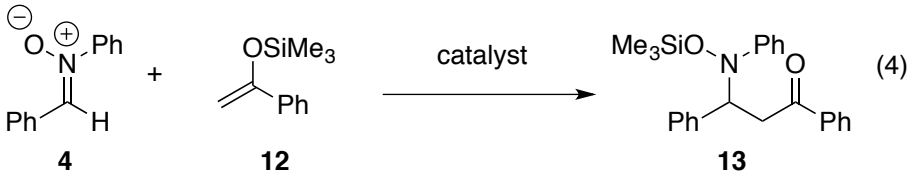

1. Results and Discussion

1.1 Reaction Optimization

To begin optimizing the Mukaiyama Mannich-type reaction of N-*phenyl* nitrones with silyl enol ethers, a number of calcium(II) complexes were tested as potential catalysts. The results of this optimization are presented in Table 6. After 21 hours at room temperature, Ca(prop) and $Ca(acac)_2$ were found to be catalytically inactive. $Ca(OTf)_2$, $Ca(NTf_2)_2$, and CaI_2 proved to be catalytically active in dicholoroethane, and CaI_2 facilitated the largest conversion of starting material to product **13** at 62% (entry 1). For all three catalysts, significant hydrolysis of the silyl enol ether was seen. When a solvent screen was performed at 50°C, hydrolysis was prevented in acetonitrile (entry 3). A second catalyst screen was performed in acetonitrile (entires 4-7), and $Ca(NTf_2)_2$, CaI_2, and $Ca(OTf)_2$ were

Table 6. Reaction Optimization

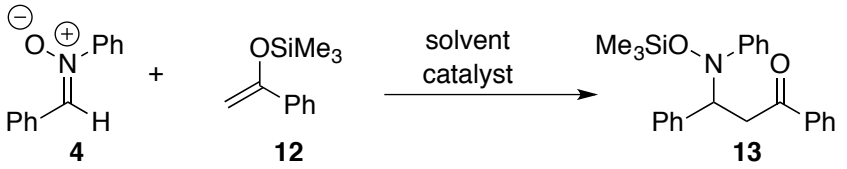

4 **12** **13**

Entry	Catalyst	Solvent[a] (1 M)	Cat. Loading (mol%)	Temp (°C)	Time (h)	Conversion[b] (%)
1	CaI_2	CH_2Cl_2	5	rt	21	62
2	CaI_2	CH_3CN	5	rt	21	58
3	CaI_2	CH_3CN	5	50	17	46
4	$Ca(prop)_2$	CH_3CN	5	50	17	0
5	$Ca(acac)_2$	CH_3CN	5	50	17	0
6	$Ca(NTf_2)_2$	CH_3CN	5	50	17	71
7	$Ca(OTf_2)$	CH_3CN	5	50	17	79
8	$Ca(OTf_2)$	CH_3CN	2	50	24	100

a Reactions were run with 0.3 mmol of 4 and 0.45 mol of 12 in dry solvents for 19-24 h.
b Conversions were determined by 1H NMR.

all found to maintain catalytic activity. Furthermore, the change in solvent resulted in 100% conversion to the desired β-amino alcohol at only 2% catalyst loading after extending the reaction to run for 24 hours (entry 8).

Despite achieving 100% conversion to product **13**, our attempts to isolate it for yield were hindered by the formation of acetophenone, a byproduct caused by the breakdown of the silyl enol ether, and by the difficulty in separating the β-amino carbonyl from excess starting materials. By monitoring the reaction via ^{1}H NMR in *d*-acetonitrile, the reaction was found to have reached completion after 4 hours. Determined by the above studies, our optimized reaction conditions were 1.0 equivalents of nitrone **4** and 1.5 equivalents silyl enol ether **12** in the presence of 2% $Ca(OTf)_2$ in 1.0M CH_3CN heated at 50°C for 4 hours. For this reaction, we were able to maximize the isolated yield to 95%.

1.2 Nitrone Scope

After optimizing the reaction, the scope of N-*phenyl* nitrones was examined. The addition of various aryl-substituted nitrones was explored, the results of which are presented in Table 7. Electron-rich, electron-deficient, sterically encumbered, and heteroaromatic nitrones **8a-i** were synthesized in our lab following literature procedure. The optimization conditions for the exploration of this scope were altered to run the reaction for 24 hours. Aryl nitrones with electron-donating and electron-withdrawing substituents both demonstrated excellent reactivity. Electron-rich nitrones **8a** and **8b** reacted in 93% and 95% yield, respectively, and electron-deficient nitrones **8e** and **8c** reacted in 94% and 96% yield, respectively. Sterically encumbered nitrones **8f** and **8g** reacted in slightly lower yields than electron-rich and electron-deficient nitrones (84%-93%). Nitrones **8h**, **8i**, and **8d** with heteroaromatic substituents were also found to be reactive, but in lower yields (72%-

Table 7. N-*phenyl* Nitrone Scope

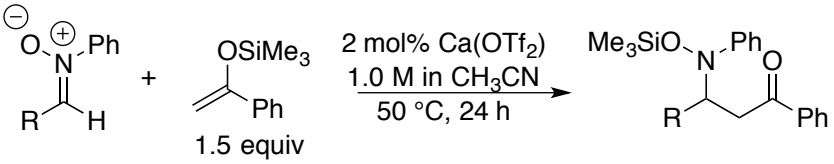

4, 8a-i **12** **13, 14a-i**

Entry	R		Isolated Yield (%)	
1	Ph	**4**	95	**13**
2	4-OMePh	**8a**	93	**14a**
3	4-MePh	**8b**	95	**14b**
4	4-BrPhl	**8e**	94	**14e**
5	4-ClPh	**8c**	96	**14c**
6	1-naphthyl	**8f**	93	**14f**
7	2-MePh	**8g**	84	**14g**
8	5-(2-Mefuranyl)	**8h**	94	**14h**
9	2-thiophenyl	**8i**	76	**14i**
10	3-(N-Ts)-indolyl	**8d**	72	**14d**

93%). The lower yield of **14d** can be attributed to the difficulty separating the β-amino carbonyl from the starting material. N-*methyl* nitrone **2** was also tested, but was unreactive. All products from silyl enol ether **12** except for **13** and **14c** were found to have trace amounts of azoxybenzene and disiloxane byproducts. Disiloxane is formed from the reaction of silicon biproducts with oxygen from water or the nitrone. It is unknown at this time how azoxybenzene is formed in this reaction.

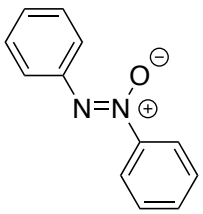

Figure 4. Azoxybenzene

1.3 Silyl Enol Ether Scope

The scope of the Mukaiyama-Mannich reaction was further explored by examining the addition of bulky and cyclic silyl enol ethers to the N-*phenyl* nitrone, the results of which are presented in Table 8. The addition of bulky silyl enol ether **15a** was found to be reactive when the optimized reaction conditions were adjusted to 5% catalyst loading at 70°C run for 24 hours. Product **16a** was isolated in a 95% yield. The reactivity of cyclic silyl enol ethers was then tested with cyclopentanone-derived and cyclohexanone-derived compounds **15b** and **15c**. We were surprised to find that these compounds, which are commonly sluggish to react, proceeded through the Mukaiyama-Mannich addition pathway to form β-amino carbonyl products. Silyl enol ether **15b** was found to form product **16b** in

Table 8. Silyl Enol Ether Scope

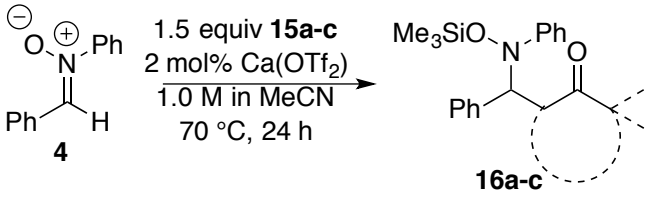

Entry					Isolated Yield (%)
1	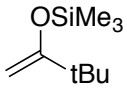	**15a**	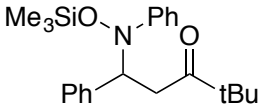	**16a**	95
2	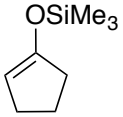	**15b**	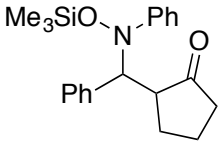	**16b**	88 3 anti:1 syn[a]
3	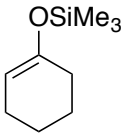	**15c**	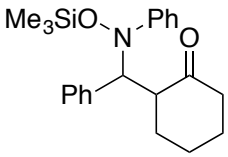	**16c**	58 2 syn:1 anti[a]

an 88% yield under the original optimized conditions. Silyl enol ether **15c** formed product **16c** when reaction conditions were adjusted to 5% catalyst loading at 70°C for 24 hours in a 58% yield. Product **16b** showed moderate diastereoselectivity for the anti diastereomer in a 3:1 ratio, while product **16c** showed moderate diastereoselectivity for the syn product in a 2:1 ratio.

2. Proposed Catalytic Cycle

The catalytic ability of calcium(II) complexes was explored due to the Lewis acidic nature of the metal, which we believed would be effective in driving the desired reaction. Scheme 2 illustrates the proposed mechanism for Mukaiyama-Mannich addition to nitrones. First, $Ca(OTf)_2$ coordinates with the nitrone, likely through exchange of one of the triflate ligands, causing an increase in electrophilicity. The nucleophilic double bond of the silyl enol ether can then add to the nitrone at the alpha position. The release of the calcium species can be envisioned in two ways. We believe that a silyl transfer occurs, possibly facilitated by the triflate anion, and our product forms directly with the release of calcium. However, there is a possibility that the formation of the silyl acetal occurs, and subsequent

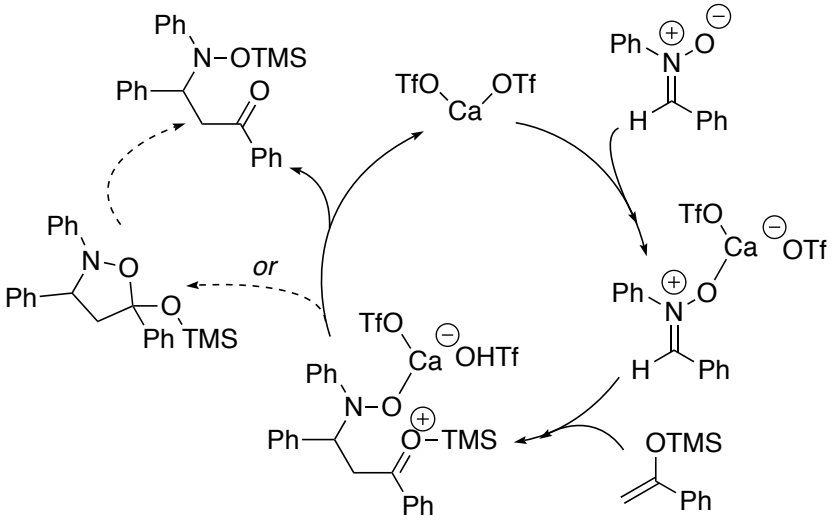

Scheme 2. Proposed Catalytic Cycle

breakdown during the reaction causes the production of our final product. However, the silyl acetal was not observed in the crude ^{1}H NMR spectrum.

3. Conclusions

The results of this study demonstrate the excellent ability of calcium to catalyze the Mukaiyama-Mannich reaction of nitrones and silyl enol ethers. Our methods provide a pathway for synthesis of β-amino carbonyls with high yield as well as the ability to utilize cyclic and bulky silyl enol ethers. The success of calcium in this reaction allows for convenient and inexpensive preparation of β-amino carbonyls and a method for the synthesis of β-amino alcohol precursors under environmentally benign conditions.

[1] Hut'ka, M.; Tsubogo, T.; Kobayashi, S. *Organometallics* **2014**, *33*, 5626-5629.
[2] Hut'ka, M.; Tsubogo, T.; Kobayashi, S. *Adv. Synth. Catal.* **2013**, *355*, 1561-1569.
[3] Davies, J.; Leonori, D. *Chem. Commun.* **2014**, *50*, 15171- 151174.
[4] Begouin, J.; Niggemann, M. *Chem. Pub. Soc. Europe* **2013,** *19*, 8030-8041.
[5] Murahashi, S.; Imada, Y.; Kawakami, T.; Harada, K.; Yonemushi, Y.; Tomita, N. *J. Am. Chem. Soc.* **2002**, *124*, 2888-2889.
[6] Confalone, P.; Huie, E.; *Organic Reactions* **2004**.
[7] Black, D.; Crozier, R. Davis, V. *Synthesis* **1975**, *4*, 205-221.
[8] Young, I.; Kerr, M. *Angew Chem. Int. Ed. Engl.* **2003**, *42*, 3023-3026.
[9] Grossman, R. *The Art of Writing Reasonable Reaction Mechanism.* **2005**.
[10] Wong, H.; Hon, M.; Tse, C.; Yip, Y. *Chem. Rev.* **1989,** *89*, 165-198.
[11] Braun, C.; Shema, A.; Dulin, C.; Nolin, K. *Tetrahedron Lett.* **2013**, *54*, 5889-5891.
[12] Carson, C.; Young, I.; Kerr, M. *Synthesis* **2008**, *3*, 485-489.
[13] Nagase, R.; Osada, J.' Tamagaki, H.; Tanabe, Y. *Adv. Synth. Catal.* **2010**, *352,* 1128-1134.
[14] Hosomi, A.; Shoji, H.; Sakurai, H. *Chem. Lett.* **1985**, *7*, 1049-1052.
[15] Ranieri, B.; Curti, C.; Battistini, L.; Sartori, A.; Pinna, L.; Casiraghi, G.; Zanardi, F. *J. Org. Chem.* **2011**, *76*, 10291-1098.
[16] Ikeda, S.; Shibuya, M.; Kanoh, N.; Iwabuchi, Y. *Chem. Lett.* **2008**, *37*, 962-963.
[17] Merino, P.; Jimenez, P.; Tejero, T. *J. Org. Chem.* **2006**, *71,* 4685-4688.
[18] Domingo, L.; Arno, M.; Merino, P.; Tejero, T. *Eur. J. Org. Chem.* **2006**, 3464-3472.
[19] Congdon, E.; Nolin, K. *Catal. Commun.* **2016**, *79*, 35-38.
[20] Kingler, D. *Acc. Chem. Res.* **2007**, *40*, 1367-1376.

Calcium(II) Catalyzed Nitrone Additions

Elizabeth Congdon
Department of Chemistry, University of Richmond, VA

Appendices

1. Experimental Information for Addition of Nitrones to Electron Deficient Cylopropanes

General Information. Unless otherwise noted, all commercial materials were used without purification. Calcium triflate and *N*,α-Diphenyl nitrone (**4**) were obtained from commercial sources and used without further purification. DA cyclopropanes and nitrones were synthesized according to literature procedures. Diastereomeric ratios were determined by ^{1}H NMR. NMR data for major diastereomer has been reported. Minor diastereomers were not able to be isolated.

General Procedure for the Addition of Nitrones to Cyclopropanes:

In an inert glovebox, calcium triflate (6.8 mg, 0.02 mmol, 0.02 equiv) was added to a 3 mL conical glass vial with a stir bar. After vial was removed from the glovebox, cyclopropane (1 mmol, 1.0 equiv), nitrone (1.2 mmol, 1.2 equiv) and dry MeCN (1.0 mL, 1.0 M) were added. The reaction solution was heated to 50 or 70 °C and the reaction progress was monitored by TLC. Upon completion, the vial was removed from the heat, and cooled to room temperature while stirring. The reaction was then loaded directly onto a silica gel column and purified by flash chromatography (5-20% EtOAc in hexanes).

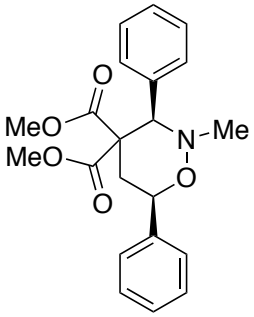

Dimethyl 2-methyl-3,6-diphenyl-1,2-oxazinane-4,4-dicarboxylate (3): white solid, mp 84-86 °C (345.7 mg, 94% yield); ^{1}H NMR (300 MHz, $CDCl_3$): δ 7.66 – 7.57 (m, 2H), 7.54 – 7.26 (m, 8H), 4.89 (dd, *J* = 11.7, 3.1 Hz, 1H), 4.84 (s, 1H), 3.89 (s, 3H), 3.39 (s, 3H), 2.74 (dd, *J* = 14.5, 11.8 Hz, 1H), 2.63 (dd, *J* = 14.4, 3.2 Hz, 1H), 2.54 (s, 3H); ^{13}C NMR (126 MHz, $CDCl_3$): δ 170.3, 168.5, 140.2, 134.8, 130.9, 128.6, 128.2, 128.1, 128.1, 126.4, 77.9, 68.0, 59.4, 53.3, 52.4, 43.4, 31.1. Spectral data was consistent with reported literature values.[i]

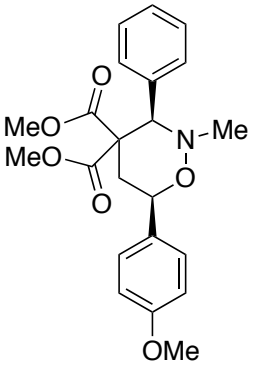

Dimethyl 6-(4-methoxyphenyl)-2-methyl-3-phenyl-1,2-oxazinane-4,4-dicarboxylate (10a): white solid, mp 86-91 °C (343.2 mg, 86% yield). ^{1}H NMR (300 MHz, $CDCl_3$): δ 7.61 (dd, *J* = 6.5, 3.0 Hz, 2H), 7.48 – 7.37 (m, 2H), 7.39 – 7.26 (m, 3H), 7.01 – 6.89 (m, 2H), 4.89 – 4.77 (m, 2H), 3.88 (s, *3*H), 3.83 (s, 3H), 3.39 (s, 3H), 2.75 (dd, *J* = 14.4, 12.2 Hz, 1H), 2.61-2.53 (m, 1H), 2.53 (s, 3H), 1.29 – 1.18 (m, 1H); ^{13}C NMR (126 MHz, $CDCl_3$): δ 170.4, 168.5, 159.6, 130.9, 128.2, 128.0, 128.0, 120.0, 114.0, 77.6, 68.0, 59.4, 55.3, 53.3, 52.4, 43.4, 30.7, 15.3; IR (cm^{-1}): 3060, 3028, 2955, 2873, 2841, 1725, 1587, 1490, 1252, 1239, 1181, 1081. HRMS (+ve ESI/APCI TOF, $C_{22}H_{26}NO_6(MH^+)$) Calc'd 400.1755, Measured Mass 400.1754.

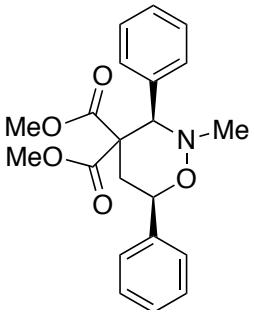

Dimethyl 6-(4-chlorophenyl)-2-methyl-3-phenyl-1,2-oxazinane-4,4-dicarboxylate (10b): white solid, mp 105-108 C (334.6 mg, 83% yield); ^{1}H NMR (300 MHz, $CDCl_3$): δ 7.56 (d, *J*

= 5.6 Hz, 2H), 7.47 – 7.28 (m, 7H), 4.85 (m, 2H), 3.89 (s, 3H), 3.38 (s, 3H), 2.78 – 2.57 (m, 2H), 2.53 (s, 3H); ^{13}C NMR (75 MHz, $CDCl_3$): δ 170.2, 168.3,138.7, 134.7, 133.8, 130.8, 128.7, 128.3, 128.1, 127.7, 67.8, 59.4, 53.4, 52.5, 43.4, 31.0; IR (cm^{-1}): 3037, 2993, 2955, 2892, 1736, 1492, 1429, 1255, 1169, 1150.[ii] HRMS (+ve ESI/APCI TOF, $C_{21}H_{23}NO_5Cl(MH^+)$) Calc'd 404.1259, Measured Mass 404.1265.

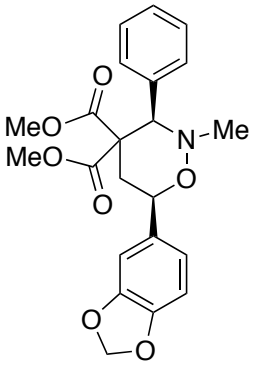

Dimethyl 6-(benzo[*d*][1,3]dioxol-5-yl)-2-methyl-3-phenyl-1,2-oxazinane-4,4-dicarboxylate (10c): white solid, mp 115-117 °C380.8 mg, 92% yield; ^{1}H NMR (300 MHz, $CDCl_3$): δ 7.64 – 7.54 (m, 2H), 7.39 – 7.26 (m, 3H), 7.04 – 6.90 (m, 2H), 6.84 (d, *J* = 8.0 Hz, 1H), 5.98 (s, 2H), 4.85 – 4.73 (m, 2H), 3.88 (s, 3H), 3.39 (s, 3H), 2.78 – 2.49 (m, 2H), 2.52 (s, 3H); ^{13}C NMR (126 MHz, $CDCl_3$): δ 170.3, 168.4, 147.8, 147.4, 134.7, 130.9, 128.3, 128.1, 120.1, 108.3, 107.3, 101.1, 77.8, 59.4, 53.3, 52.4, 43.4, 31.0; IR (cm^{-1}): 3063, 3025, 2952, 2873, 1726, 1596, 1487, 1234, 1171, 1070, 751. HRMS (+ve ESI/APCI TOF, $C_{22}H_{24}NO_7(MH^+)$) Calc'd 414.1547, Measured Mass 414.1545.

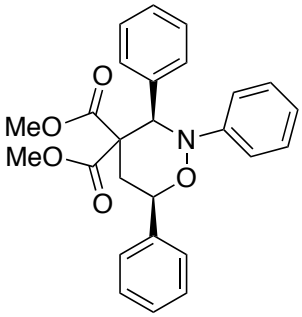

Dimethyl 2,3,6-triphenyl-1,2-oxazinane-4,4-dicarboxylate (5): white solid, mp 161-162 °C **(**406.5 mg, 94% yield); ^{1}H NMR (500 MHz, $CDCl_3$): δ 7.62 – 7.54 (m, 4H), 7.49 – 7.44 (m, 2H), 7.42 – 7.37 (m, 1H), 7.23 – 7.17 (m, 3H), 7.17 – 7.08 (m, 4H), 6.81 (tt, *J* = 7.2, 1.3 Hz, 1H), 5.80 (s, 1H), 5.04 (dd, *J* = 12.1, 2.6 Hz, 1H), 3.93 (s, 3H), 3.47 (s, 3H), 2.87 (dd, *J* = 14.4, 12.0 Hz,

1H), 2.79 (ddd, *J* = 14.4, 2.7, 0.9 Hz, 1H); ^{13}C NMR (126 MHz, $CDCl_3$): δ 170.1, 168.3, 148.6, 139.4, 135.0, 130.4, 128.6, 128.5, 128.3, 128.1, 128.0, 126.5, 121.6, 115.8, 78.8, 65.8, 59.6, 53.5, 52.6, 31.7. Spectral data was consistent with reported literature values.[iii]

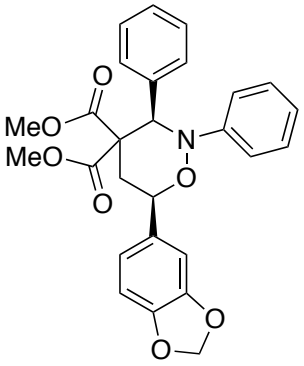

Dimethyl 6-(benzo[*d*][1,3]dioxol-5-yl)-2,3-diphenyl-1,2-oxazinane-4,4-dicarboxylate (7a): white solid, mp 152-155 °C (474.7 mg, 99% yield); ^{1}H NMR (300 MHz, $CDCl_3$): δ 7.63 – 7.50 (m, 2H), 7.22-7.06 (m, 8), 7.02 (ddd, *J* = 8.0, 1.8, 0.6 Hz, 1H), 6.89 (d, *J* = 8.0 Hz, 1H), 6.81 (tt, *J* = 6.7, 1.4 Hz, 1H), 6.02 (s, 2H), 5.78 (s, 1H), 4.93 (dd, *J* = 11.9, 2.6 Hz, 1H), 3.92 (s, 3H), 3.48 (s, 3H), 2.84 (dd, *J* = 14.4, 11.9 Hz, 1H), 2.72 (ddd, *J* = 14.4, 2.7, 0.9 Hz, 1H); ^{13}C NMR (75 MHz, $CDCl_3$): δ 170.1, 168.3, 148.5, 147.9, 147.6, 135.0, 133.1, 130.4, 128.6, 128.1, 128.0, 121.6, 120.3, 115.8, 108.4, 107.4, 101.2, 78.7, 65.6, 59.5, 53.5, 52.7, 31.5; IR (cm^{-1}): 2946, 2895, 1730, 1600, 1492, 1249, 1033. HRMS (+ve ESI/APCI TOF, $C_{27}H_{26}NO(MH^+)$) Calc'd 476.1704, Measured Mass 476.1710.

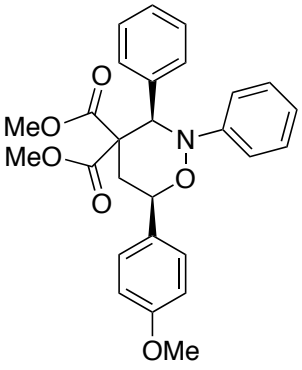

Dimethyl 6-(4-methoxyphenyl)-2,3-diphenyl-1,2-oxazinane-4,4-dicarboxylate (7b): pale yellow solid, mp 137-139 °C (394.2 mg, 85% yield); ^{1}H NMR (300 MHz, $CDCl_3$): δ 7.67 – 7.55 (m, 2H), 7.55 – 7.46 (m, 2H), 7.25 – 7.05 (m, 7H), 7.05 – 6.95 (m, 2H), 6.85 – 6.76 (m, 1H), 5.79 (s, 1H), 4.97 (dd, *J* = 12.1, 2.4 Hz, 1H), 3.92 (s, 3H), 3.86 (s, 3H), 3.49 (s, 3H), 2.90 (dd, *J* = 14.4, 12.1 Hz,

1H), 2.74 (ddd, *J* = 14.4, 2.6, 0.9 Hz, 1H); ^{13}C NMR (75 MHz, $CDCl_3$): δ 170.1, 168.4, 159.7, 148.6, 135.1, 131.3, 130.4, 128.5, 128.2, 128.1, 128.0, 121.5, 115.7, 114.0, 78.5, 65.5, 59.6, 55.4, 53.5, 52.7, 31.2; IR (cm^{-1}): 2949, 2892, 2854, 1733, 1597, 1242, 1169, 1043. HRMS (+ve ESI/APCI TOF, $C_{27}H_{28}NO_6$(MH+)) Calc'd 462.1911, Measured Mass 462.1927.

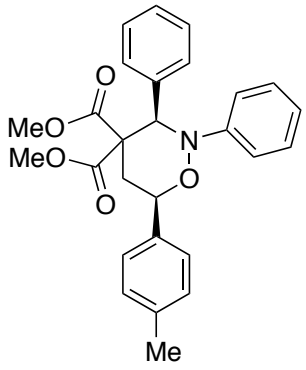

Dimethyl 2,3-diphenyl-6-(*p*-tolyl)-1,2-oxazinane-4,4-dicarboxylate (7c): pale yellow solid, mp 147-149 °C (385.9 mg, 87% yield); ^{1}H NMR (500 MHz, $CDCl_3$): δ 7.62 – 7.55 (m, 2H), 7.48 – 7.42 (m, 2H), 7.31 – 7.24 (m, 2H), 7.24 – 7.04 (m, 7H), 6.80 (tt, *J* = 7.2, 1.3 Hz, 1H), 5.79 (s, 1H), 4.99 (dd, *J* = 12.2, 2.4 Hz, 1H), 3.92 (s, 3H), 3.47 (s, 3H), 2.87 (dd, *J* = 14.4, 12.2 Hz, 1H), 2.76 (ddd, *J* = 14.4, 2.5, 0.9 Hz, 1H), 2.41 (s, 3H); ^{13}C NMR (75 MHz, $CDCl_3$): δ 170.1, 168.3, 148.6, 138.2, 136.3, 135.1, 130.4, 129.3, 128.5, 128.1, 128.0, 126.6, 121.5, 115.7, 78.7, 65.6, 59.5, 53.5, 52.7, 31.4, 21.3; IR (cm^{-1}): 3028, 2958, 2927, 2873, 1735, 1593, 1241, 1179, 1076. HRMS (+ve ESI/APCI TOF, $C_{27}H_{28}NO_5(MH^+)$) Calc'd 446.1962, Measured Mass 446.1962.

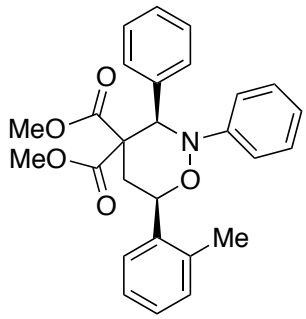

Dimethyl 2,3-diphenyl-6-(*o*-tolyl)-1,2-oxazinane-4,4-dicarboxylate (7d): white solid, mp 173-175 °C **(**376.9 mg, 85% yield); ^{1}H NMR (500 MHz, $CDCl_3$): δ 7.71 – 7.65 (m, 1H), 7.64 – 7.57 (m, 2H), 7.39 – 7.32 (m, 1H), 7.29 (td, *J* = 7.4, 1.4 Hz, 1H), 7.25 – 7.06 (m, 8H), 6.80 (tt, *J* = 7.2, 1.3 Hz,

1H), 5.82 (s, 1H), 5.18 (dd, *J* = 11.8, 2.4 Hz, 1H), 3.94 (s, 3H), 3.47 (s, 3H), 2.82 (dd, *J* = 14.4, 11.8 Hz, 1H), 2.74 (ddd, *J* = 14.4, 2.5, 1.0 Hz, 1H), 2.39 (s, 3H); ^{13}C NMR (75 MHz, $CDCl_3$): δ 170.1, 168.3, 148.6, 137.8, 135.7, 135.0, 130.6, 130.4, 128.6, 128.1, 128.0, 126.4, 125.2, 121.6, 115.7, 76.3, 66.0, 59.6, 53.5, 52.7, 31.1, 19.0; IR (cm^{-1}): 3022, 2955, 2927, 2870, 1727, 1600, 1432, 1239, 1176, 1070. HRMS (+ve ESI/APCI TOF, $C_{27}H_{28}NO_5(MH^+)$) Calc'd 446.1962, Measured Mass 446.1970.

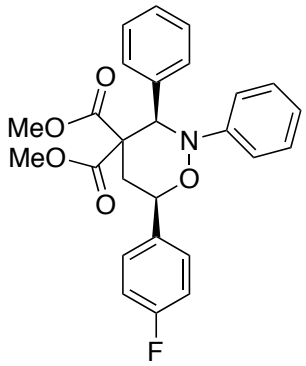

Dimethyl 6-(4-fluorophenyl)-2,3-diphenyl-1,2-oxazinane-4,4-dicarboxylate (7e): white solid, mp 134-137 °C (409.9 mg, 91% yield); ^{1}H NMR (300 MHz, $CDCl_3$): δ 7.62 – 7.47 (m, 4H), 7.24 – 7.04 (m, 9H), 6.88 – 6.76 (m, 1H), 5.79 (s, 1H), 5.01 (dd, *J* = 11.4, 3.2 Hz, 1H), 3.93 (s, 3H), 3.48 (s, 3H), 2.92 – 2.69 (m, 2H); ^{13}C NMR (75 MHz, $CDCl_3$): δ 170.0, 168.2, 162.7 (d, *J* = 246.9 Hz), 148.5, 135.2 (d, *J* = 3.3 Hz), 134.9, 130.4, 128.6, 128.4 (d, *J* = 8.2 Hz), 128.1, 128.0, 121.7, 115.8, 115.6 (d, *J* = 21.5 Hz), 78.2, 65.8, 59.5, 53.6, 52.7, 31.6; IR (cm^{-1}): 3034, 2955, 1739, 1597, 1508, 1226, 1176. HRMS (+ve ESI/APCI TOF, $C_{26}H_{25}NO_5F(MH^+)$) Calc'd 450.1711, Measured Mass 450.1714.

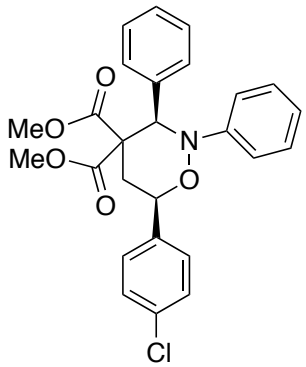

Dimethyl 6-(4-chlorophenyl)-2,3-diphenyl-1,2-oxazinane-4,4-dicarboxylate (7f): white solid, mp 164-170 °C (432.1 mg, 93% yield); ^{1}H NMR (300 MHz, $CDCl_3$): δ 7.61 – 7.38 (m, 6H), 7.27 – 7.01 (m, 7H), 6.83 (tt, *J* = 7.1, 1.3 Hz, 1H), 5.78 (s, 1H), 5.00 (dd, *J* = 10.6, 4.1 Hz, 1H), 3.93 (s,

3H), 3.48 (s, 3H), 2.89 – 2.69 (m, 2H); ^{13}C NMR (75 MHz, $CDCl_3$): δ 170.0, 168.1, 148.5, 137.9, 134.9, 134.2, 130.4, 128.8, 128.6, 128.1, 128.0, 127.8, 121.8, 115.9, 78.2, 66.0, 59.5, 53.5, 52.7, 31.7; IR (cm^{-1}): 2949, 2898, 1739, 1597, 1492, 1230, 1174. HRMS (+ve ESI/APCI TOF, $C_{26}H_{25}NO_5Cl(MH^+)$) Calc'd 466.1416, Measured Mass 466.1418.

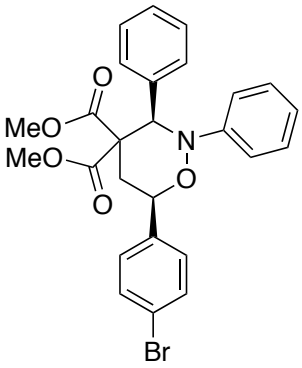

Dimethyl 6-(4-bromophenyl)-2,3-diphenyl-1,2-oxazinane-4,4-dicarboxylate (7g): white solid, mp 180-181 °C (395.5 mg, 78% yield); ^{1}H NMR (300 MHz, $CDCl_3$): δ 7.64 – 7.49 (m, 4H), 7.48 – 7.39 (m, 2H), 7.24 – 7.02 (m, 7H), 6.83 (tt, *J* = 7.0, 1.3 Hz, 1H), 5.78 (s, 1H), 5.00 (dd, *J* = 10.0, 4.6 Hz, 1H), 3.93 (s, 3H), 3.47 (s, 3H), 2.89 – 2.69 (m, 2H); ^{13}C NMR (75 MHz, $CDCl_3$): δ 169.9, 168.1, 148.5, 138.4, 134.9, 131.8, 130.4, 128.6, 128.1, 128.0, 121.8, 115.9, 78.2, 66.0, 59.5, 53.5, 52.7, 31.6; IR (cm^{-1}): 2949, 2920, 1739, 1591, 1496, 1258, 1173, 1068. HRMS (+ve ESI/APCI TOF, $C_{26}H_{25}NO_5Br(MH^+)$) Calc'd 510.0911, Measured Mass 510.0902.

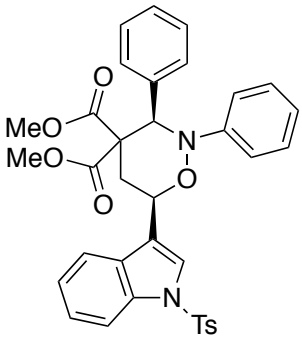

Dimethyl 2,3-diphenyl-6-(1-tosyl-1*H*-indol-3-yl)-1,2-oxazinane-4,4-dicarboxylate (7h): white solid, mp 118-125 °C (569.7 mg, 91% yield); ^{1}H NMR (300 MHz, $CDCl_3$): δ 8.03 (dt, *J* = 8.3, 0.9 Hz, 1H), 7.90 – 7.81 (m, 2H), 7.78 (d, *J* = 1.1 Hz, 1H), 7.75 – 7.68 (m, 1H), 7.58 – 7.45 (m, 2H), 7.37 (ddd, *J* = 8.4, 7.2, 1.3 Hz, 1H), 7.32 – 7.22 (m, 3H), 7.22 – 7.10 (m, 5H), 7.10 – 7.02 (m,

2H), 6.83 (tt, *J* = 7.4, 1.3 Hz, 1H), 5.80 (s, 1H), 5.28 (ddd, *J* = 11.6, 2.9, 1.1 Hz, 1H), 3.93 (s, 3H), 3.51 (s, 3H), 3.02 (dd, *J* = 14.2, 11.6 Hz, 1H), 2.97 – 2.87 (m, 1H), 2.37 (s, 3H); ^{13}C NMR (75 MHz, $CDCl_3$): δ 170.0, 168.2, 148.6, 145.2, 135.3, 135.3, 134.8, 130.5, 130.0, 129.5, 128.6, 128.2, 128.0, 127.0, 125.1, 123.5, 123.4, 121.8, 121.0, 120.4, 115.8, 113.7, 72.3, 66.5, 59.4, 53.6, 52.7, 29.7, 21.6; IR (cm^{-1}): 3060, 3034, 2949, 1735, 1597, 1446, 1236, 1174, 1135, 680. HRMS (+ve ESI/APCI TOF, $C_{35}H_{33}N_2O_7S(MH^+)$) Calc'd 625.2003, Measured Mass 625.2018.

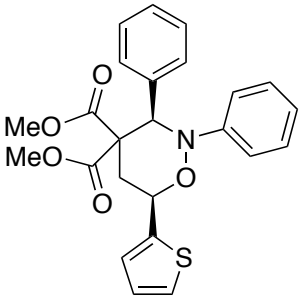

Dimethyl 2,3-diphenyl-6-(thiophen-2-yl)-1,2-oxazinane-4,4-dicarboxylate (7i): white solid, mp 124-127 °C (377.5 mg, 86% yield); ^{1}H NMR (300 MHz, $CDCl_3$): δ 7.62 – 7.51 (m, 2H), 7.41 (dd, *J* = 5.1, 1.2 Hz, 1H), 7.28 – 7.02 (m, 9H), 6.82 (tt, *J* = 7.4, 1.4 Hz, 1H), 5.76 (s, 1H), 5.25 (ddd, *J* = 11.6, 3.0, 0.9 Hz, 1H), 3.91 (s, 3H), 3.49 (s, 3H), 2.99 (dd, *J* = 14.3, 11.6 Hz, 1H), 2.88 (ddd, *J* = 14.3, 3.1, 0.8 Hz, 1H); ^{13}C NMR (75 MHz, $CDCl_3$): δ 169.9, 168.1, 148.4, 141.9, 134.8, 130.5, 128.6, 128.2, 128.0, 126.8, 126.0, 125.5, 121.8, 115.9, 74.7, 66.0, 59.5, 53.6, 52.7, 31.7; IR (cm^{-1}): 2980, 2965, 1730, 1600, 1492, 1236, 1176, 1147, 701. HRMS (+ve ESI/APCI TOF, $C_{24}H_{24}NO_5S(MH^+)$) Calc'd 438.1370, Measured Mass 438.1376.

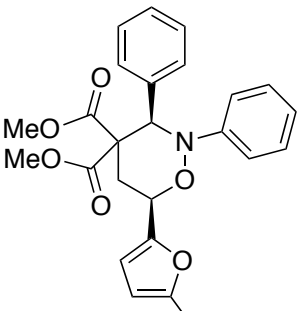

Dimethyl 6-(5-methylfuran-2-yl)-2,3-diphenyl-1,2-oxazinane-4,4-dicarboxylate (7j): white solid, mp 124-127 °C (414.9 mg, 95% yield); ^{1}H NMR (300 MHz, $CDCl_3$): δ

7.66 – 7.53 (m, 2H), 7.23 – 7.03 (m, 7H), 6.87 – 6.74 (m, 1H), 6.49 – 6.41 (m, 1H), 6.03 (dq, *J* = 3.1, 1.0 Hz, 1H), 5.72 (s, 1H), 5.01 (dd, *J* = 12.5, 2.4 Hz, 1H), 3.89 (s, 3H), 3.48 (s, 3H), 3.09 (dd, *J* = 14.5, 12.5 Hz, 1H), 2.70 (ddd, *J* = 14.5, 2.6, 0.9 Hz, 1H), 2.37 (d, *J* = 1.0 Hz, 3H); ^{13}C NMR (75 MHz, $CDCl_3$): δ 169.9, 168.2, 153.0, 150.1, 148.4, 134.9, 130.6, 128.5, 128.1, 128.0, 121.6, 116.0, 110.0, 106.4, 72.4, 65.9, 59.3, 53.5, 52.7, 28.2, 13.8; IR (cm^{-1}): 3006, 2958, 1736, 1591, 1489, 1252, 1198, 1154, 755. HRMS (+ve ESI/APCI TOF, $C_{25}H_{26}NO_6(MH^+)$) Calc'd 436.1755, Measured Mass 436.1769.

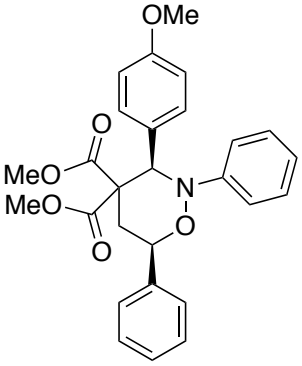

Dimethyl 3-(4-methoxyphenyl)-2,6-diphenyl-1,2-oxazinane-4,4-dicarboxylate (9a): pale yellow solid, mp 162-164 °C (404.7 mg, 88% yield); ^{1}H NMR (300 MHz, $CDCl_3$): δ 7.61 – 7.34 (m, 7H), 7.20 – 7.05 (m, 4H), 6.87 – 6.77 (m, 1H), 6.77 – 6.67 (m, 2H), 5.75 (s, 1H), 5.03 (dd, *J* = 11.5, 3.1 Hz, 1H), 3.92 (s, 3H), 3.71 (s, 3H), 3.50 (s, 3H), 2.86 (dd, *J* = 14.4, 11.5 Hz, 1H), 2.77 (ddd, *J* = 14.3, 3.2, 0.9 Hz, 1H); ^{13}C NMR (75 MHz, $CDCl_3$): δ 170.1, 168.3, 159.1, 148.6, 139.4, 131.6, 128.6, 128.5, 128.3, 126.9, 126.5, 121.6, 115.8, 113.3, 78.8, 65.3, 59.5, 55.0, 53.5, 52.7, 31.5. Spectral data was consistent with reported literature values.

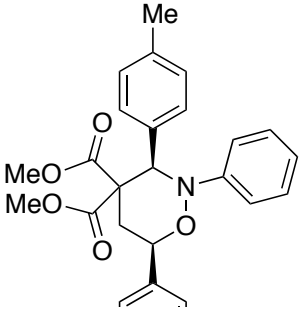

Dimethyl 2,6-diphenyl-3-(*p*-tolyl)-1,2-oxazinane-4,4-dicarboxylate (9b): white solid, mp 186-188 °C (425.2 mg, 95% yield); ^{1}H NMR (300 MHz, $CDCl_3$): δ 7.60 – 7.52 (m,

2H), 7.51 – 7.33 (m, 5H), 7.20 – 7.05 (m, 4H), 7.04 – 6.94 (m, 2H), 6.81 (tt, *J* = 7.3, 1.5 Hz, 1H), 5.77 (s, 1H), 5.02 (dd, *J* = 11.7, 2.9 Hz, 1H), 3.92 (s, 3H), 3.50 (s, 3H), 2.86 (dd, *J* = 14.4, 11.7 Hz, 1H), 2.76 (ddd, *J* = 14.3, 3.0, 0.8 Hz, 1H), 2.22 (s, 3H); ^{13}C NMR (75 MHz, $CDCl_3$): δ 170.2, 168.3, 148.6, 139.4, 137.7, 131.8, 130.3, 128.8, 128.6, 128.5, 128.3, 126.6, 121.5, 115.7, 78.8, 65.4, 59.5, 53.5, 52.7, 31.6, 21.1; IR (cm^{-1}): 3012, 2965, 2923, 2863, 1733, 1597, 1489, 1233, 1198, 1052. HRMS (+ve ESI/APCI TOF, $C_{27}H_{28}NO_5(MH^+)$) Calc'd 446.1962, Measured Mass 446.1952.

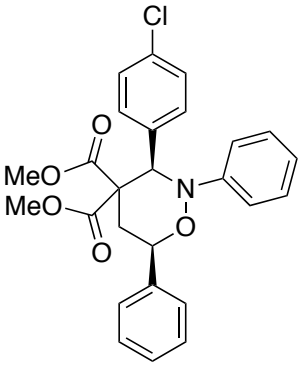

Dimethyl 3-(4-chlorophenyl)-2,6-diphenyl-1,2-oxazinane-4,4-dicarboxylate (9c): white solid, 150-152 °C (411.3 mg, 88% yield); ^{1}H NMR (300 MHz, $CDCl_3$): δ 7.59 – 7.34 (m, 7H), 7.22 – 7.11 (m, 4H), 7.11 – 7.02 (m, 2H), 6.90 – 6.78 (m, 1H), 5.77 (s, 1H), 5.03 (dd, *J* = 7.8, 6.7 Hz, 1H), 3.93 (s, 3H), 3.51 (s, 3H), 2.87 – 2.75 (m, 2H); ^{13}C NMR (75 MHz, $CDCl_3$): δ 169.8, 168.1, 148.3, 139.1, 134.1, 133.5, 131.7, 128.7, 128.7, 128.5, 128.3, 126.5, 121.9, 115.8, 78.8, 65.3, 59.4, 53.6, 52.8, 31.5; IR (cm^{-1}): 3034, 2952, 2876, 1733, 1599, 1486, 1235, 1198, 1181. HRMS (+ve ESI/APCI TOF, $C_{26}H_{25}NO_5Cl(MH^+)$) Calc'd 466.1416, Measured Mass 466.1421.

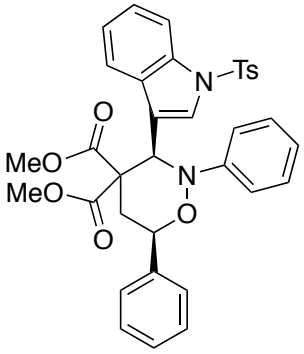

Dimethyl 2,6-diphenyl-3-(1-tosyl-1*H*-indol-3-yl)-1,2-oxazinane-4,4-dicarboxylate (9d): yellow solid, mp 188-193 °C (459.2 mg, 74% yield); ^{1}H NMR (300 MHz, $CDCl_3$): δ 8.11 (s, 1H), 7.86 – 7.74 (m, 1H), 7.64 – 7.56 (m, 2H), 7.56 –

7.48 (m, 3H), 7.48 – 7.38 (m, 3H), 7.24 – 7.12 (m, 2H), 7.11 – 6.99 (m, 6H), 6.85 – 6.71 (m, 1H), 6.12 (s, 1H), 5.08 (dd, *J* = 11.5, 3.0 Hz, 1H), 3.96 (s, 3H), 3.14 (s, 3H), 2.84 (ddd, *J* = 14.5, 3.1, 0.9 Hz, 1H), 2.75 (dd, *J* = 14.5, 11.5 Hz, 1H), 2.28 (s, 3H); ^{13}C NMR (75 MHz, $CDCl_3$): δ 169.7, 167.9, 148.6, 144.6, 139.0, 134.8, 134.0, 131.2, 129.7, 128.9, 128.6, 128.5, 127.3, 126.5, 126.4, 124.6, 123.1, 122.1, 119.2, 116.0, 115.6, 113.5, 79.1, 58.8, 58.6, 53.6, 52.6, 31.9, 21.; IR (cm^{-1}): 3066, 3031, 2955, 2923, 1736, 1597, 1445, 1230, 1173, 1119, 660. HRMS (+ve ESI/APCI TOF, $C_{35}H_{33}N_2O_7S(MH^+)$) Calc'd 476.1704, Measured Mass 476.1710.Calc'd 625.2003, Measured Mass 625.2003.

2. Experimental Information for the Mukaiyama-Mannich Reaction

General Information. Unless otherwise noted, all commercial materials were used without purification. Calcium triflate, N,α-Diphenyl nitrone, and 1-Phenyl-1-trimethylsiloxyethylene, 1-(Trimethylsiloxy)cyclopentene, 1-(Trimethylsiloxy)cyclophexene, and (1-Tert-Butylvinyloxy)trimentylsilane were obtained from commercial sources and used without further purification. Nitrones were synthesized according to literature procedures. Diastereomeric ratios were determined by ^{1}HNMR. NMR data for the major diastereomer has been reported. Minor diastereomers were not able to be isolated.

General Procedure for the Addition of Nitrones to Silyl Enol Ethers

In an inert glovebox, calcium triflate (6.8 mg, 0.02 mmols, 0.02 eq) was added to a 3 mL conical glass vial with a stir bar. After the vial was removed from the glove box,

nitrone (1.0 eq, 1.0 mmol), silyl enol ether (1.5 mmols, 1.5 eq), and dry MeCN (1.0 mL, 1.0 M) were added. The reaction solution was heated to 50 °C, and the reaction progress was monitored by TLC. Upon completion, the vial was removed from the heat and cooled to room temperature while stirring. The reaction was loaded directly onto a silica gel column and purified by flash chromatography (10-20% EtOAc or ether in hexanes).

In an inert glovebox, calcium triflate (16.9mg, 0.05 mmols, 0.05 eq) was added to a 3 mL conical glass vial with a stir bar. After the vial was removed from the glove box, nitrone (1.0 eq, 1.0 mmol), silyl enol ether (1.5 mmols, 1.5 eq), and dry MeCN (1.0 mL, 1.0 M) were added. The reaction solution was heated to 70 °C, and the reaction progress was monitored by TLC. Upon completion, the vial was removed from the heat and cooled to room temperature while stirring. The reaction was loaded directly onto a silica gel column and purified by flash chromatography (10-20% ether in hexanes).

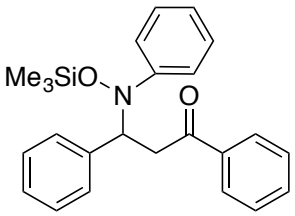

1,3-diphenyl-3-(phenyl((trimethylsilyl)oxy)amino)propan-1-one (13): (384.5 mg, 98% yield); ^{1}H NMR (500 MHz, Chloroform-*d*) δ 7.91 – 7.86 (m, 2H), 7.56 – 7.50 (m, 1H), 7.42 (dd, *J* = 8.3, 7.1 Hz, 2H), 7.33 – 7.17 (m, 8H), 7.15 – 7.09 (m, 2H), 6.98 (tt, *J* = 7.2, 1.2 Hz, 1H), 5.11 (dd, *J* = 8.5, 4.9 Hz, 1H), 3.73 (dd, *J* = 17.2, 8.5 Hz, 1H), 3.60 (dd, *J* = 17.2, 4.9 Hz, 1H), -0.13 (s, 9H); ^{13}C NMR (75 MHz, $CDCl_3$) δ 197.95, 152.31, 138.80, 137.15, 132.88, 129.50, 128.46, 128.16,

128.00, 127.81, 127.53, 123.48, 120.29, 69.45, 37.70, -0.70; Spectral data was consistent with reported literature values. [iv]

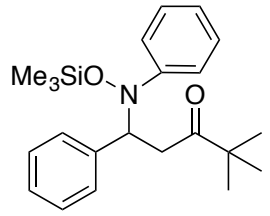

4,4-dimethyl-1-phenyl-3-(phenyl((trimethylsilyl)oxy)amino)pentan-1-one (16a): (351.6 mg, 95% yield); ^{1}H NMR (300 MHz, Chloroform-*d*) δ 7.28 – 7.15 (m, 7H), 7.11 – 7.05 (m, 2H), 7.00 – 6.93 (m, 1H), 4.90 (dd, *J* = 9.5, 3.8 Hz, 1H), 3.42 (dd, *J* = 17.8, 9.4 Hz, 1H), 3.00 (dd, *J* = 17.8, 3.8 Hz, 1H), 1.01 (s, 9H), -0.12 (s, 9H); ^{13}C NMR (75 MHz, $CDCl_3$) δ 213.20, 152.40, 139.02, 129.60, 128.08, 127.65, 127.38, 123.33, 120.26, 69.06, 44.22, 36.71, 26.29, -0.65; IR (cm^{-1}): 3040, 2962, 1695, 1486, 1343, 1250, 1099, 1074. HRMS (+ve ESI/APCI TOF, $C_{22}H_{31}NO_2Si(MH^+)$) Calcd 370.2197, Measured Mass 370.2208.

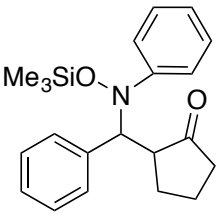

2-(phenyl(phenyl((trimethylsilyl)oxy)amino)methyl)cyclopentanone (16b): (311.1 mg, 88% yield); ^{1}H NMR (300 MHz, Chloroform-*d*) δ 7.24 – 6.92 (m, 10H), 4.55 (d, *J* = 6.2 Hz, 1H), 2.69 (tdd, *J* = 8.9, 6.2, 1.2 Hz, 1H), 2.42 – 1.96 (m, 5H), 1.89 – 1.66 (m, 1H), -0.06 (s, 9H); ^{13}C NMR (75 MHz, $CDCl_3$) δ 217.47, 152.78, 138.27, 129.69, 127.99, 127.46, 127.31, 124.30, 122.00, 73.84, 52.45, 37.95, 26.94, 20.31, -0.20; IR(cm^{-1}): 3032, 2958, 1744, 1593, 1491, 1450, 1254, 1156. HRMS (+ve ESI/APCI TOF, $C_{21}H_{27}NO_2Si(MH^+)$) Calcd 354.1884, Measured Mass 354.1891.

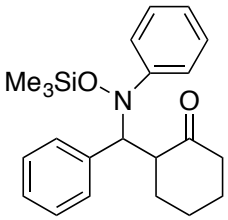

2-(phenyl(phenyl((trimethylsilyl)oxy)amino)methyl)cyclohexanone (16c):

(213.5 mg, 58% yield); ^{1}H NMR (500 MHz, Chloroform-*d*) δ 7.20 – 7.07 (m, 5H), 6.99 – 6.87 (m, 3H), 6.86 – 6.80 (m, 2H), 4.46 (d, *J* = 11.1 Hz, 1H), 3.45 – 3.35 (m, 1H), 2.62 – 2.51 (m, 1H), 2.29 – 1.76 (m, 5H), 0.05 (s, 9H); ^{13}C NMR (75 MHz, $CDCl_3$) δ 212.02, 152.97, 135.40, 130.08, 127.98, 127.21, 126.88, 123.11, 119.89, 73.19, 52.93, 42.35, 32.71, 29.32, 23.59, -0.19; IR (cm^{-1}): 3685, 3060, 3035, 2941, 2864, 1712, 1601, 1495, 1458, 1249, 1209, 1127, 1061, 1033, 1004. HRMS (+ve ESI/APCI TOF, $C_{22}H_{29}NO_2Si(MH^+)$) Calcd 368.2040, Measured Mass 368.2043.

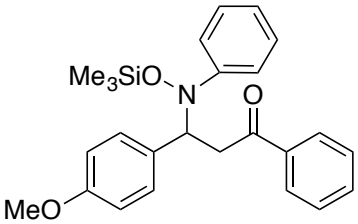

3-(4-methoxyphenyl)-1-phenyl-3-(phenyl((trimethylsilyl)oxy)amino)propan-1-one (14a):

(389.8 mg, 93% yield); ^{1}H NMR (300 MHz, Chloroform-*d*) δ 7.92 – 7.84 (m, 2H), 7.56 – 7.38 (m, 3H), 7.24 – 7.06 (m, 6H), 7.03 – 6.94 (m, 1H), 6.82 – 6.73 (m, 2H), 5.05 (dd, *J* = 8.1, 5.4 Hz, 1H), 3.77 (s, 3H), 3.73 – 3.52 (m, 2H), -0.10 (s, 9H); ^{13}C NMR (75 MHz, $CDCl_3$) δ 198.07, 158.97, 152.28, 137.17, 132.85, 130.93, 130.54, 128.46, 128.11, 128.01, 123.43, 120.39, 113.18, 68.92, 55.15, 38.11, -0.62; Spectral data was consistent with reported literature values.[iv]

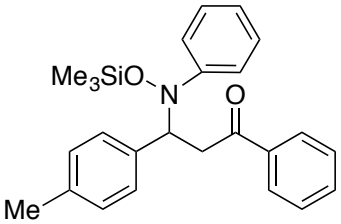

1-phenyl-3-(phenyl((trimethylsilyl)oxy)amino)-3-(*p*-tolyl)propan-1-one (14b)

(382.6 mg, 95% yield); ^{1}H NMR (300 MHz, Chloroform-*d*) δ 7.93 – 7.84 (m, 2H), 7.57 – 7.36 (m, 3H), 7.29 – 6.93 (m, 10H), 5.08 (dd, *J* = 8.1, 5.3 Hz, 1H), 3.76 – 3.54 (m, 2H), 2.30 (s, 3H), -0.11 (s, 9H); ^{13}C NMR (75 MHz, $CDCl_3$) δ 198.04, 152.33, 137.18, 137.06, 135.70, 132.84, 129.35, 128.49, 128.44, 128.11, 128.01, 123.38, 120.31, 69.16, 37.92, 21.10, -0.65; Spectral data was consistent with reported literature values. [iv]

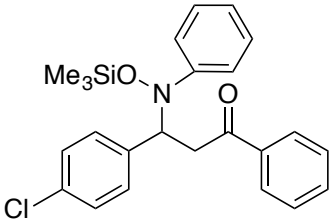

3-(4-chlorophenyl)-1-phenyl-3-(phenyl((trimethylsilyl)oxy)amino)propan-1-one (14c)

(406.2 mg, 96% yield); ^{1}H NMR (500 MHz, Chloroform-*d*) δ 7.90 – 7.86 (m, 2H), 7.57 – 7.51 (m, 1H), 7.43 (dd, *J* = 8.4, 7.1 Hz, 2H), 7.25 – 7.17 (m, 6H), 5.04 (dd, *J* = 8.5, 5.0 Hz, 1H), 3.69 (dd, *J* = 17.3, 8.6 Hz, 1H), 3.60 (dd, *J* = 17.3, 4.9 Hz, 1H), -0.10 (s, 9H); ^{13}C NMR (75 MHz, $CDCl_3$) δ 197.61, 152.11, 137.11, 136.97, 133.32, 133.06, 130.82, 128.54, 128.26, 127.96, 127.93, 123.74, 120.33, 68.87, 38.22, -0.61; Spectral data was consistent with reported literature values.[v]

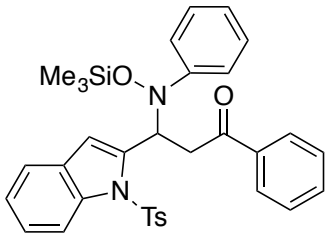

1-phenyl-3-(phenyl((trimethylsilyl)oxy)amino)-3-(1-tosyl-1*H*-indol-3-yl)propan-1-one (14d):

(419.0 mg, 72% yield); ^{1}H NMR (300 MHz, Chloroform-*d*) δ 7.96 – 7.83 (m, 3H), 7.65 – 7.35 (m, 7H), 7.31 – 7.04 (m,

11H), 7.01 – 6.91 (m, 1H), 5.34 (t, *J* = 6.6 Hz, 1H), 3.73 – 3.63 (m, 2H), 2.33 (s, 3H), -0.18 (s, 9H); IR(cm^{-1}): 3027, 2954, 2893, 1687, 1597, 1487, 1450, 1334, 1291, 1258, 1213, 1021. HRMS (+ve ESI/APCI TOF, $C_{33}H_{34}N_2O_4SSi(MNa^+)$) Calcd 605.1901, Measured Mass 605.1904.

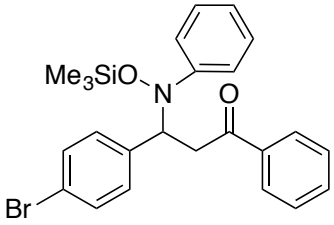

3-(4-bromophenyl)-1-phenyl-3-(phenyl((trimethylsilyl)oxy)amino)propan-1-one (14e):

441.8 mg, 94% yield); ^{1}H NMR (500 MHz, Chloroform-*d*) δ 7.90 – 7.85 (m, 2H), 7.57 – 7.51 (m, 1H), 7.47 – 7.40 (m, 2H), 7.39 – 7.33 (m, 2H), 7.24 – 7.18 (m, 2H), 7.16 – 7.08 (m, 4H), 7.00 (tt, *J* = 7.2, 1.2 Hz, 1H), 5.03 (dd, *J* = 8.5, 5.1 Hz, 1H), 3.69 (dd, *J* = 17.3, 8.5 Hz, 1H), 3.60 (dd, *J* = 17.3, 5.0 Hz, 1H), -0.10 (s, 9H); ^{13}C NMR (75 MHz, $CDCl_3$) δ 197.57, 152.09, 137.60, 136.95, 133.07, 131.18, 130.88, 128.55, 128.26, 127.96, 123.75, 121.53, 120.32, 68.92, 38.21, -0.61; Spectral data was consistent with reported literature values. [iv]

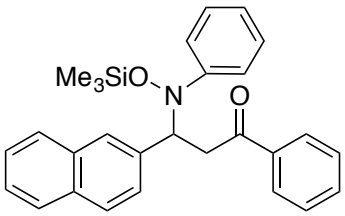

3-(naphthalen-1-yl)-1-phenyl-3-(phenyl((trimethylsilyl)oxy)amino)propan-1-one (14f):

(410.6 mg, 93% yield); ^{1}H NMR (300 MHz, Chloroform-*d*) δ 8.49 (d, *J* = 8.5 Hz, 1H), 7.92 – 7.73 (m, 4H), 7.64 – 7.18 (m, 13H), 7.04 – 6.94 (m, 1H), 6.06 (dd, *J* = 8.7, 4.7 Hz, 1H), 4.03 (dd, *J* = 17.2, 8.7 Hz, 1H), 3.61 (dd, *J* = 17.2, 4.7 Hz, 1H), -0.38 (s, 9H); ^{13}C NMR (75 MHz, $CDCl_3$) δ 198.12, 152.46, 137.15, 134.87, 134.01, 132.86, 132.77,

128.68, 128.46, 128.43, 128.00, 126.11, 126.02, 125.33, 124.72, 123.86, 123.41, 119.75, 64.51, 36.41, -0.97; IR(cm $^{-1}$): 3861, 3652, 3060, 2962, 2905, 1684, 1601, 1491, 1450, 1348, 1291, 1250, 1213, 1005. HRMS (+ve ESI/APCI TOF, $C_{28}H_{29}NO_2Si(MH^+)$) Calcd 440.2040, Measured Mass 440.2054.

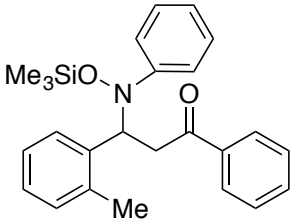

1-phenyl-3-(phenyl((trimethylsilyl)oxy)amino)-3-(*o*-tolyl)propan-1-one (14g):

(339.4 mg, 84% yield); ^{1}H NMR (500 MHz, Chloroform-*d*) δ 7.86 – 7.81 (m, 2H), 7.54 – 7.48 (m, 1H), 7.40 (dd, *J* = 8.4, 7.1 Hz, 2H), 7.34 – 7.28 (m, 1H), 7.28 – 7.19 (m, 5H), 7.17 – 7.06 (m, 3H), 6.99 (tt, *J* = 6.6, 2.1 Hz, 1H), 5.39 (dd, *J* = 9.1, 4.4 Hz, 1H), 3.92 (dd, *J* = 17.3, 9.0 Hz, 1H), 3.42 (dd, *J* = 17.3, 4.4 Hz, 1H), 2.51 (s, 3H), -0.26 (s, 9H); ^{13}C NMR (75 MHz, $CDCl_3$) δ 198.28, 152.65, 138.07, 137.26, 137.19, 132.80, 130.37, 128.40, 128.35, 128.21, 127.94, 127.47, 125.31, 123.34, 119.78, 65.05, 36.39, 19.76, -0.98; IR (cm^{-1}): 3027, 2954, 2893, 1687, 1597, 1487, 1450, 1339, 1291, 1258, 1213, 1021. HRMS (+ve ESI/APCI TOF, $C_{25}H_{29}NO_2Si(MH^+)$) Calcd 404.2040, Measured Mass 404.2052.

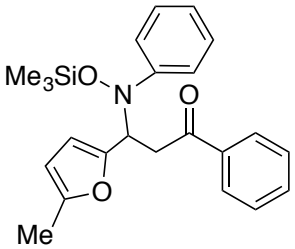

3-(5-methylfuran-2-yl)-1-phenyl-3-(phenyl((trimethylsilyl)oxy)amino)propan-1-one (14h):

(371.5 mg, 94% yield); ^{1}H NMR (300 MHz, Chloroform-*d*) δ 7.94 – 7.85 (m, 2H), 7.54 (ddt, *J* = 8.3, 6.6, 1.4 Hz, 1H), 7.47 – 7.38 (m, 2H), 7.31 – 7.14 (m, 5H), 7.06 – 6.99 (m, 1H), 6.02 (d, *J* = 3.1 Hz, 1H), 5.86 (dq, *J* = 3.1, 1.0 Hz, 1H), 5.15 (dd, *J* = 9.3, 4.1 Hz, 1H), 3.68 (dd, *J* = 17.0, 9.3 Hz, 1H),

3.41 (dd, *J* = 17.0, 4.1 Hz, 1H), 2.27 (d, *J* = 1.0 Hz, 3H), -0.03 (s, 9H); ^{13}C NMR (75 MHz, $CDCl_3$) δ 197.81, 151.74, 151.27, 150.95, 136.96, 132.92, 128.44, 128.25, 128.09, 123.30, 119.66, 109.44, 106.19, 63.29, 35.61, 13.58, -0.91; IR(cm^{-1}): 3068, 2966, 1691, 1601, 1491, 1450, 1344, 1250, 1221, 1070. HRMS (+ve ESI/APCI TOF, $C_{23}H_{27}NO_3Si(MH^+)$) Calcd 394.1833, Measured Mass 394.1846.

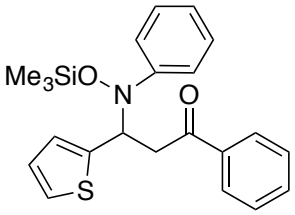

1-phenyl-3-(phenyl((trimethylsilyl)oxy)amino)-3-(thiophen-2-yl)propan-1-one (24i)

(301.0 mg, 76% yield); ^{1}H NMR (300 MHz, Chloroform-*d*) δ 7.96 – 7.87 (m, 2H), 7.59 – 7.50 (m, 1H), 7.50 – 7.39 (m, 2H), 7.28 – 7.08 (m, 5H), 7.04 – 6.95 (m, 1H), 6.88 – 6.73 (m, 2H), 5.42 – 5.33 (m, 1H), 3.65 (dd, *J* = 6.6, 1.7 Hz, 2H), -0.01 (s, 9H); ^{13}C NMR (75 MHz, $CDCl_3$) δ 197.28, 151.96, 141.49, 136.98, 133.04, 128.54, 128.17, 128.04, 126.59, 125.86, 125.07, 123.59, 120.02, 65.20, -0.61; IR(cm^{-1}): 3068, 2958, 1683, 1597, 1486, 1450, 1352, 1287, 1254, 1217. HRMS (+ve ESI/APCI TOF, $C_{22}H_{25}NO_2SSi(MH^+)$ Calcd 396.1448, Measured Mass 396.1456.

---

[i] Kang, Y. B.; Sun, X. L.; Tang, Y. *Angew. Chem. Int. Ed.* **2007**, *46*, 3918-3921.

[ii] A peak for the ^{13}C NMR in $CDCl_3$ was obscured under the $CDCl_3$ peaks. It was confirmed by ^{13}C NMR in C_6D_6 at 77.12 ppm.

[iii] Sapeta, K.; Kerr, M. A. *J. Org. Chem.* **2007**, *72*, 8597-8599.

[iv] Downey, C. W.; Dombrowski, C. M.; Maxwell, E. N.; Safran, C. L.; Akomah, O. A. *Eur. J. Org. Chem.* **2013**, 25, 5716–5720.

[v] Ito, S.; Kubota, Y.; Asami, M. *Tetrahedron Lett.* **2014**, *55*, 4930-4932.

3. Spectral Data

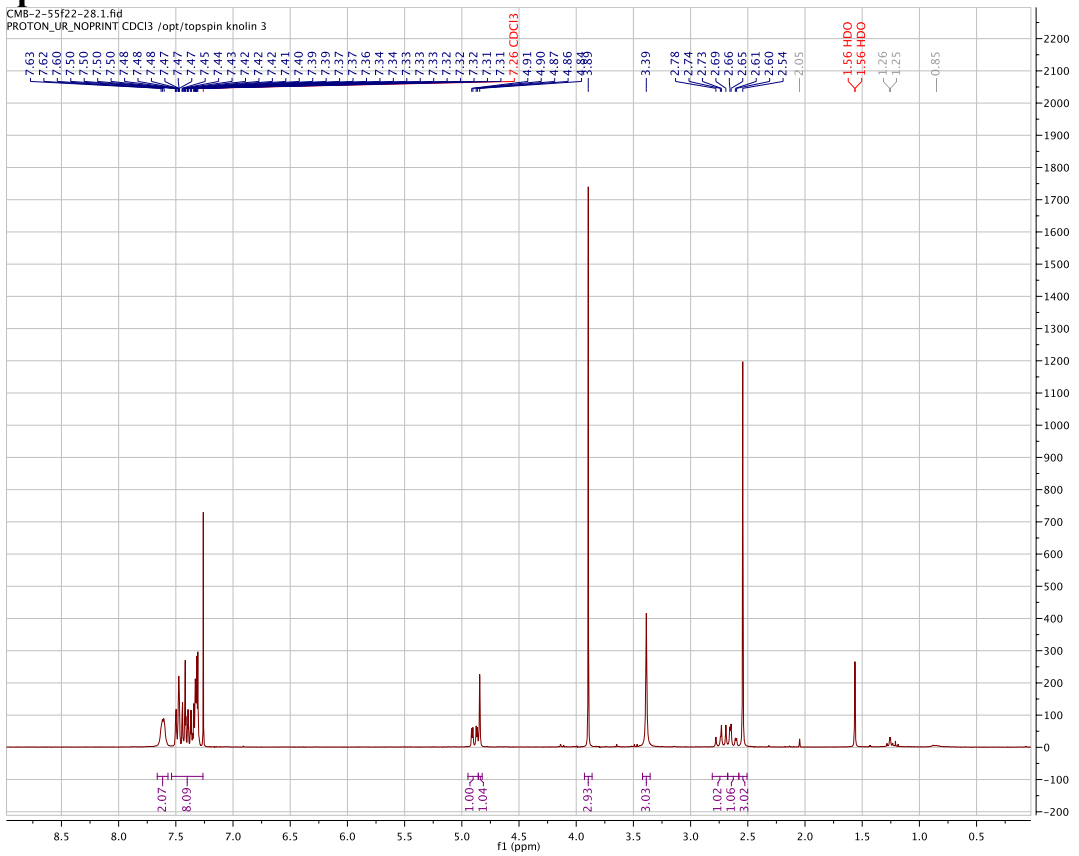

3

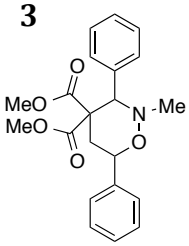

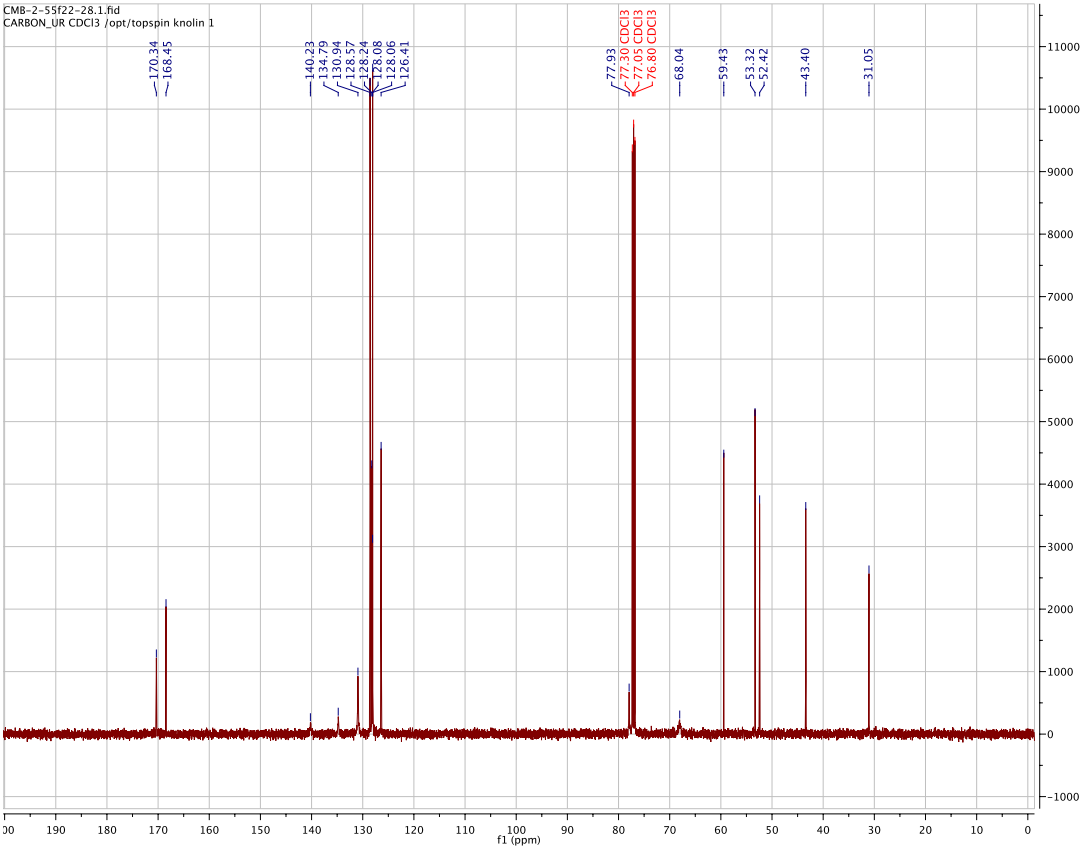

10a

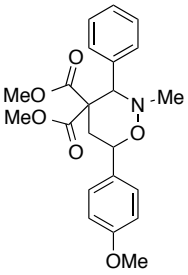
MeO
MeO
O
O
N
Me
O
OMe

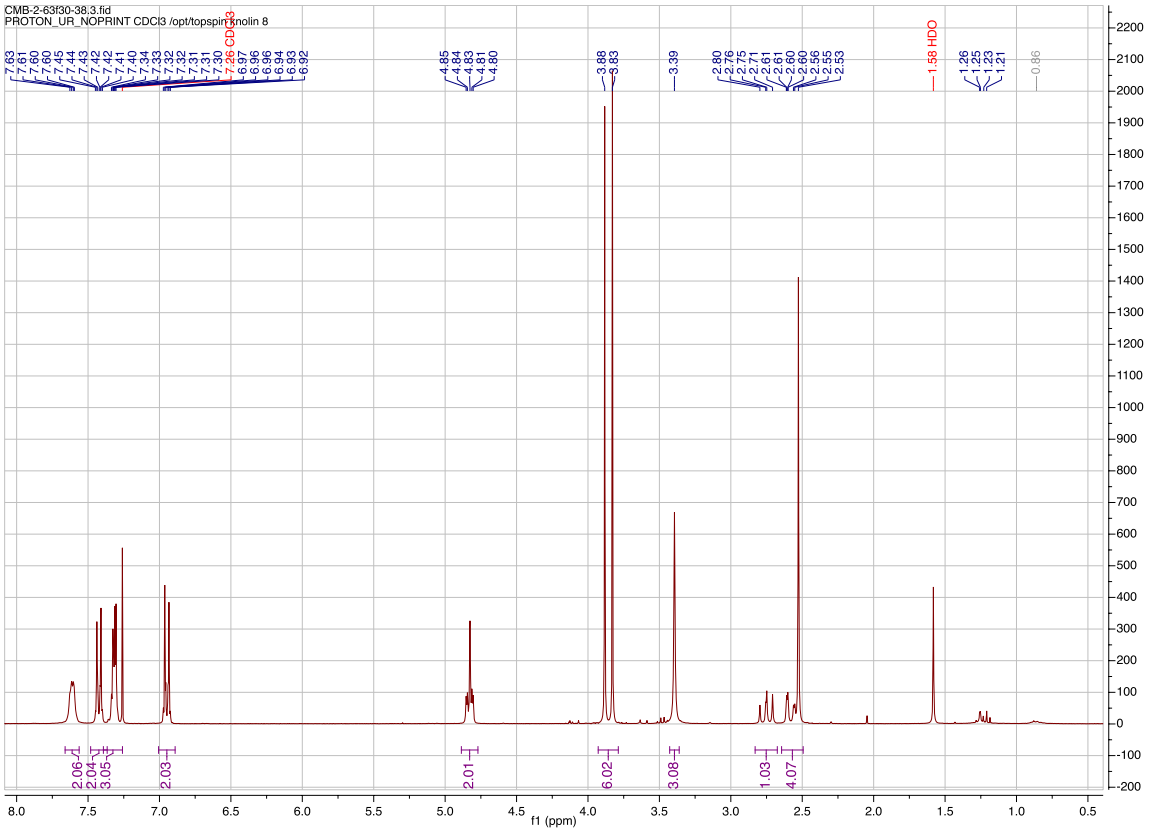
CMB-2-63f30-38.3.fid
PROTON_UR_NOPRINT CDCl3 /opt/topspin knolin 8
7.63
7.61
7.60
7.45
7.44
7.43
7.42
7.42
7.41
7.40
7.34
7.33
7.32
7.32
7.31
7.31
7.30
7.26 CDCl3
6.97
6.96
6.96
6.94
6.93
6.92
4.85
4.84
4.83
4.81
4.80
3.88
3.83
3.39
2.80
2.76
2.75
2.71
2.61
2.61
2.60
2.60
2.56
2.55
2.53
1.58 HDO
1.26
1.25
1.23
1.21
0.86
2.06
2.04
3.05
2.03
2.01
6.02
3.08
1.03
4.07
f1 (ppm)

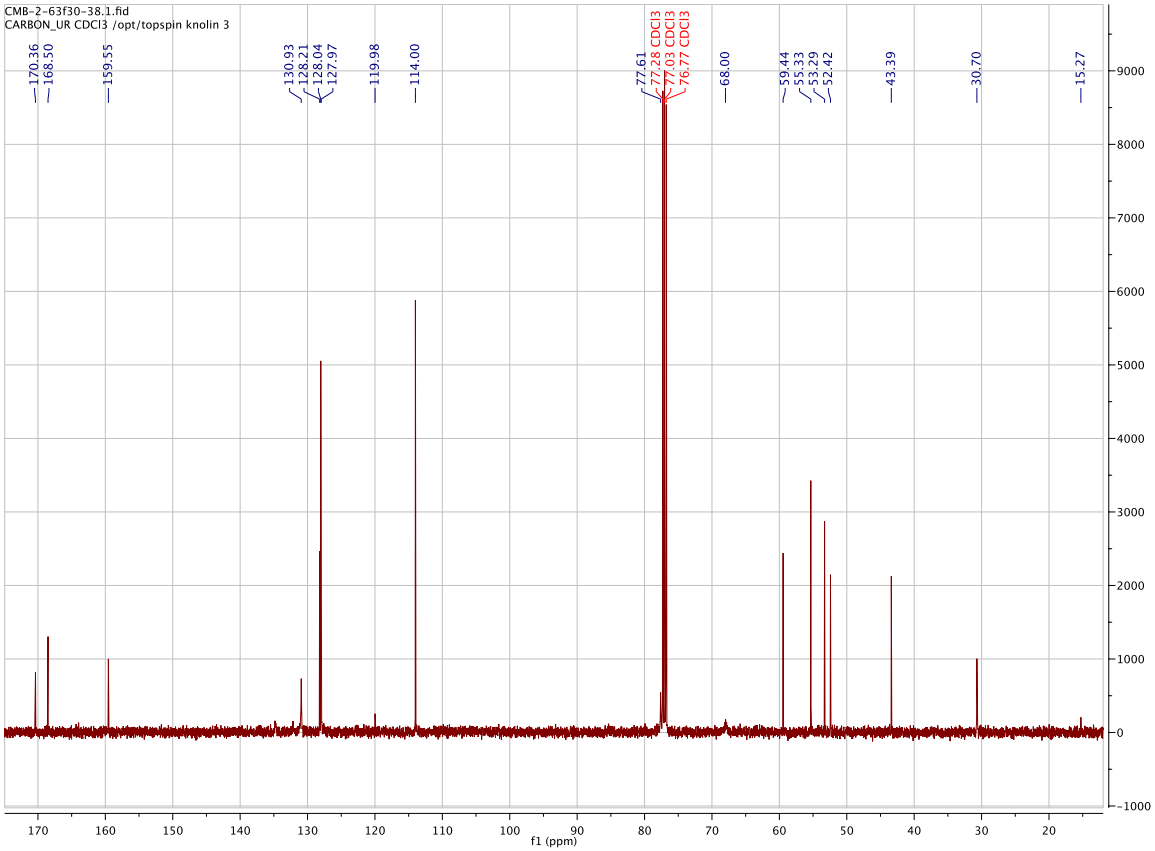
CMB-2-63f30-38.1.fid
CARBON_UR CDCl3 /opt/topspin knolin 3
170.36
168.50
159.55
130.93
128.21
128.04
127.97
119.98
114.00
77.61
77.28 CDCl3
77.03 CDCl3
76.77 CDCl3
68.00
59.44
55.33
53.29
52.42
43.39
30.70
15.27
f1 (ppm)

10b

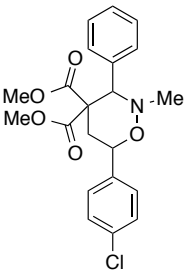
MeO
MeO
O
O
N
Me
O
Cl

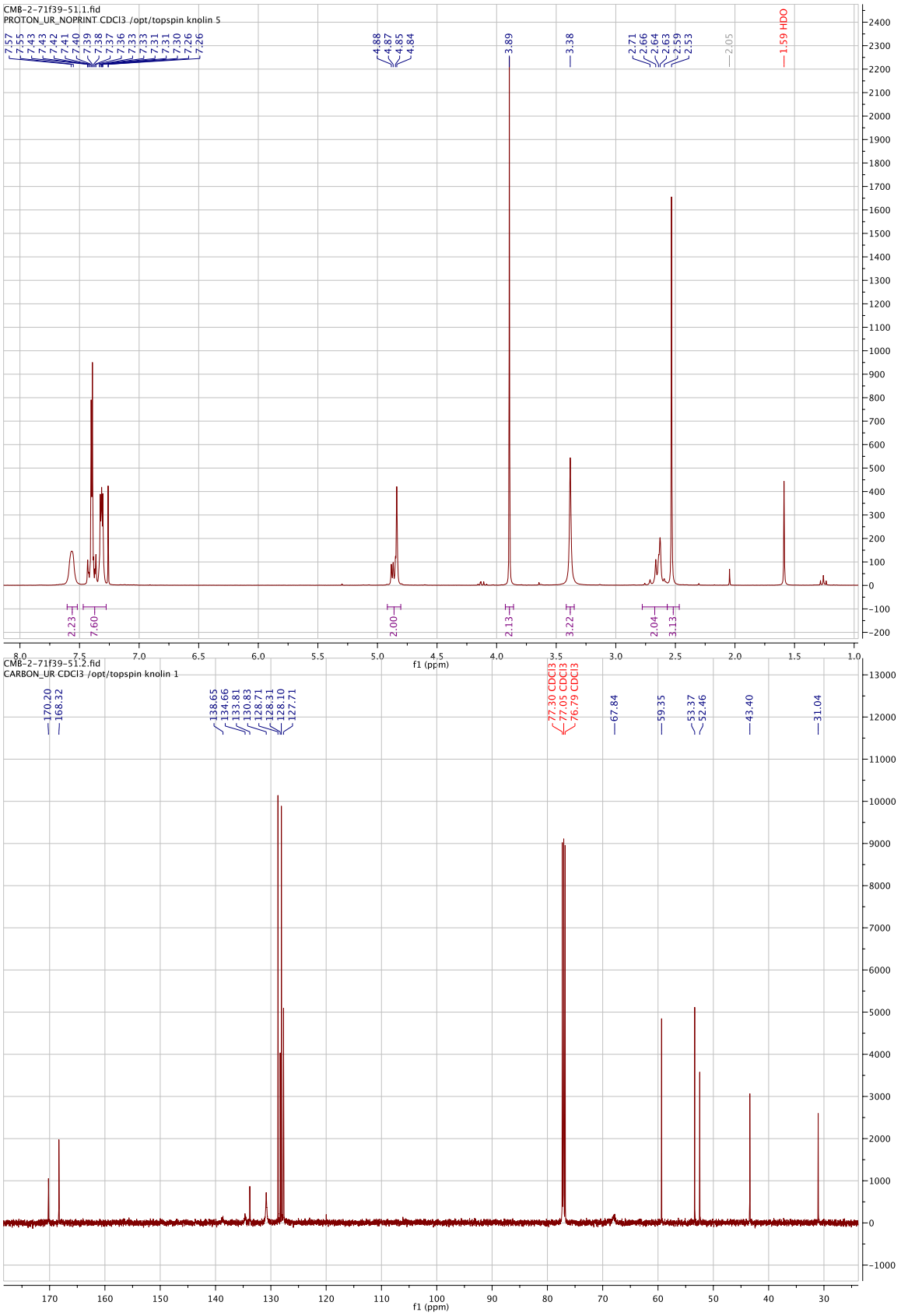
CMB-2-71f39-51.1.fid
PROTON_UR_NOPRINT CDCl3 /opt/topspin knolin 5
7.57
7.55
7.43
7.43
7.42
7.41
7.40
7.39
7.38
7.37
7.36
7.33
7.33
7.31
7.31
7.30
7.26
7.26
4.88
4.87
4.85
4.84
3.89
3.38
2.71
2.66
2.64
2.63
2.59
2.53
2.05
1.59 HDO
2.23
7.60
2.00
2.13
3.22
2.04
3.13
f1 (ppm)
CMB-2-71f39-51.2.fid
CARBON_UR CDCl3 /opt/topspin knolin 1
170.20
168.32
138.65
134.66
133.81
130.83
128.71
128.31
128.10
127.71
77.30 CDCl3
77.05 CDCl3
76.79 CDCl3
67.84
59.35
53.37
52.46
43.40
31.04
f1 (ppm)

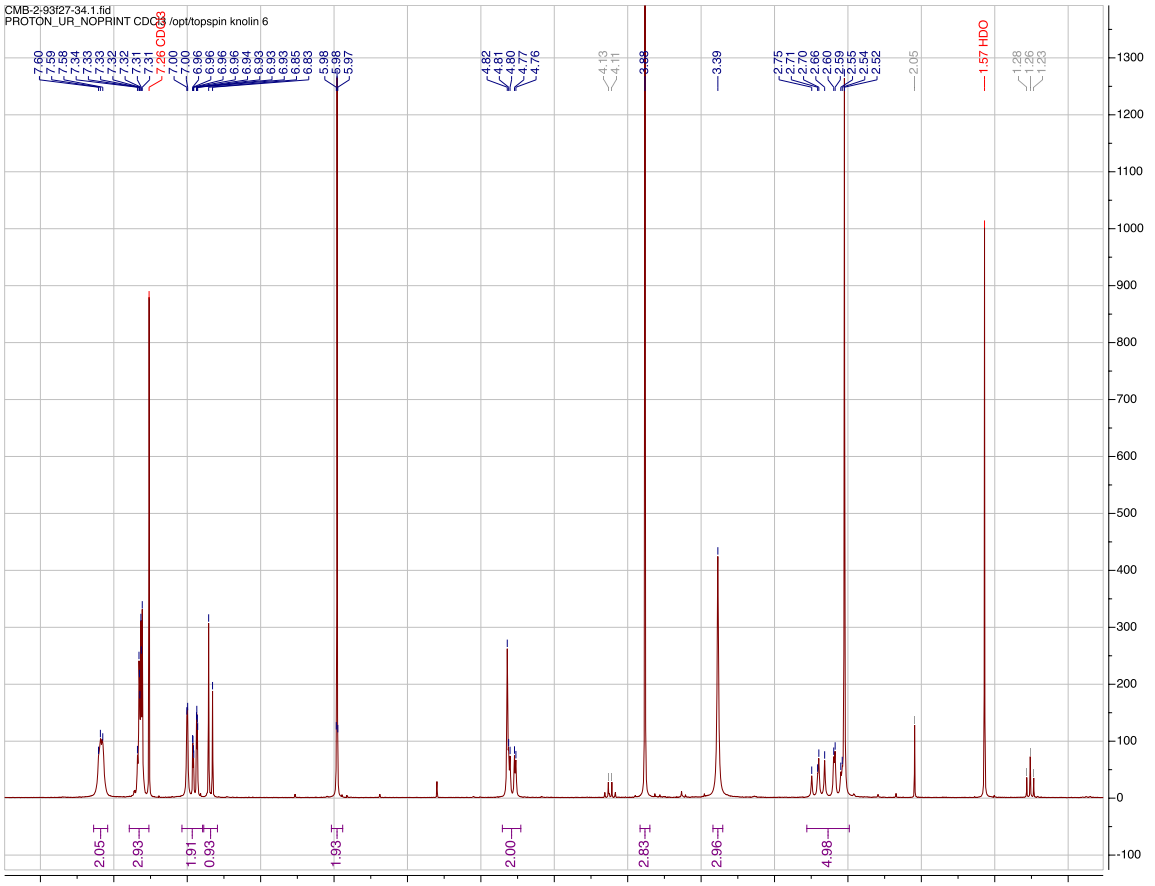
CMB-2-93f27-34.1.fid
PROTON_UR_NOPRINT CDCl3 /opt/topspin knolin 6
7.60
7.59
7.58
7.34
7.33
7.32
7.32
7.31
7.31
7.26 CDCl3
7.00
7.00
6.96
6.96
6.96
6.96
6.94
6.93
6.93
6.85
6.83
5.98
5.98
5.97
4.82
4.81
4.80
4.77
4.76
4.13
4.11
3.88
3.39
2.75
2.71
2.70
2.66
2.60
2.59
2.55
2.54
2.52
2.05
1.57 HDO
1.28
1.26
1.23
2.05
2.93
1.91
0.93
1.93
2.00
2.83
2.96
4.98
f1 (ppm)

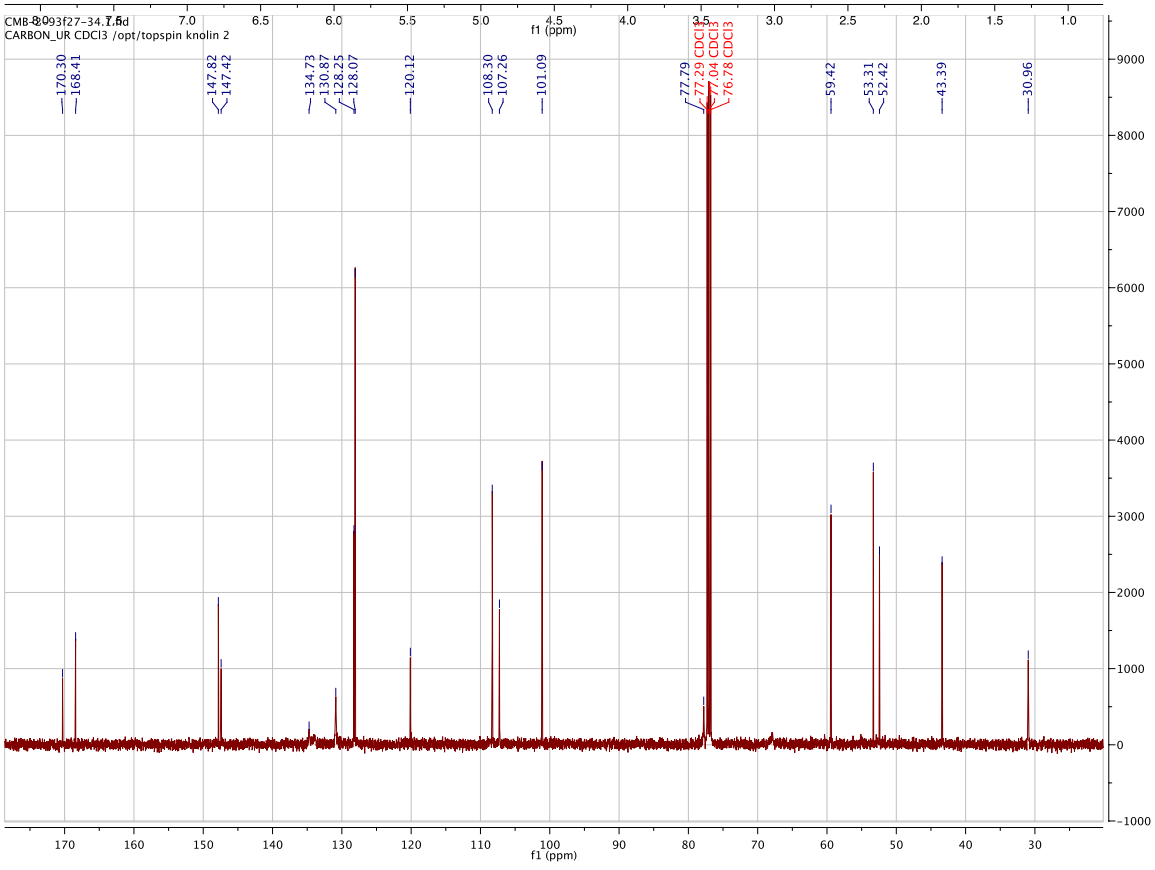
CMB-2-93f27-34.1.fid
CARBON_UR CDCl3 /opt/topspin knolin 2
170.30
168.41
147.82
147.42
134.73
130.87
128.25
128.07
120.12
108.30
107.26
101.09
77.79
77.29 CDCl3
77.04 CDCl3
76.78 CDCl3
59.42
53.31
52.42
43.39
30.96
f1 (ppm)

10c

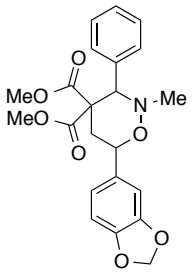
MeO
MeO
N
Me
O
O
O
O
O

5

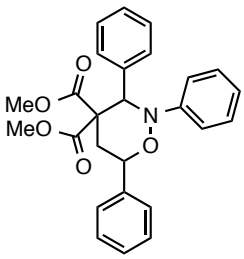
MeO
MeO
O
O
N
O

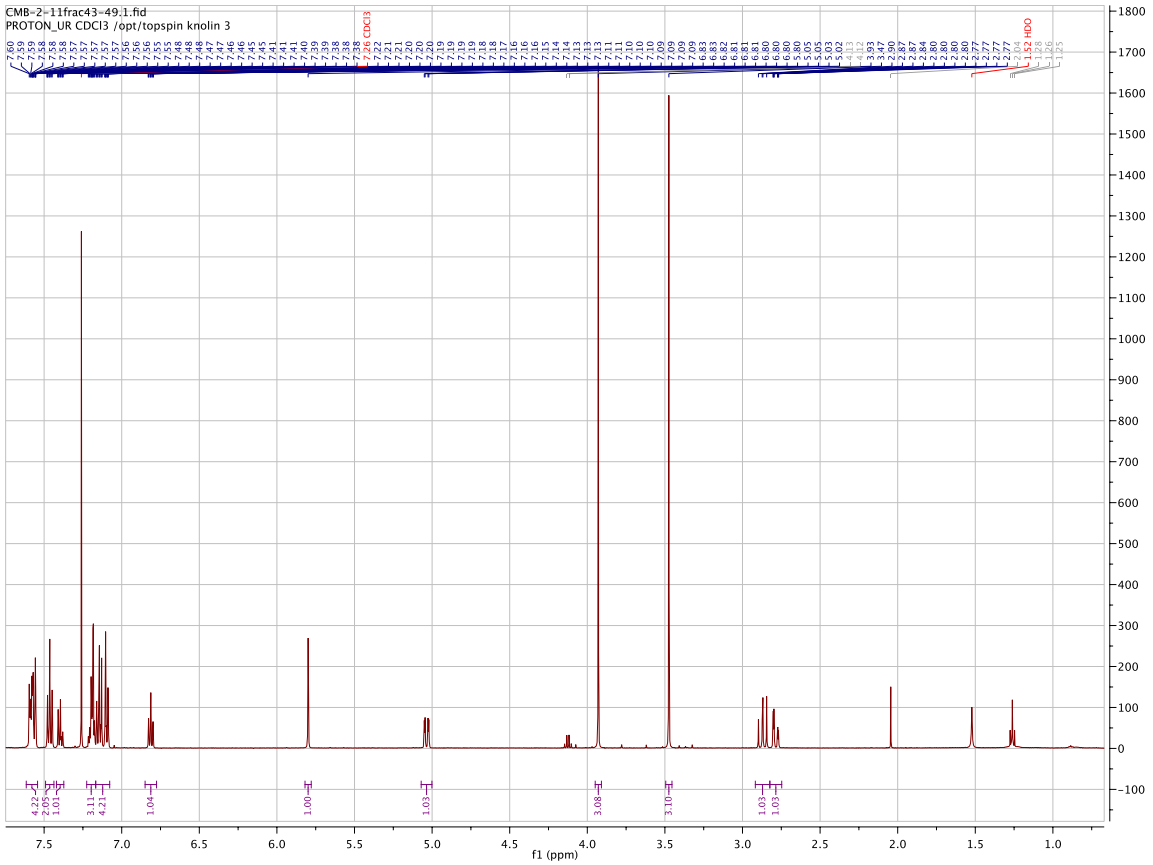
CMB-2-11frac43-49.1.fid
PROTON_UR CDCl3 /opt/topspin knolin 3
7.26 CDCl3
1.62 HDO
f1 (ppm)

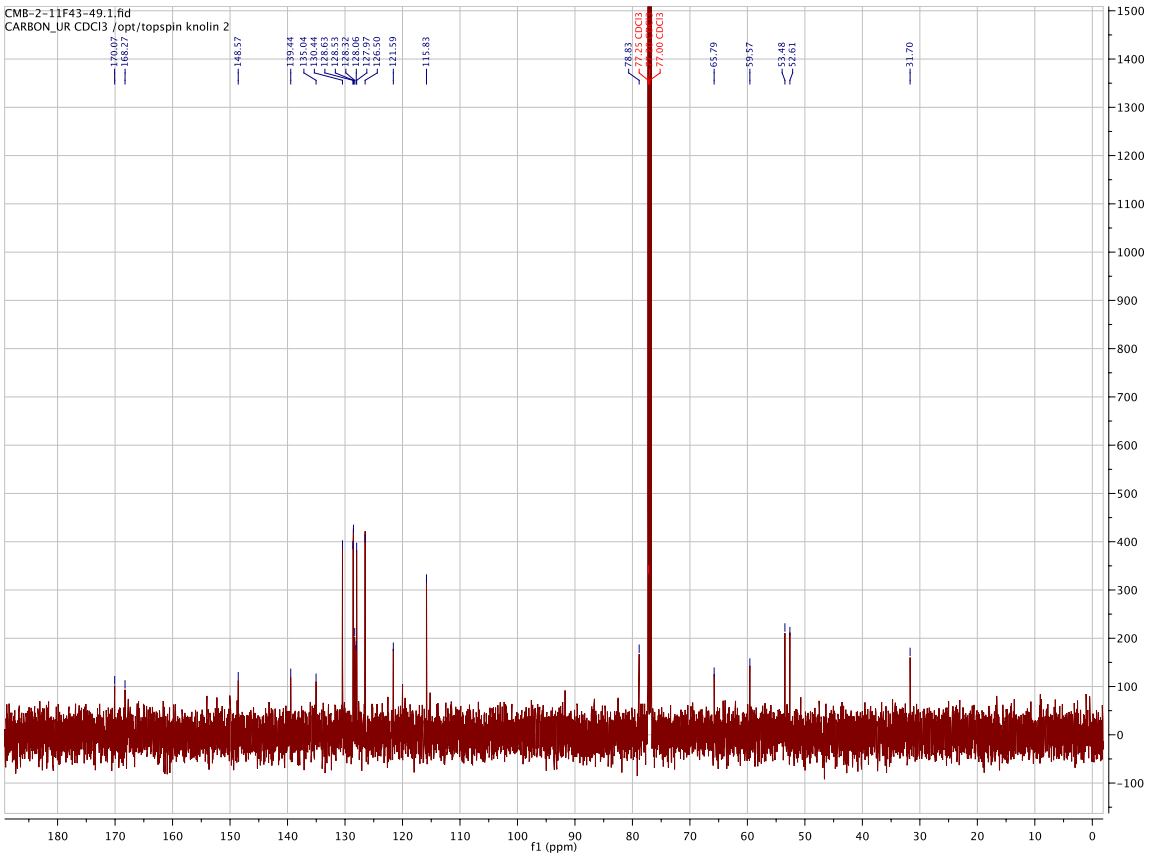
CMB-2-11F43-49.1.fid
CARBON_UR CDCl3 /opt/topspin knolin 2
170.07
168.27
148.57
139.44
135.04
130.44
129.63
128.53
128.32
128.06
127.57
126.50
121.59
115.83
78.83
77.25 CDCl3
77.00 CDCl3
65.79
59.57
53.48
52.61
31.70
f1 (ppm)

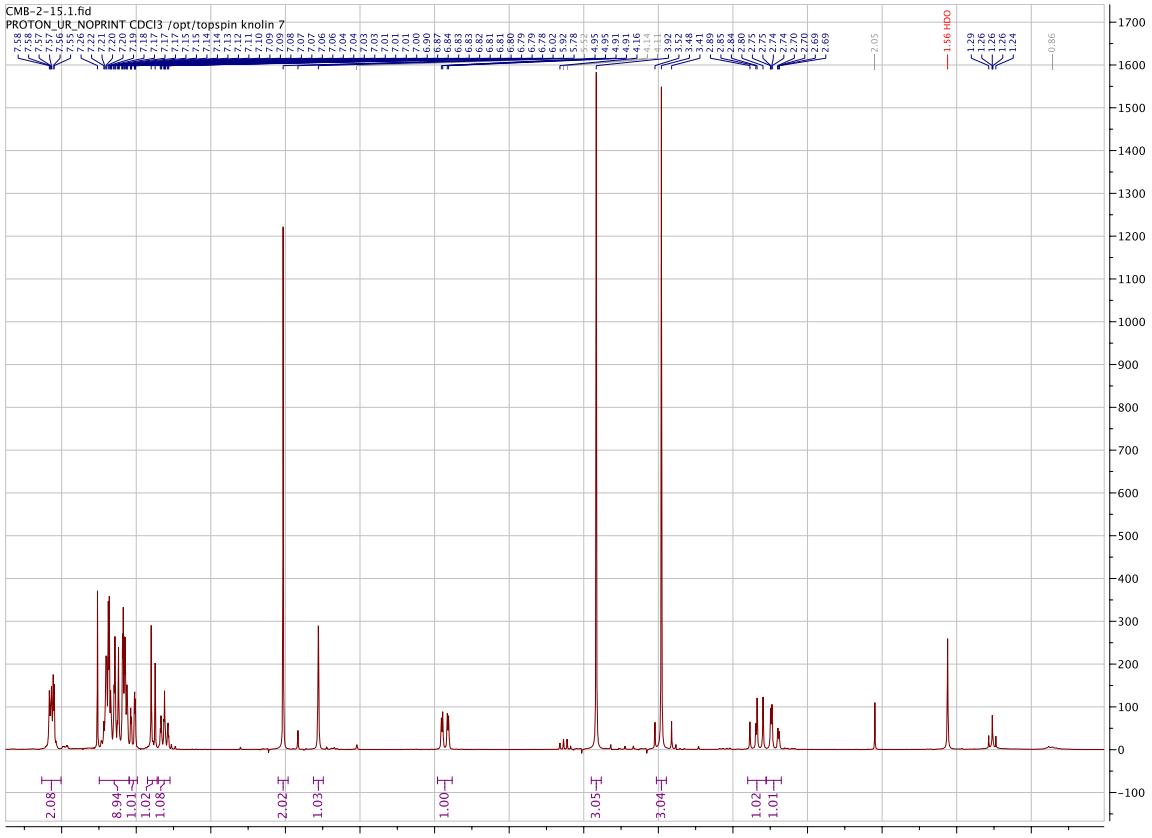
CMB-2-15.1.fid
PROTON_UR_NOPRINT CDCl3 /opt/topspin knolin 7
1.56 HDO
2.05
0.86
2.08
8.94
1.01
1.02
1.08
2.02
1.03
1.00
3.05
3.04
1.02
1.01
f1 (ppm)

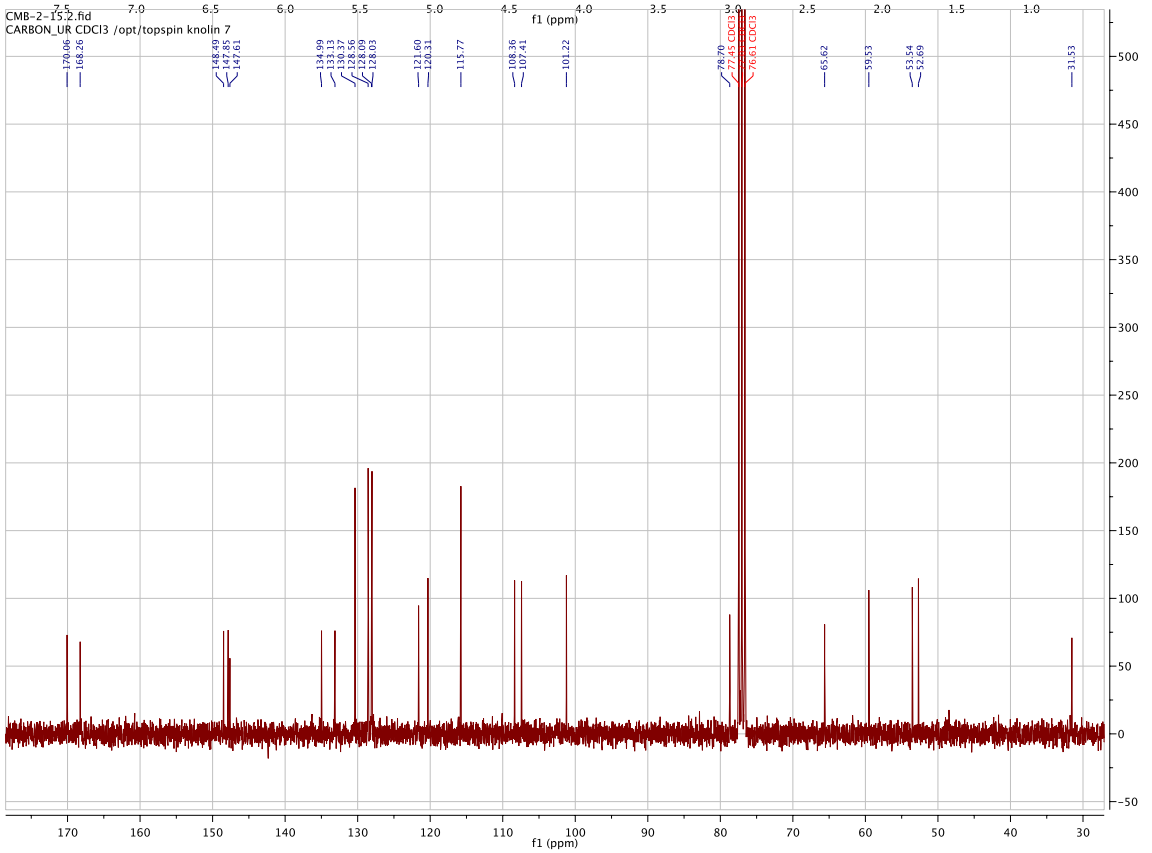
CMB-2-15.2.fid
CARBON_UR CDCl3 /opt/topspin knolin 7
170.06
168.26
148.49
147.85
147.61
134.99
133.13
130.37
128.56
128.03
121.60
120.31
115.77
108.36
107.41
101.22
78.70
77.45 CDCl3
76.61 CDCl3
65.62
59.53
53.54
52.69
31.53
f1 (ppm)

7a

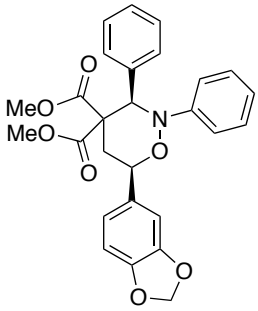
MeO
MeO
O
O
O
N
O
O
O

7b

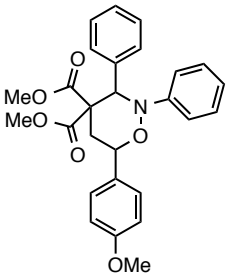
O
MeO
MeO
N
O
O
OMe

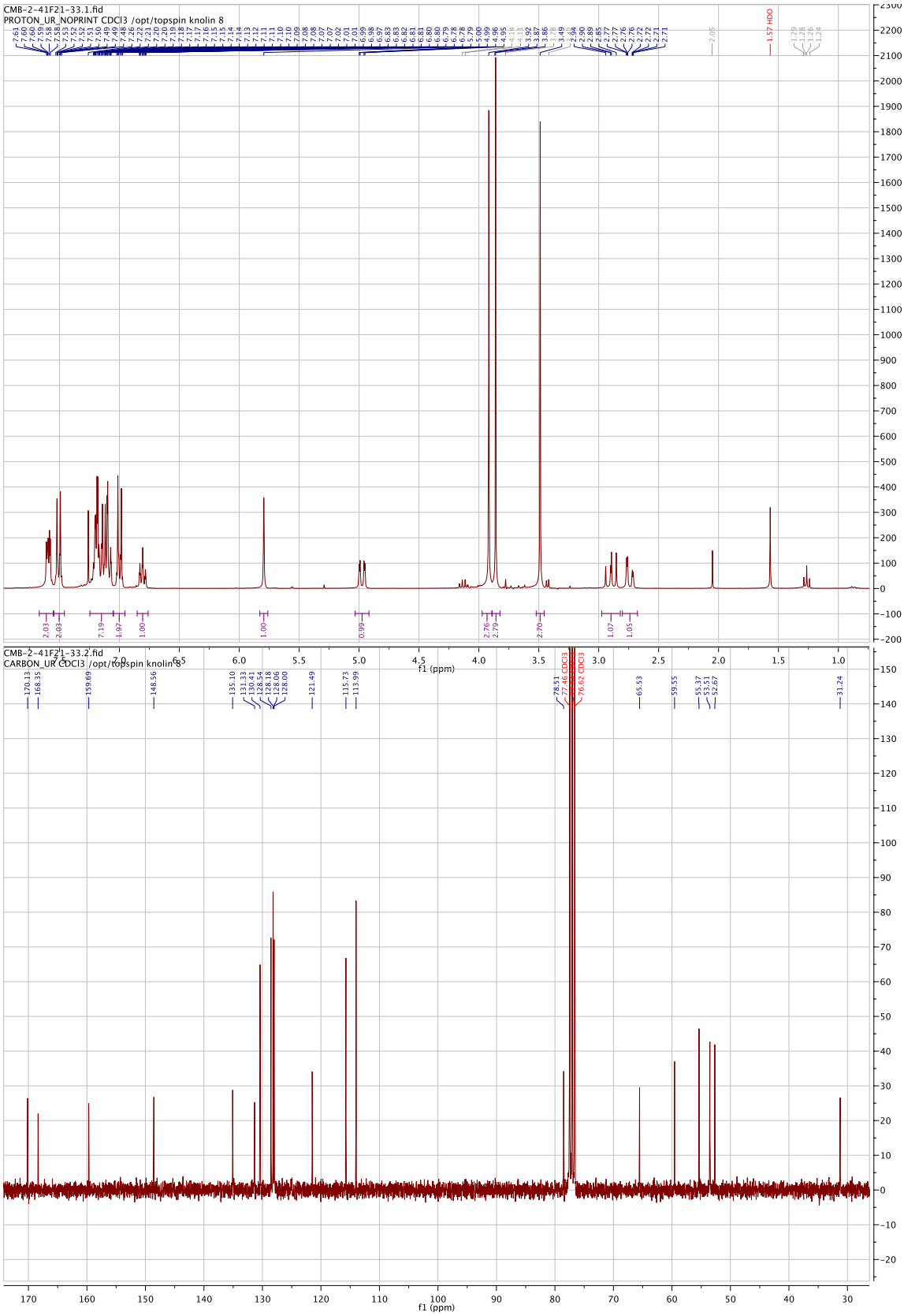
CMB-2-41F21-33.1.fid
PROTON_UR_NOPRINT CDCl3 /opt/topspin knolin 8
1.57 HDO
2.05
2.03
2.03
7.19
1.97
1.00
1.00
0.99
2.76
2.79
2.70
1.07
1.05
f1 (ppm)
CMB-2-41F21-33.2.fid
CARBON_UR CDCl3 /opt/topspin knolin 8
170.13
168.35
159.69
148.56
135.10
131.33
130.41
128.54
126.48
128.06
128.00
121.49
115.73
113.99
78.51
77.46 CDCl3
77.04 CDCl3
76.62 CDCl3
65.53
59.55
55.37
53.51
52.67
31.24
f1 (ppm)

7c

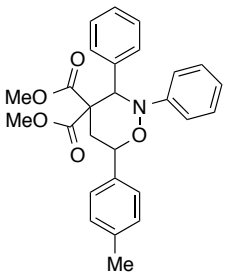
O
MeO
MeO
O
N
O
Me

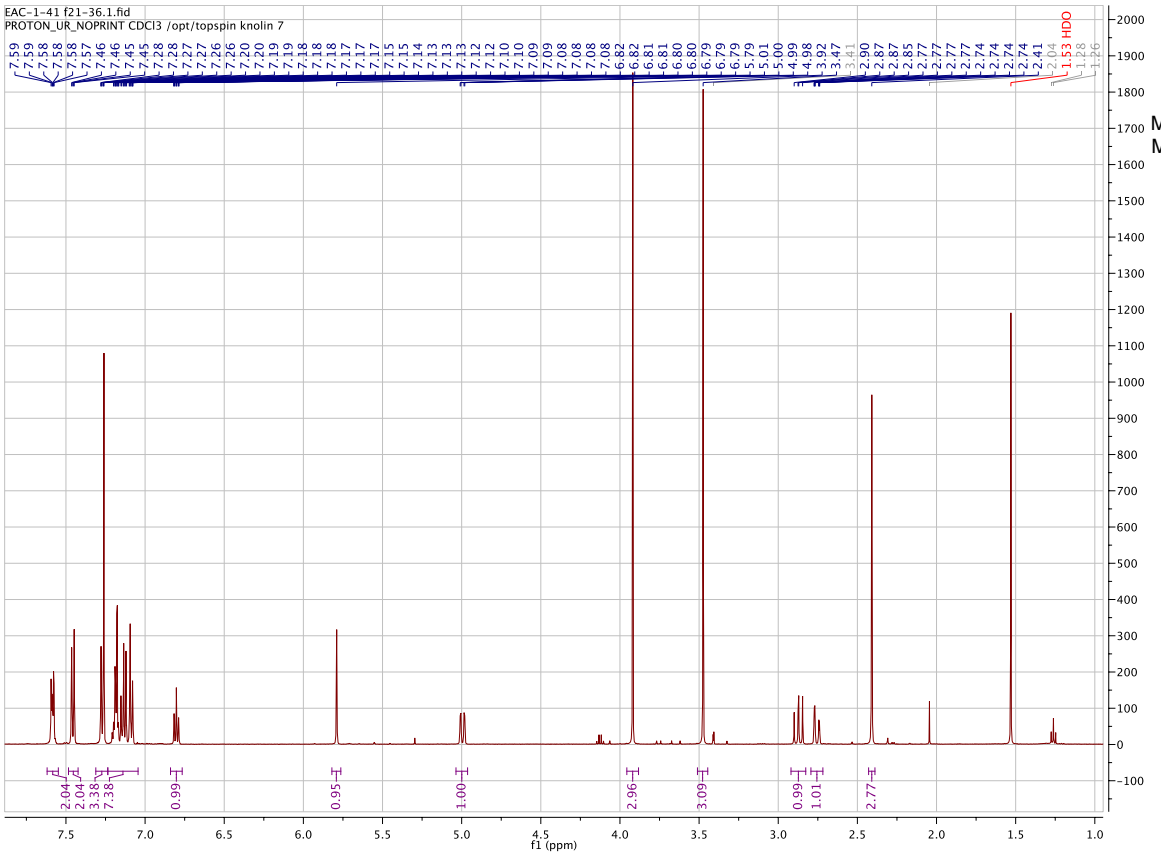
EAC-1-41 f21-36.1.fid
PROTON_UR_NOPRINT CDCl3 /opt/topspin knolin 7
1.53 HDO
2.04
2.04
3.38
7.38
0.99
0.95
1.00
2.96
3.09
0.99
1.01
2.77
f1 (ppm)

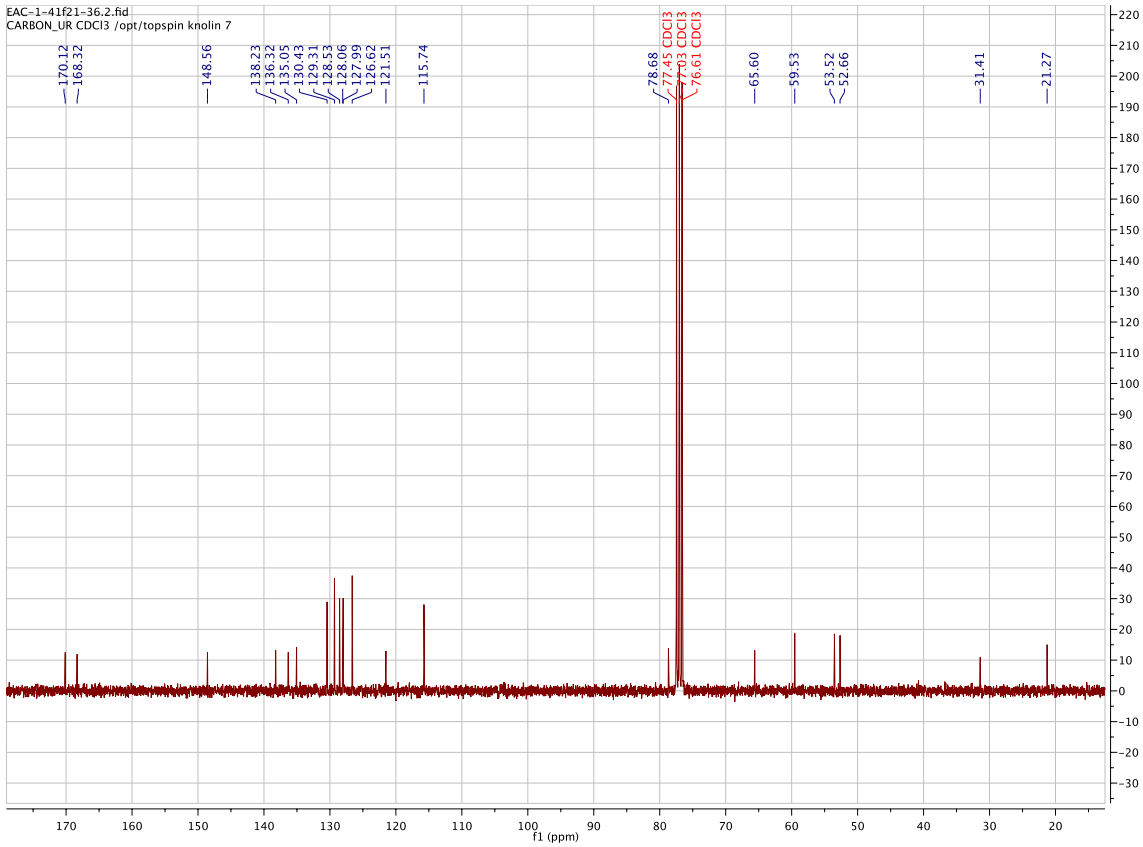
EAC-1-41f21-36.2.fid
CARBON_UR CDCl3 /opt/topspin knolin 7
170.12
168.32
148.56
138.23
136.32
135.05
130.43
129.31
128.53
128.06
127.99
126.62
121.51
115.74
78.68
77.45 CDCl3
77.03 CDCl3
76.61 CDCl3
65.60
59.53
53.52
52.66
31.41
21.27
f1 (ppm)

7d

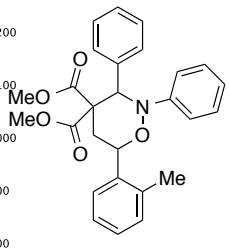
MeO
MeO
O
O
O
N
O
Me

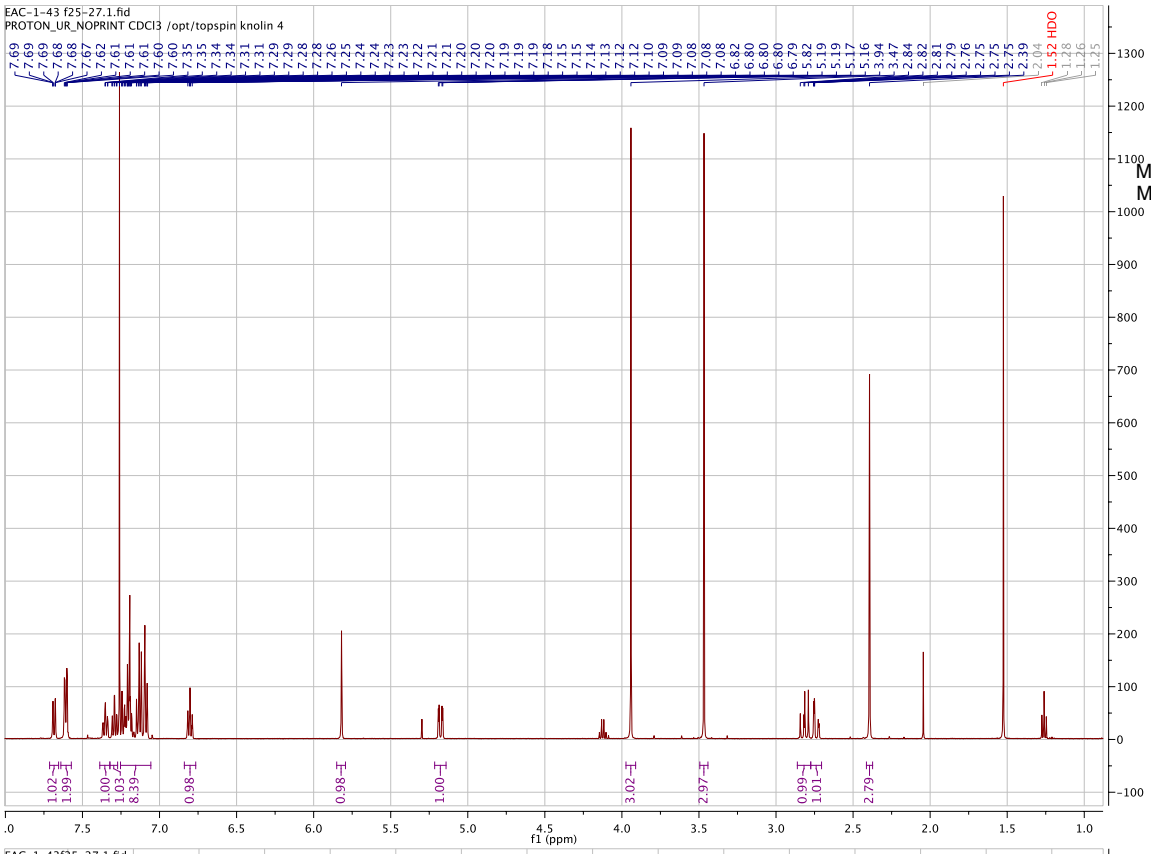
EAC-1-43 f25-27.1.fid
PROTON_UR_NOPRINT CDCl3 /opt/topspin knolin 4
1.52 HDO
1.02
1.99
1.00
1.03
8.39
0.98
0.98
1.00
3.02
2.97
0.99
1.01
2.79
f1 (ppm)

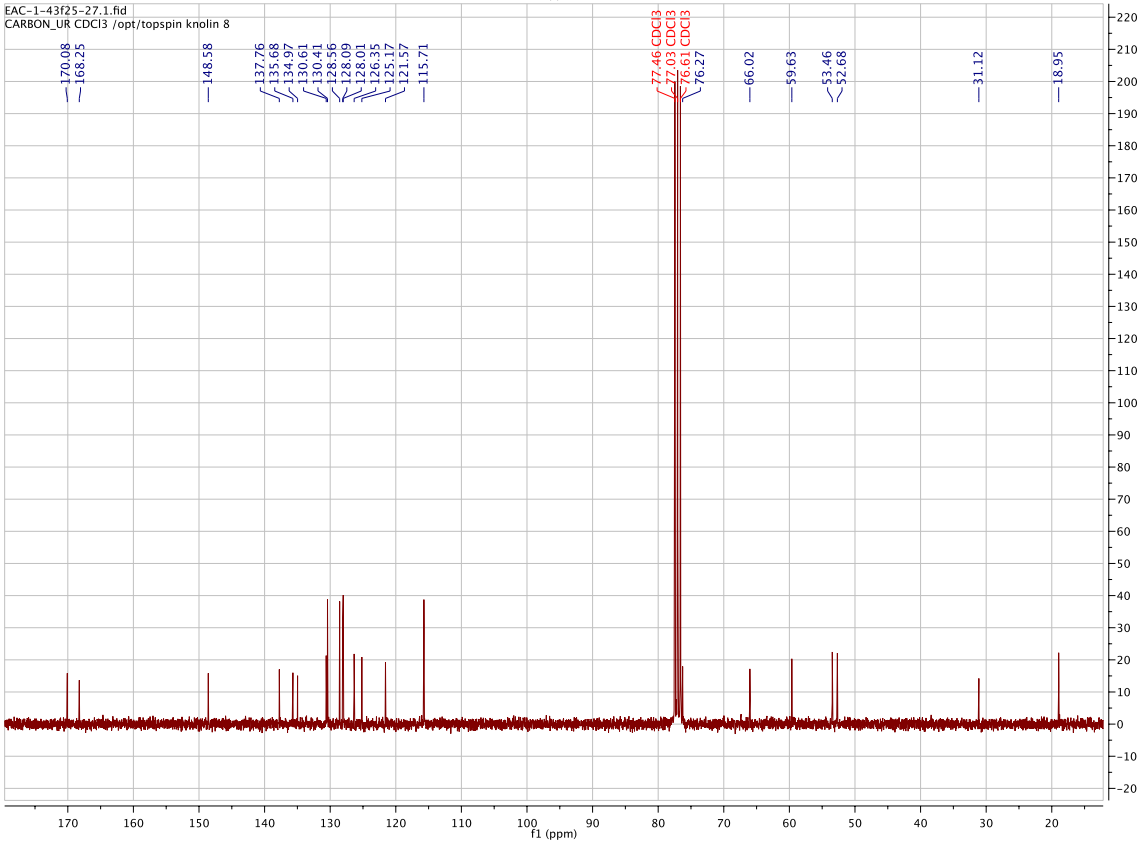
EAC-1-43f25-27.1.fid
CARBON_UR CDCl3 /opt/topspin knolin 8
170.08
168.25
148.58
137.76
135.68
134.97
130.61
130.41
128.56
128.09
128.01
126.35
125.17
121.57
115.71
77.46 CDCl3
77.03 CDCl3
76.61 CDCl3
76.27
66.02
59.63
53.46
52.68
31.12
18.95
f1 (ppm)

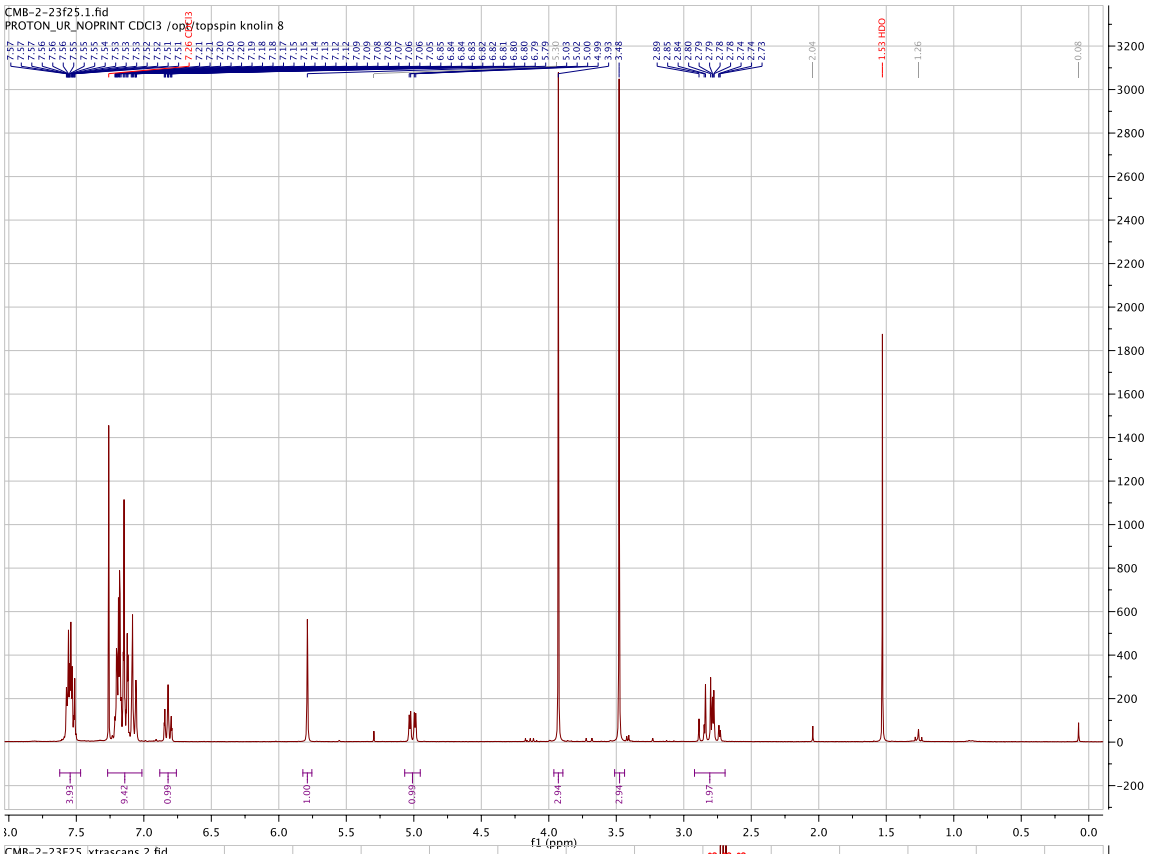
CMB-2-23f25.1.fid
PROTON_UR_NOPRINT CDCl3 /opt/topspin knolin 8
f1 (ppm)

7e

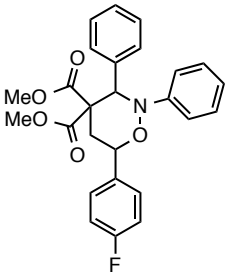
MeO
MeO
O
O
O
N
O
F

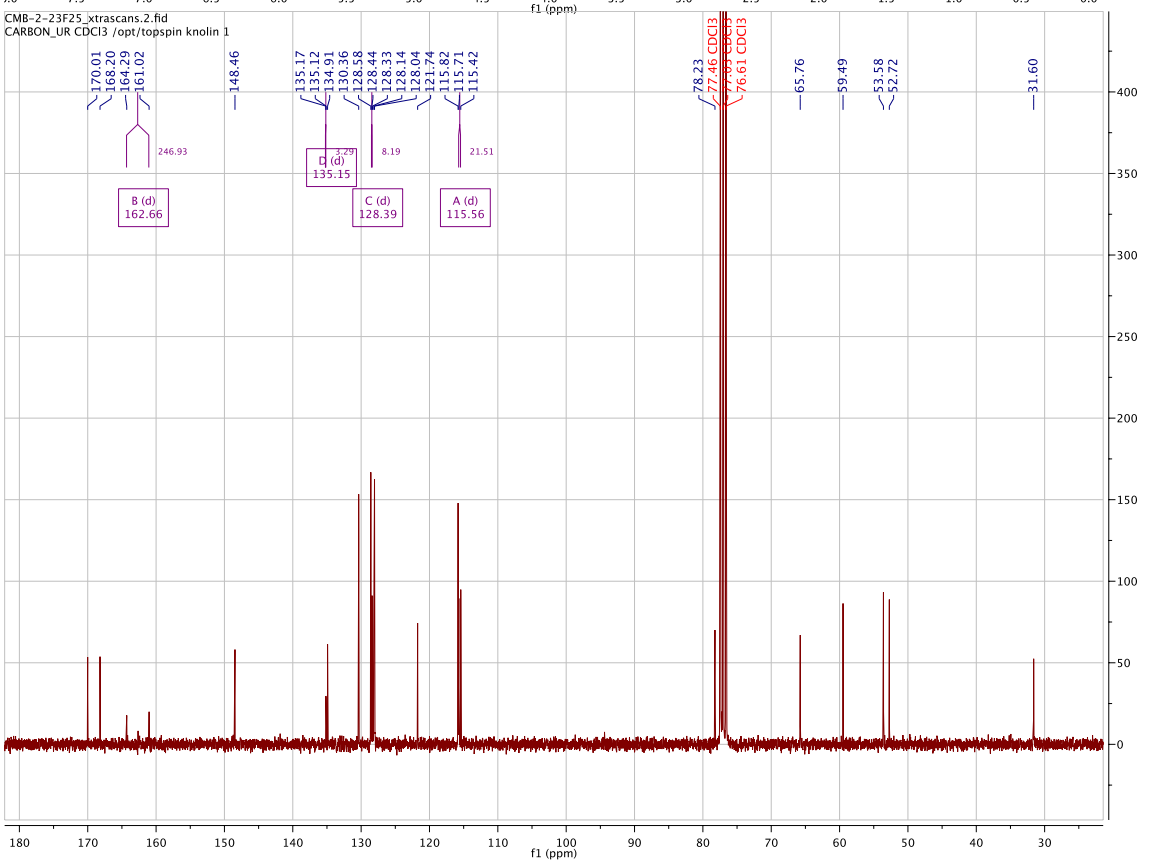
CMB-2-23F25_xtrascans.2.fid
CARBON_UR CDCl3 /opt/topspin knolin 1
170.01
168.20
164.29
161.02
148.46
135.17
135.12
134.91
130.36
128.58
128.44
128.33
128.14
128.04
121.74
115.82
115.71
115.42
78.23
77.46 CDCl3
77.03 CDCl3
76.61 CDCl3
65.76
59.49
53.58
52.72
31.60
246.93
3.29
8.19
21.51
B (d)
162.66
D (d)
135.15
C (d)
128.39
A (d)
115.56
f1 (ppm)

7f

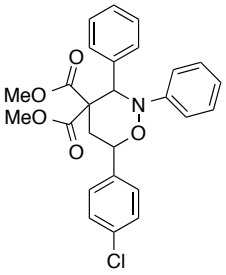
MeO
MeO
O
O
N
O
O
Cl

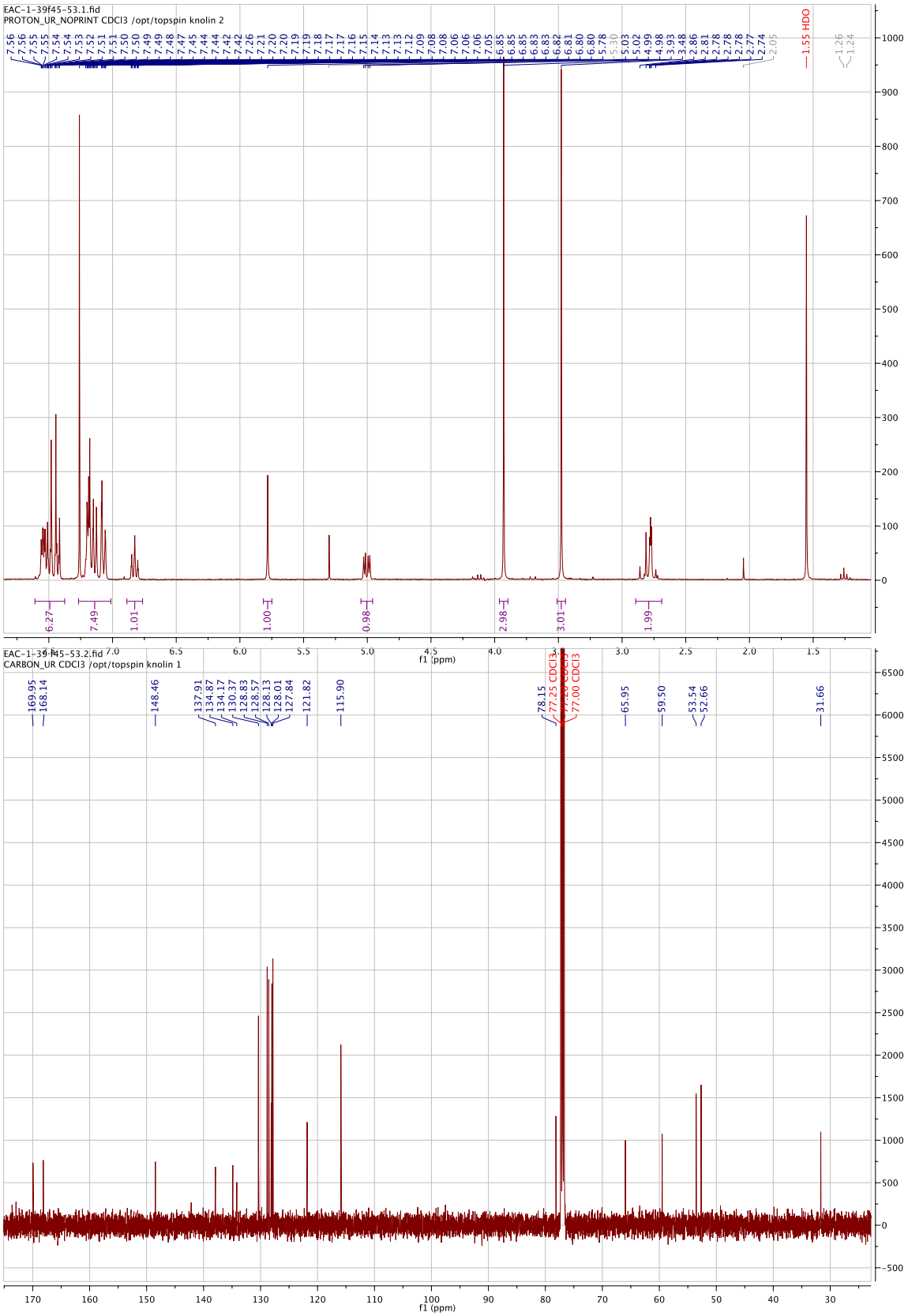
EAC-1-39f45-53.1.fid
PROTON_UR_NOPRINT CDCl3 /opt/topspin knolin 2
1.55 HDO
6.27
7.49
1.01
1.00
0.98
2.98
3.01
1.99
f1 (ppm)
EAC-1-39f45-53.2.fid
CARBON_UR CDCl3 /opt/topspin knolin 1
169.95
168.14
148.46
137.91
134.87
134.17
130.37
128.83
128.57
128.13
128.01
127.84
121.82
115.90
78.15
77.25 CDCl3
77.00 CDCl3
65.95
59.50
53.54
52.66
31.66
f1 (ppm)

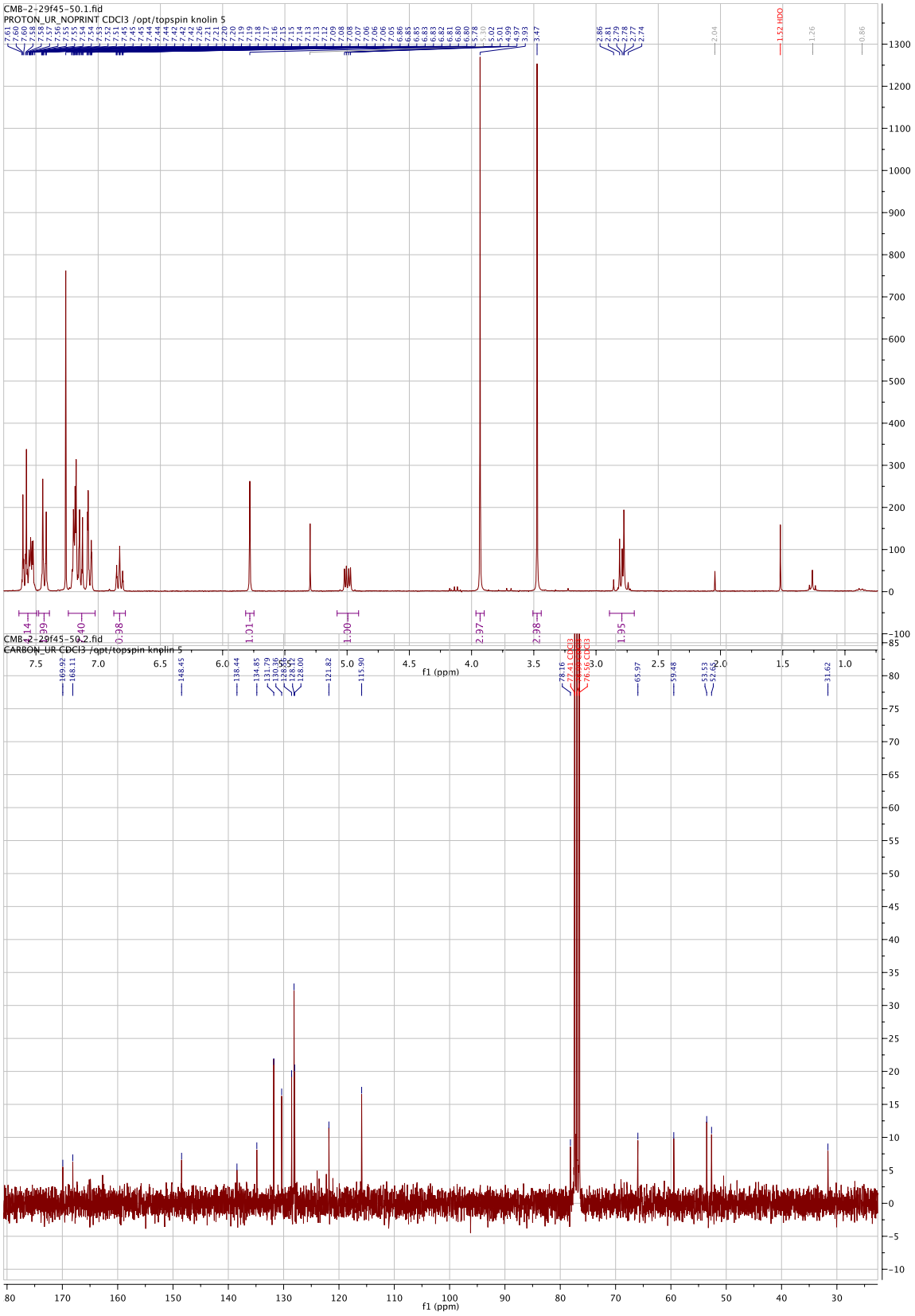
CMB-2-29f45-50.1.fid
PROTON_UR_NOPRINT CDCl3 /opt/topspin knolin 5
CMB-2-29f45-50.2.fid
CARBON_UR CDCl3 /opt/topspin knolin 5
f1 (ppm)

7g

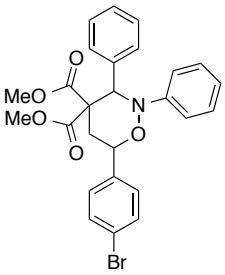
MeO
MeO
O
O
O
N
O
Br


CMB-2-31F41-49.1.fid
PROTON_UR_NOPRINT CDCl3 /opt/topspin knolin 5
1.55 HDO
2.10
7.66
1.05
1.04
1.02
1.00
1.00
3.06
3.11
1.02
1.02
2.99
f1 (ppm)

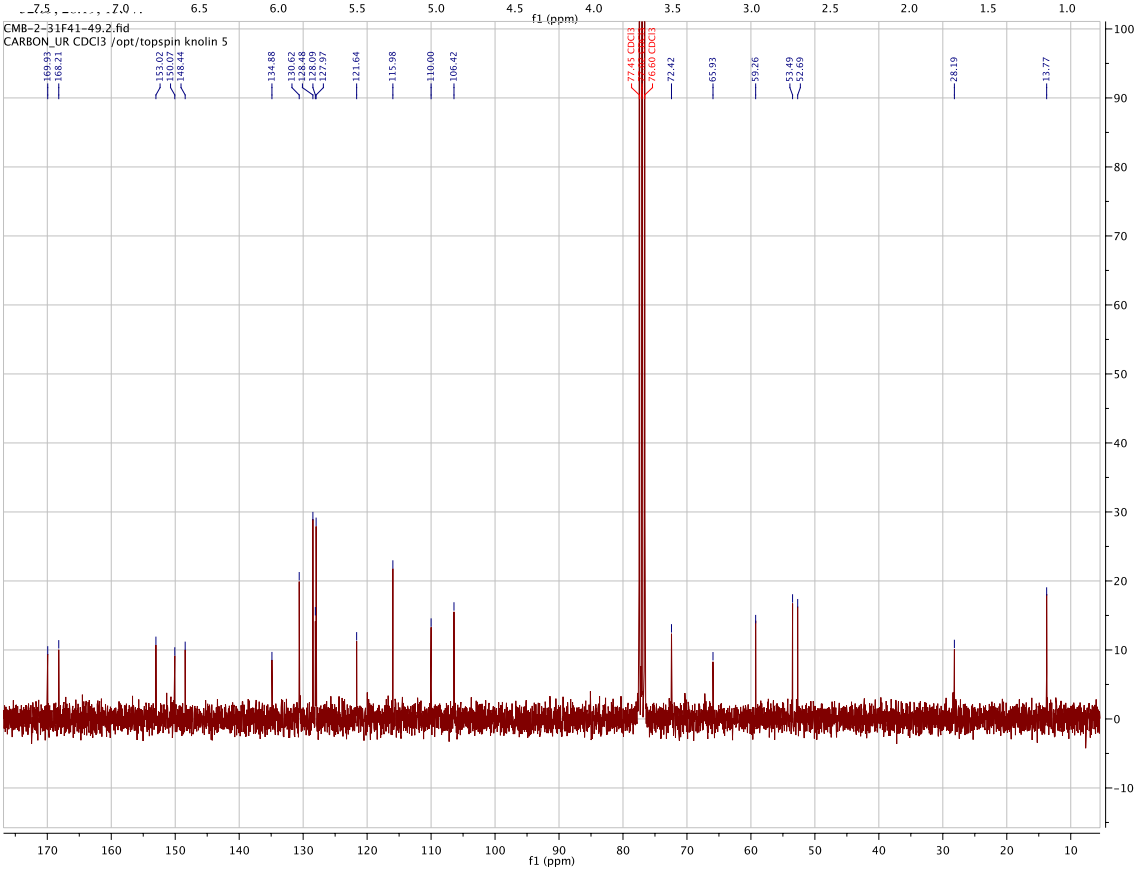
CMB-2-31F41-49.2.fid
CARBON_UR CDCl3 /opt/topspin knolin 5
169.93
168.21
153.02
150.07
148.44
134.88
130.62
128.44
128.08
127.97
121.64
115.98
110.00
106.42
77.45 CDCl3
76.80 CDCl3
72.42
65.93
59.26
53.49
52.69
28.19
13.77
f1 (ppm)

7j

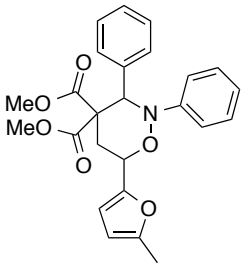
MeO
MeO
O
O
N
O
O

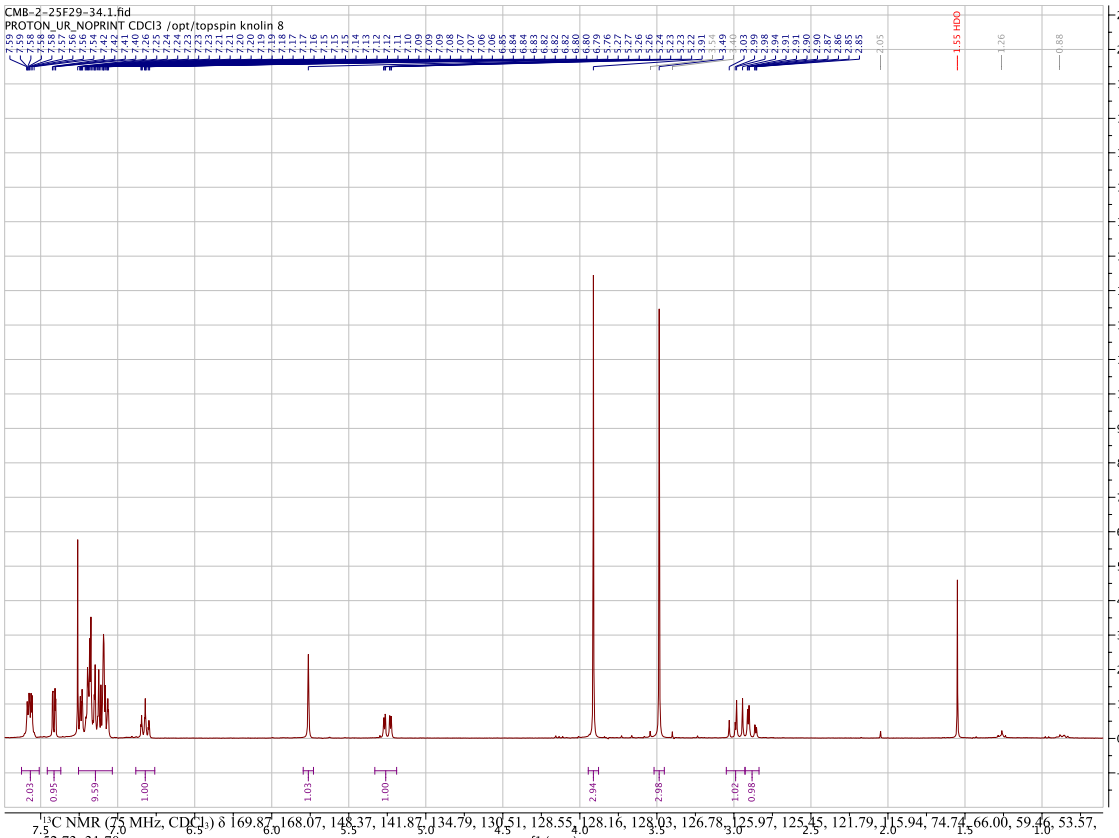

7i

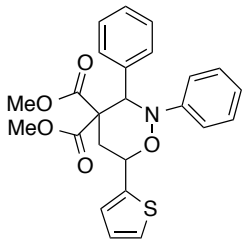

^{13}C NMR (75 MHz, $CDCl_3$) δ 169.87, 168.07, 148.37, 141.87, 134.79, 130.51, 128.55, 128.16, 128.03, 126.78, 125.97, 125.45, 121.79, 115.94, 74.74, 66.00, 59.46, 53.57, 52.73, 31.70.

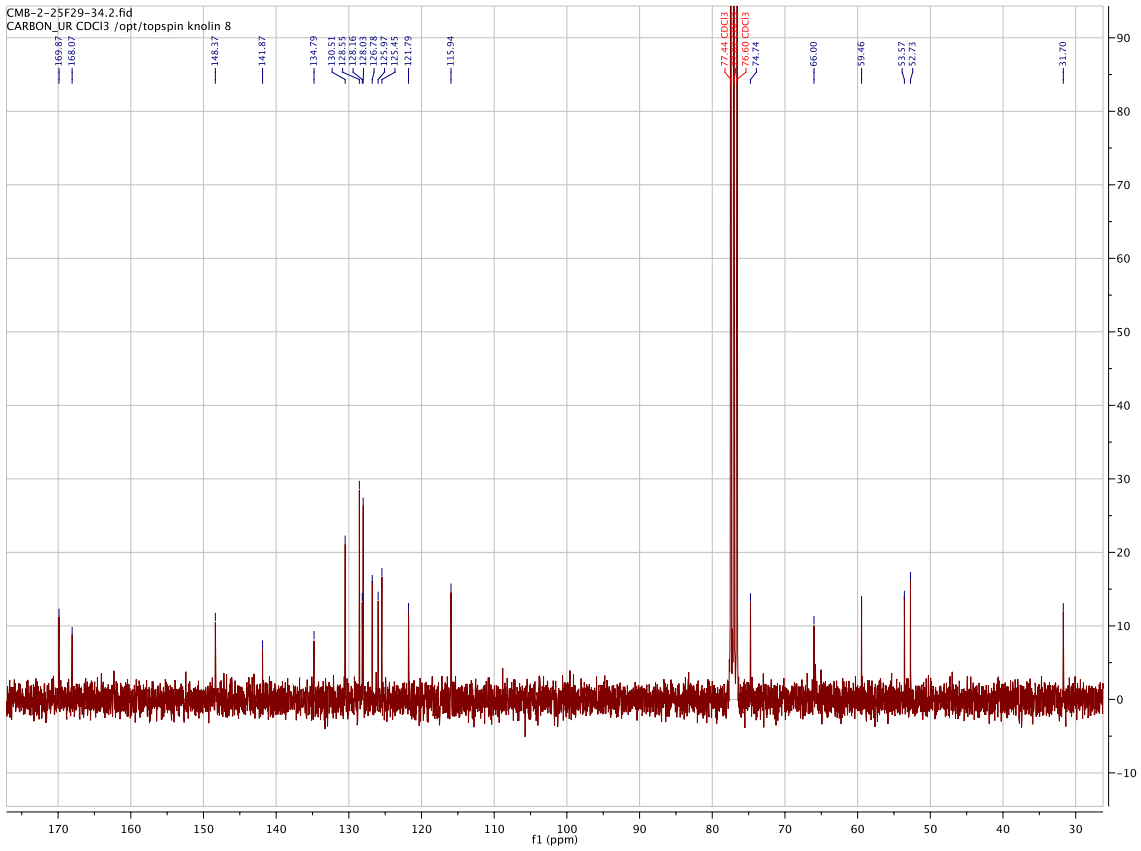

7h

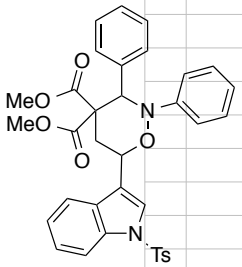
MeO
MeO
O
O
O
N
O
N
Ts

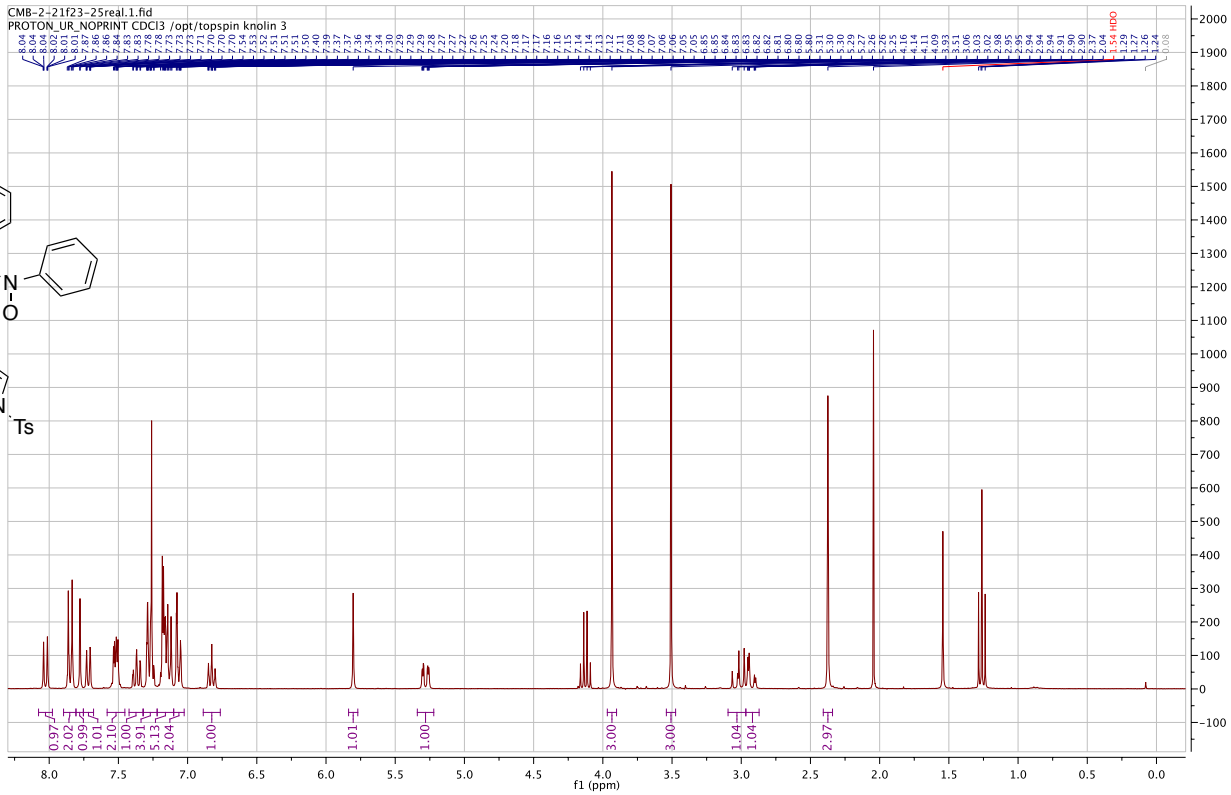
CMB-2-21f23-25real.1.fid
PROTON_UR_NOPRINT CDCl3 /opt/topspin knolin 3
HDO
0.97
2.02
0.99
1.01
2.10
1.00
3.91
5.13
2.04
1.00
1.01
1.00
3.00
3.00
1.04
1.04
2.97
f1 (ppm)

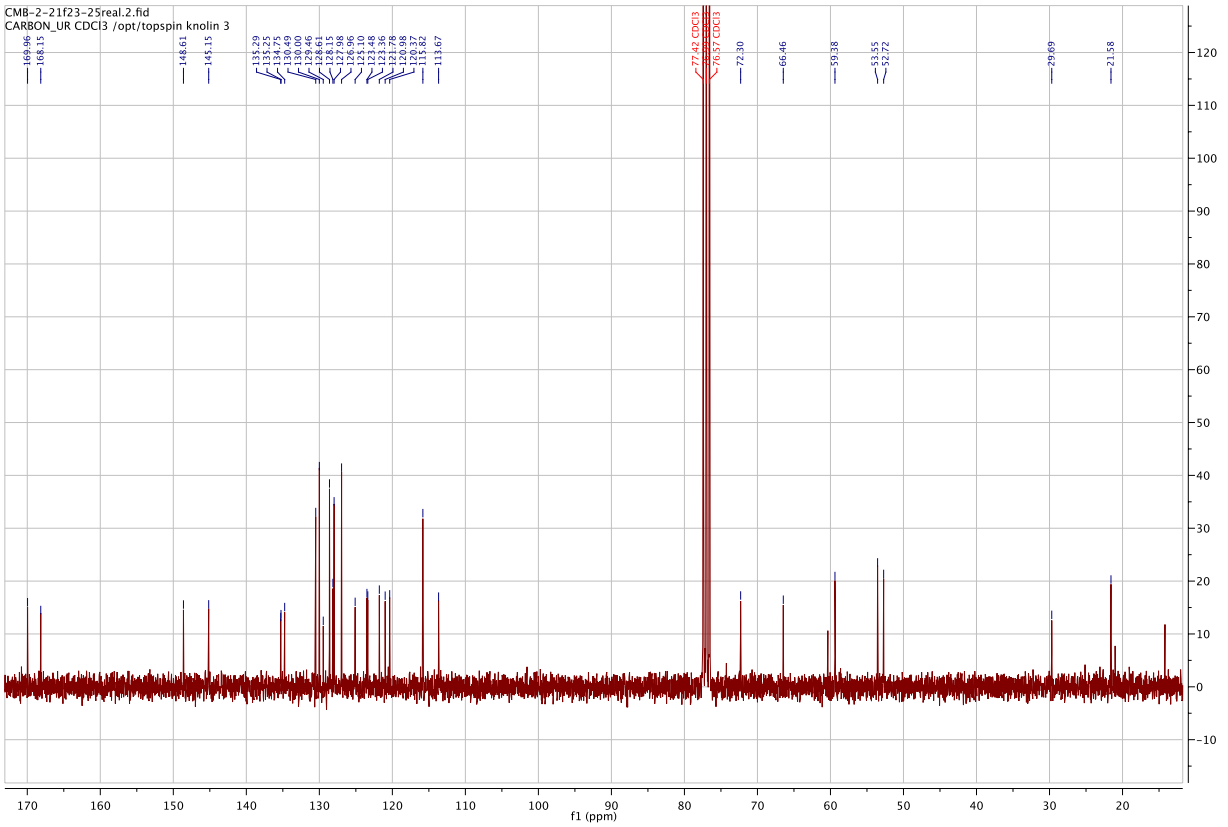
CMB-2-21f23-25real.2.fid
CARBON_UR CDCl3 /opt/topspin knolin 3
169.96
168.15
148.61
145.15
135.29
135.25
134.75
130.49
130.00
129.46
128.61
128.15
127.58
126.96
125.10
123.48
123.36
121.78
120.98
113.82
113.67
77.42 CDCl3
77.00
76.57 CDCl3
72.30
66.46
59.38
53.55
52.72
29.69
21.58
f1 (ppm)

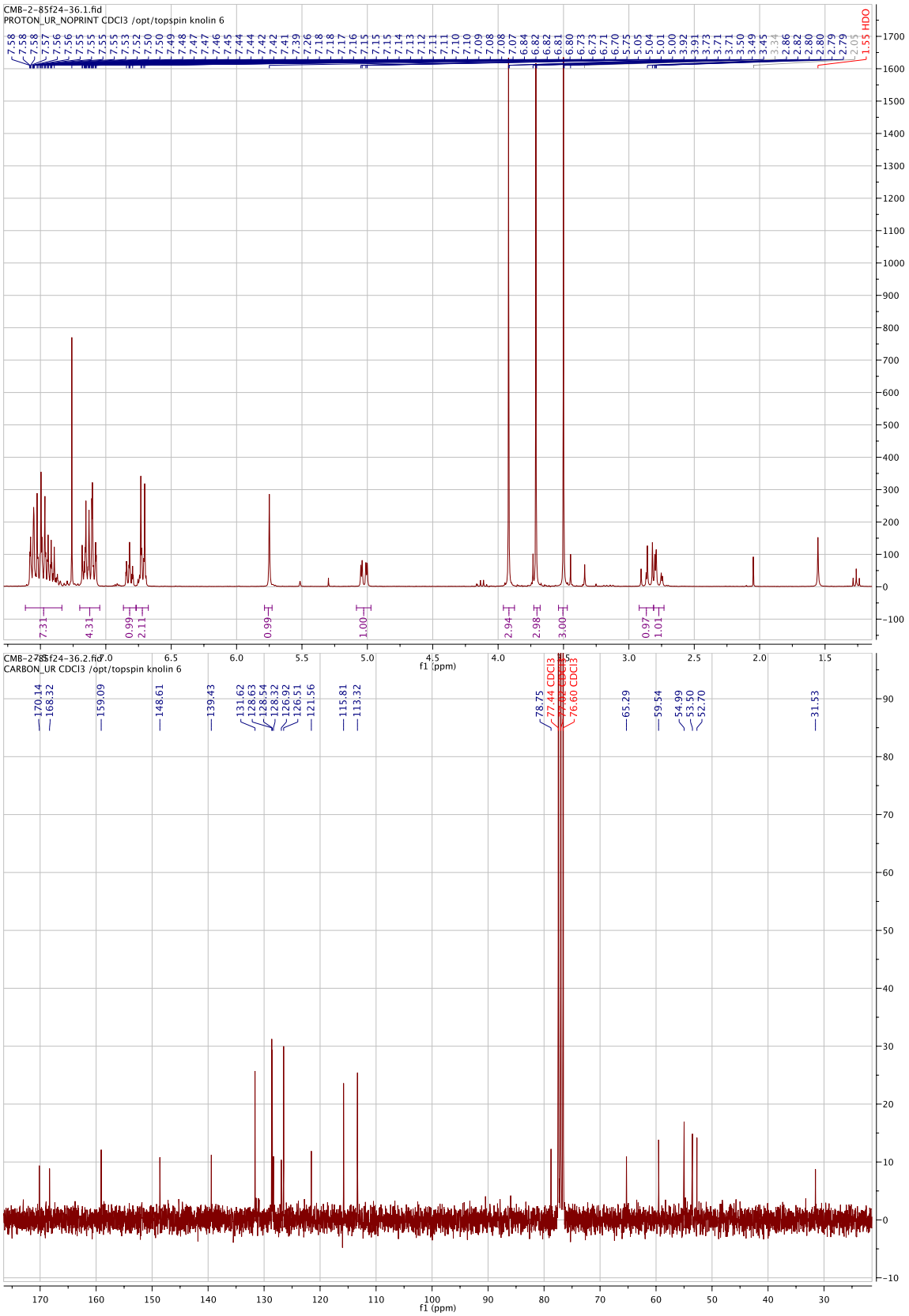
CMB-2-85f24-36.1.fid
PROTON_UR_NOPRINT CDCl3 /opt/topspin knolin 6
CMB-2-85f24-36.2.fid
CARBON_UR CDCl3 /opt/topspin knolin 6
f1 (ppm)

9a

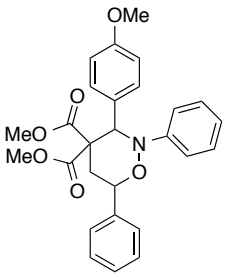
OMe
O
MeO
MeO
O
N
O

9b

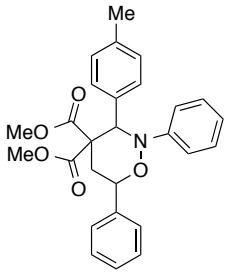
Me
O
MeO
MeO
O
N
O
O


CMB-2-83.1.fid
PROTON_UR_NOPRINT CDCl3 /opt/topspin knolin 4
7.26 CDCl3
1.55 HDO
1.95
5.30
4.16
2.21
0.98
0.95
1.00
2.90
2.92
0.98
0.94
2.73
f1 (ppm)

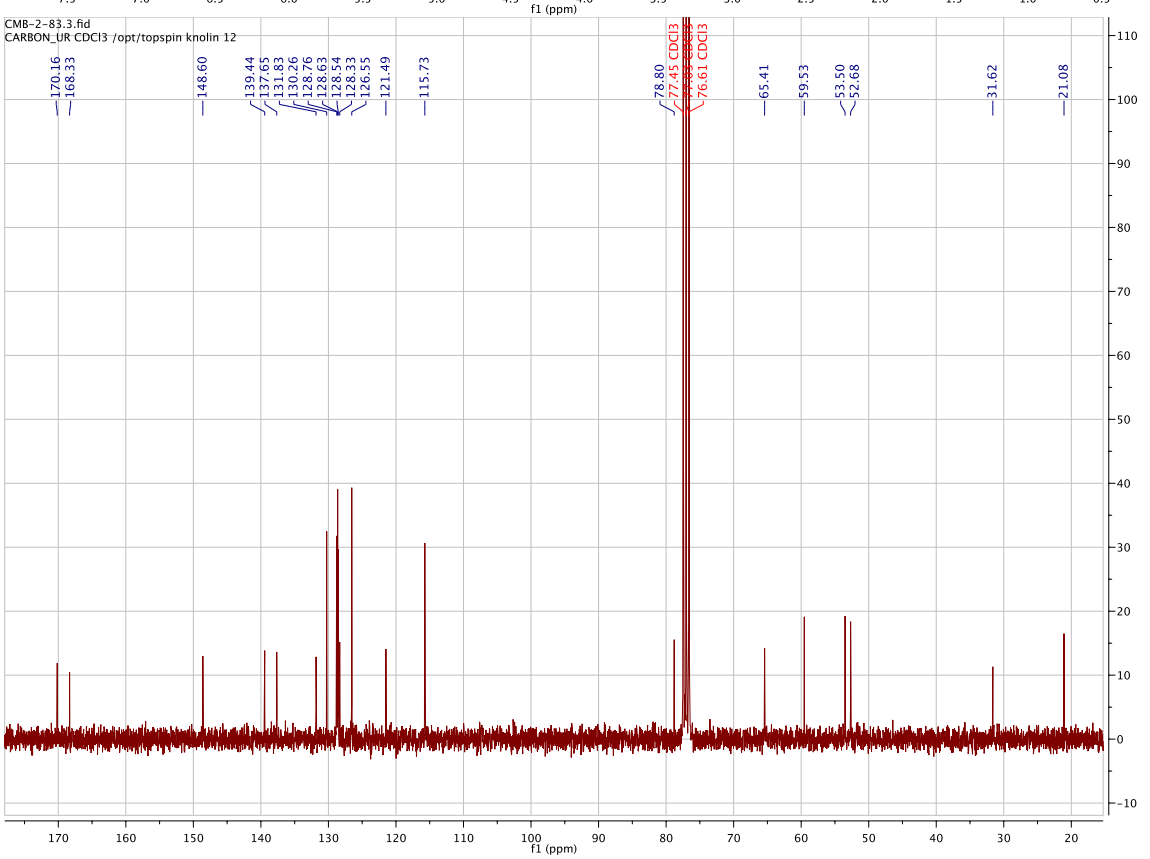
CMB-2-83.3.fid
CARBON_UR CDCl3 /opt/topspin knolin 12
170.16
168.33
148.60
139.44
137.65
131.83
130.26
128.76
128.63
128.54
128.33
126.55
121.49
115.73
78.80
77.45 CDCl3
76.61 CDCl3
65.41
59.53
53.50
52.68
31.62
21.08
f1 (ppm)

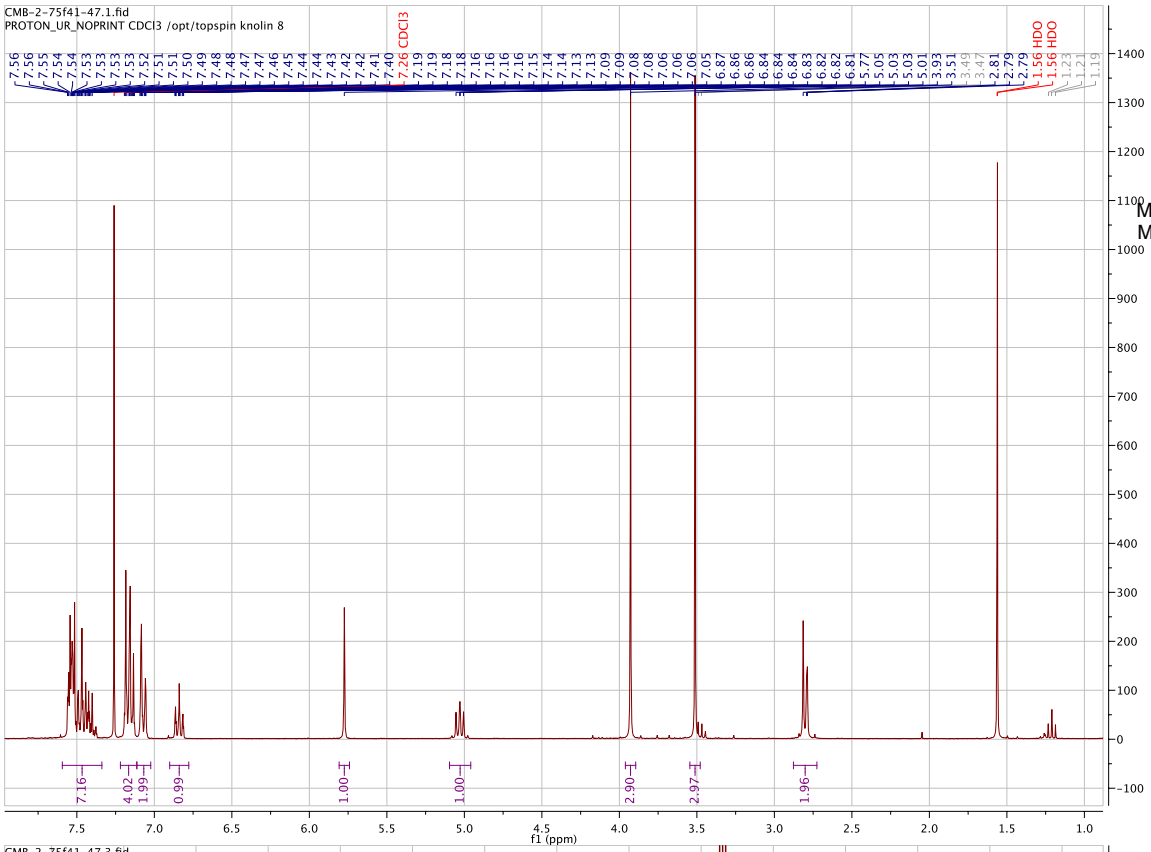
CMB-2-75f41-47.1.fid
PROTON_UR_NOPRINT CDCl3 /opt/topspin knolin 8
f1 (ppm)

9c

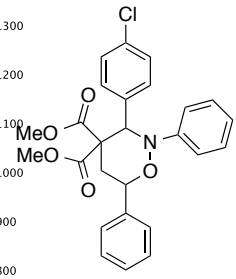
Cl
O
MeO
MeO
O
N
O

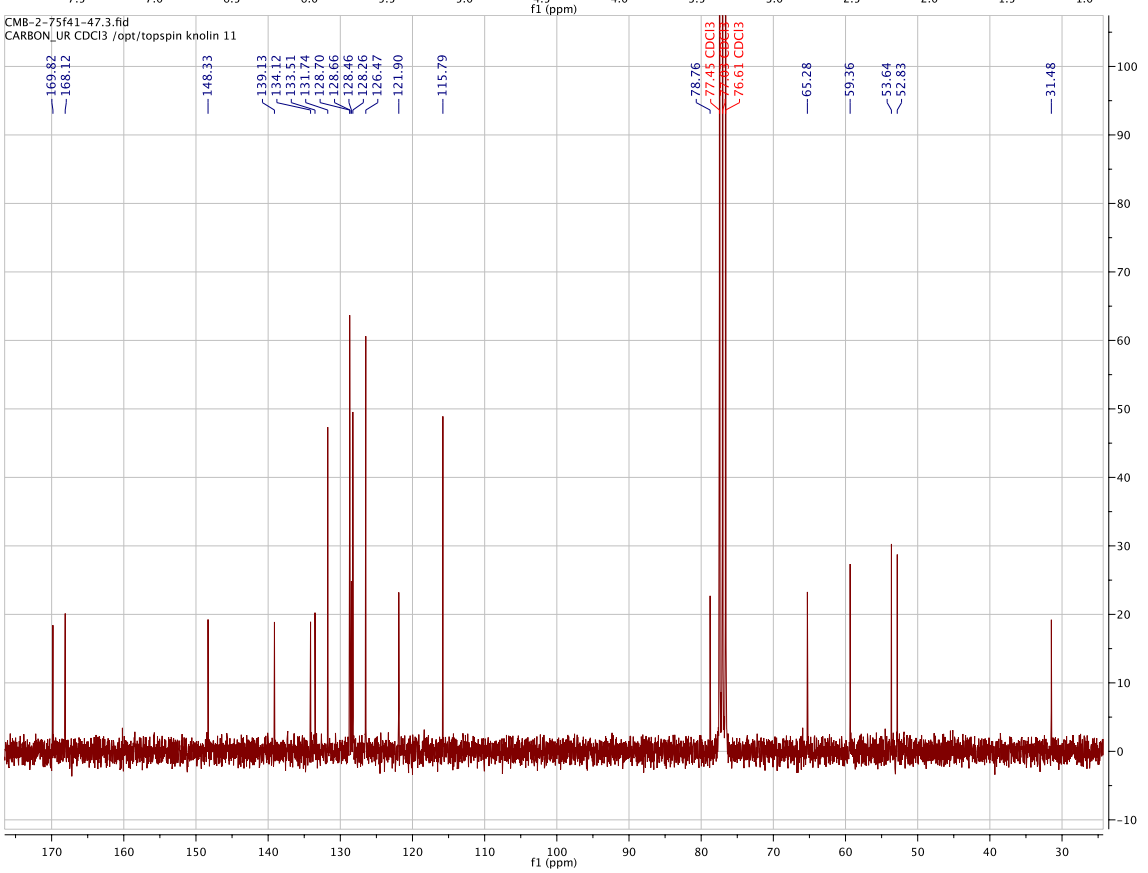
CMB-2-75f41-47.3.fid
CARBON_UR CDCl3 /opt/topspin knolin 11
f1 (ppm)

9d

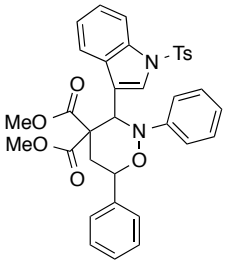
N
Ts
O
MeO
MeO
O
N
O

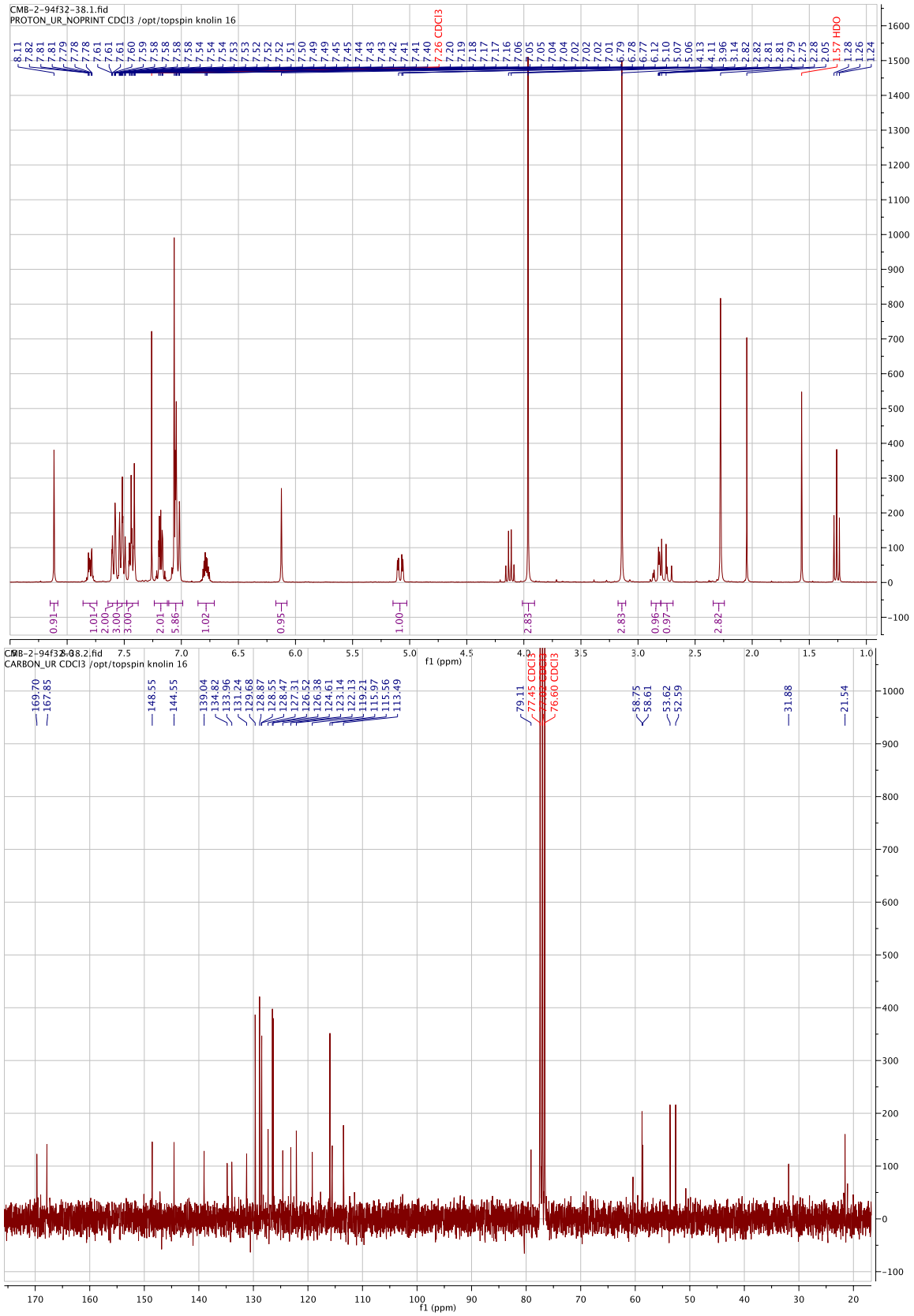
CMB-2-94f32-38.1.fid
PROTON_UR_NOPRINT CDCl3 /opt/topspin knolin 16
7.26 CDCl3
1.57 HDO
f1 (ppm)
CMB-2-94f32-38.2.fid
CARBON_UR CDCl3 /opt/topspin knolin 16
169.70
167.85
148.55
144.55
139.04
134.82
133.96
131.24
129.68
128.87
128.55
128.47
127.31
126.52
126.38
124.61
123.14
122.13
119.21
115.97
115.56
113.49
79.11
77.45 CDCl3
76.60 CDCl3
58.75
58.61
53.62
52.59
31.88
21.54
f1 (ppm)

13

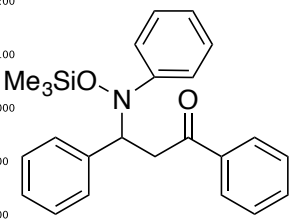
Me3SiO
N
O

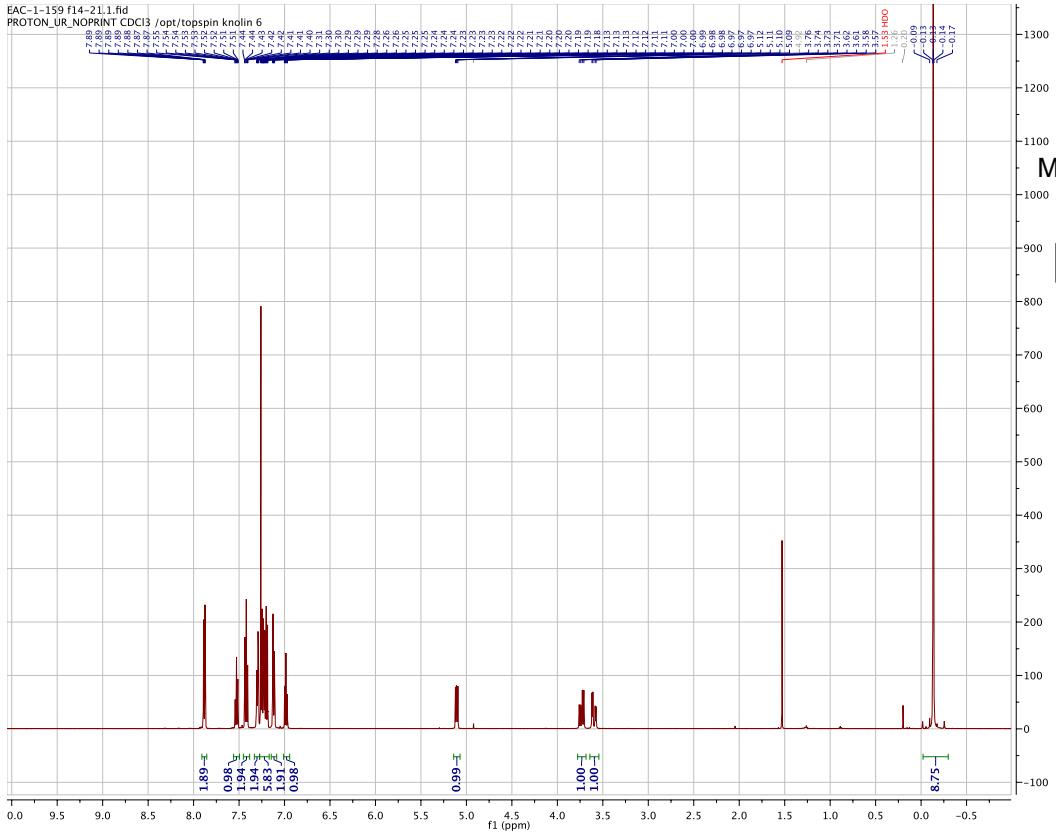
EAC-1-159 f14-21.1.fid
PROTON_UR_NOPRINT CDCl3 /opt/topspin knolin 6
f1 (ppm)

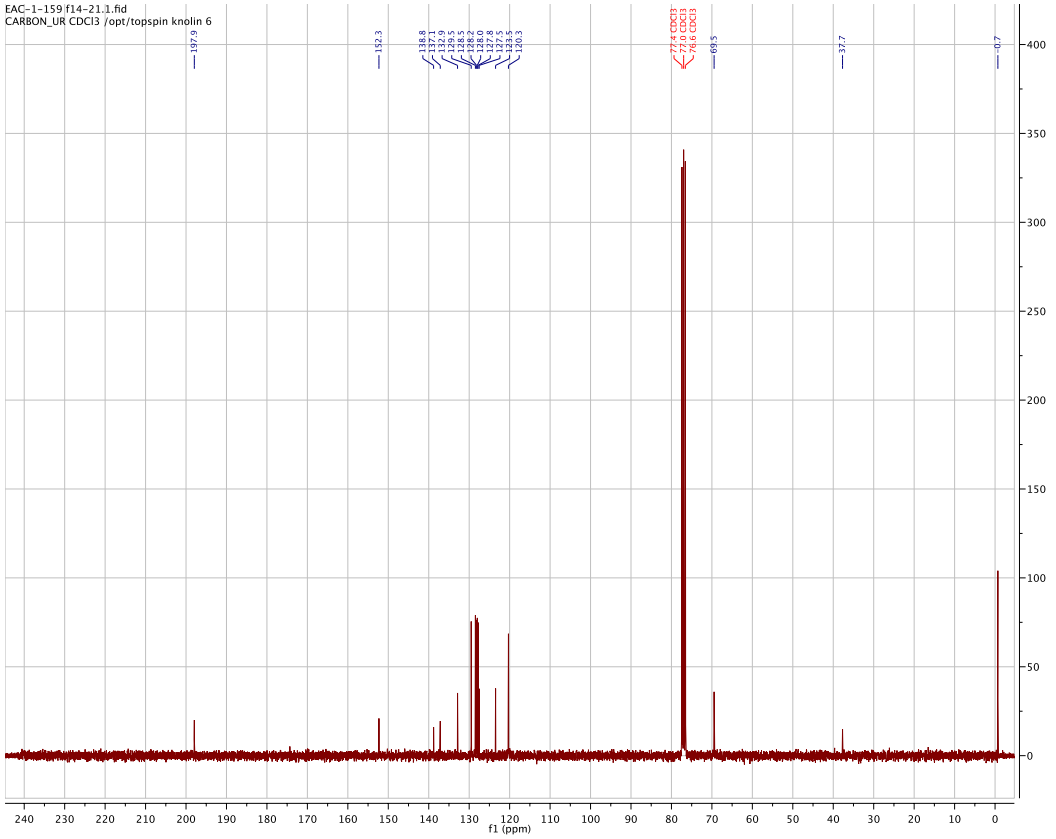
EAC-1-159 f14-21.1.fid
CARBON_UR CDCl3 /opt/topspin knolin 6
f1 (ppm)

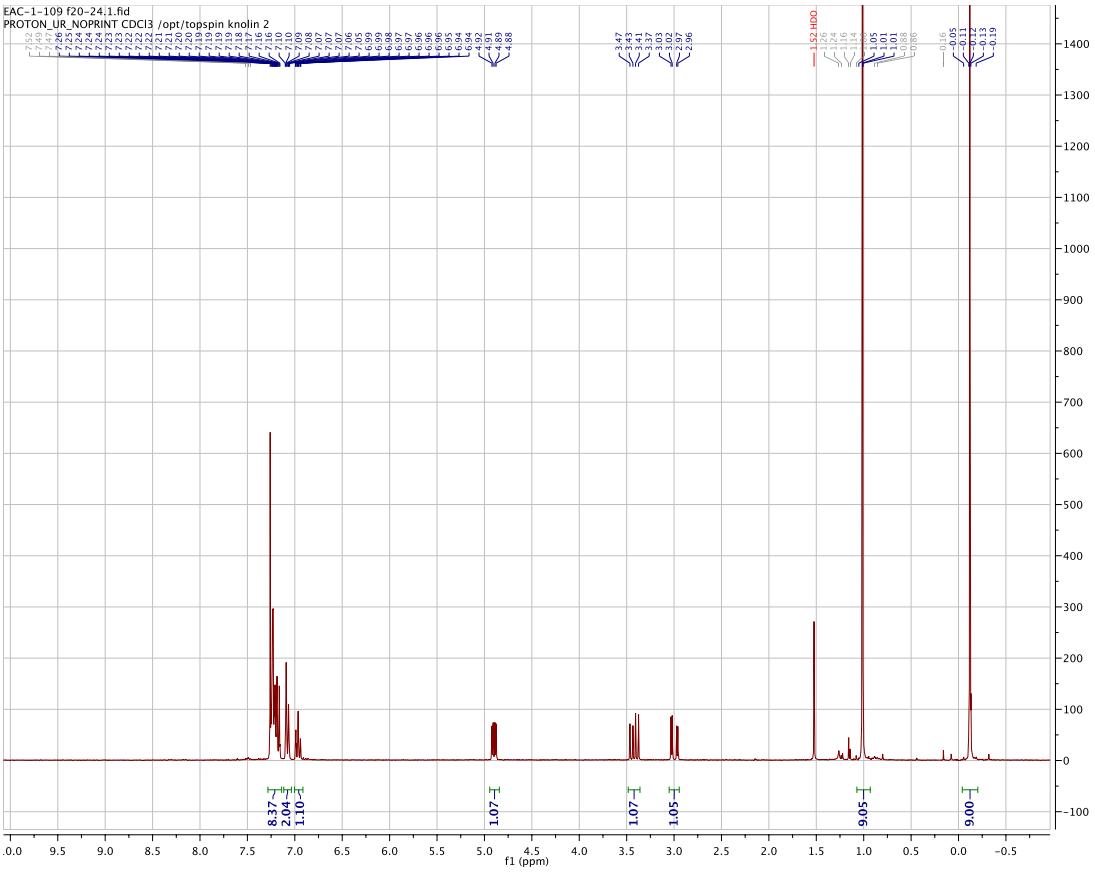
EAC-1-109 f20-24.1.fid
PROTON_UR_NOPRINT CDCl3 /opt/topspin knolin 2
1.52 HDO
8.37
2.04
1.10
1.07
1.07
1.05
9.05
9.00
f1 (ppm)

16a

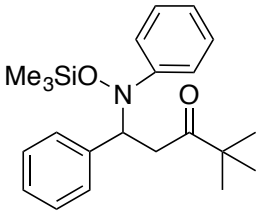
Me3SiO
N
O

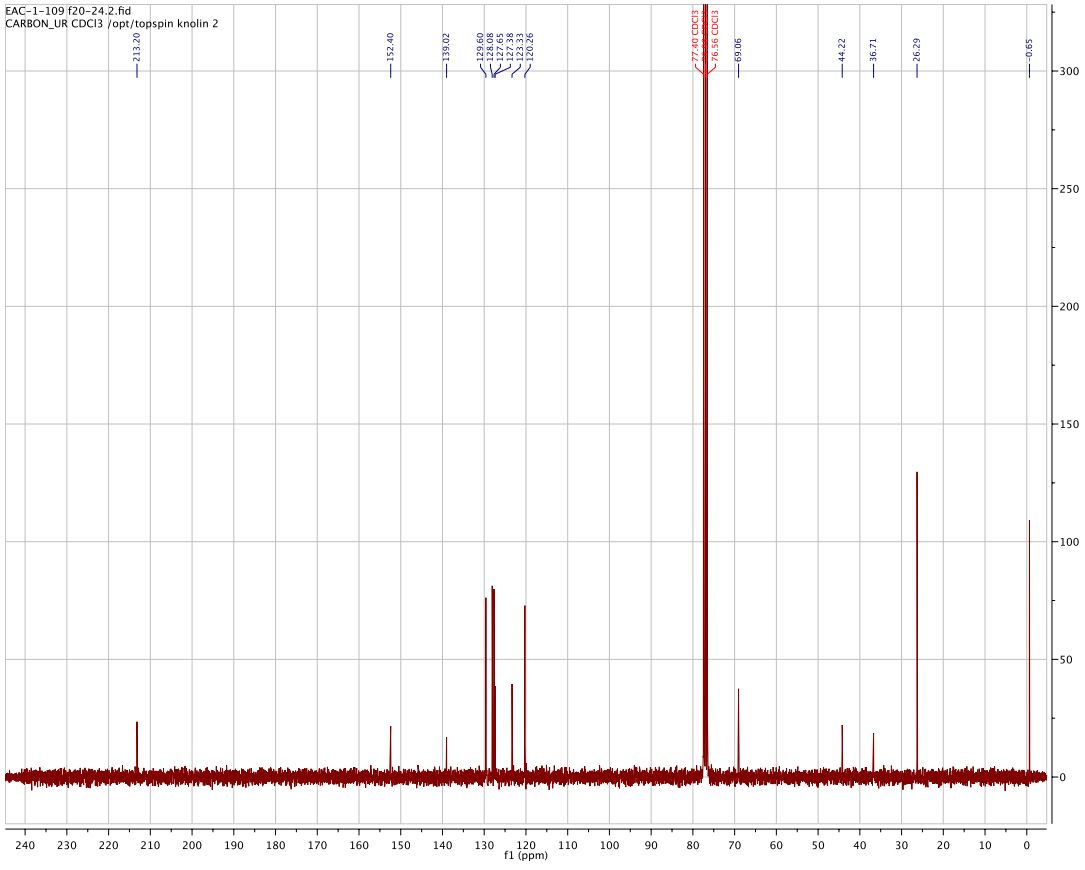
EAC-1-109 f20-24.2.fid
CARBON_UR CDCl3 /opt/topspin knolin 2
213.20
152.40
139.02
129.60
128.08
127.65
127.38
125.33
120.26
77.40 CDCl3
76.56 CDCl3
69.06
44.22
36.71
26.29
-0.65
f1 (ppm)

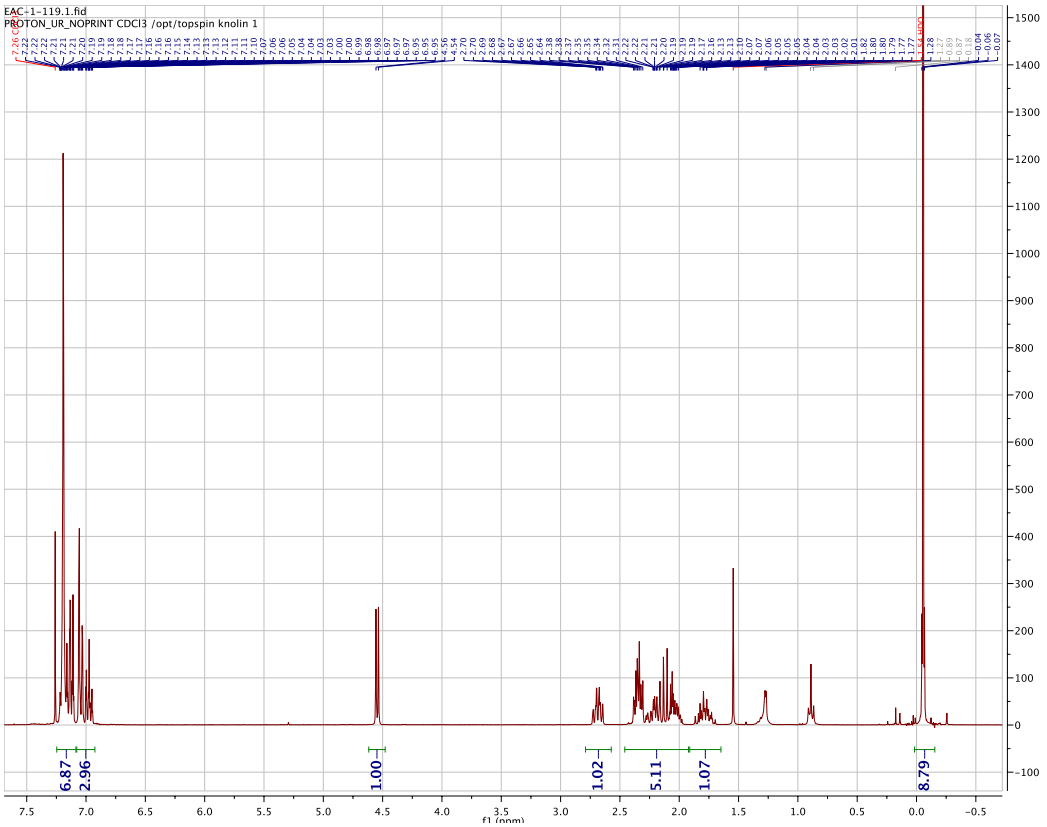
EAC-1-119.1.fid
PROTON_UR_NOPRINT CDCl3 /opt/topspin knolin 1
6.87
2.96
1.00
1.02
5.11
1.07
8.79
f1 (ppm)

16b

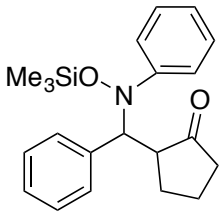
Me3SiO
N
O

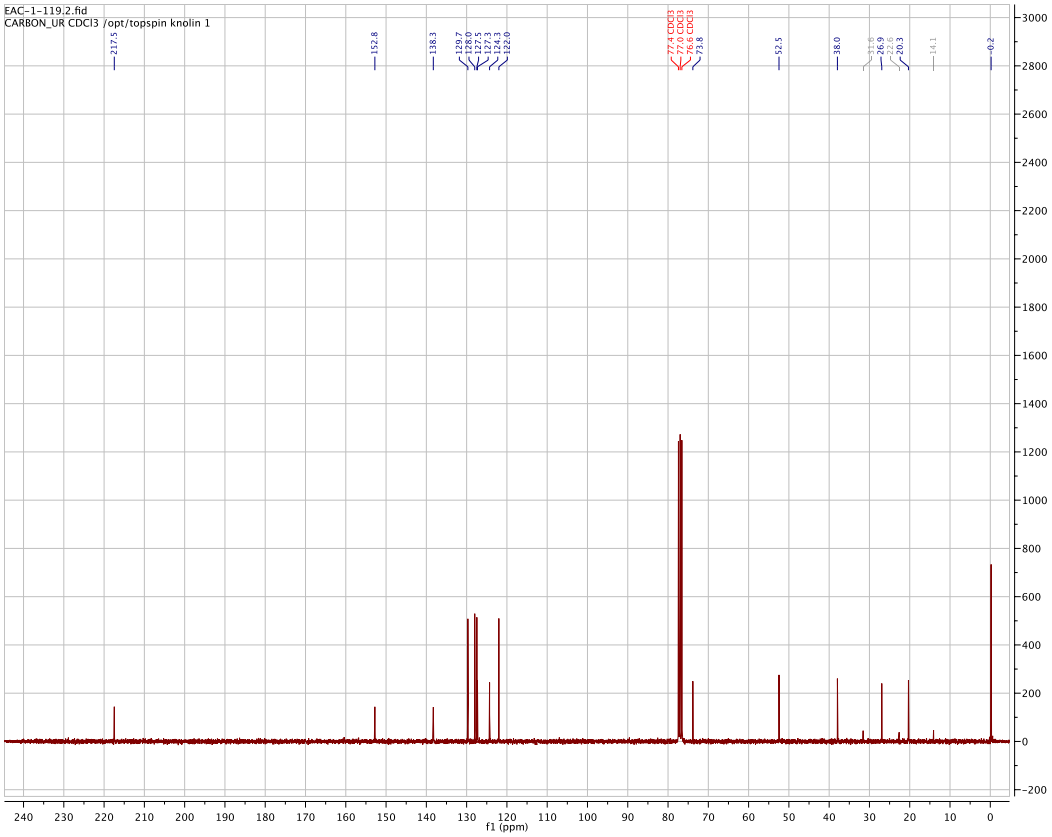
EAC-1-119.2.fid
CARBON_UR CDCl3 /opt/topspin knolin 1
217.4
152.8
138.3
129.7
128.0
127.5
127.3
124.3
122.0
77.4 CDCl3
77.0 CDCl3
76.6 CDCl3
73.8
52.5
38.0
31.6
26.9
25.5
20.3
14.1
0.2
f1 (ppm)

16c

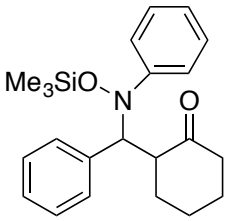
Me3SiO
N
O

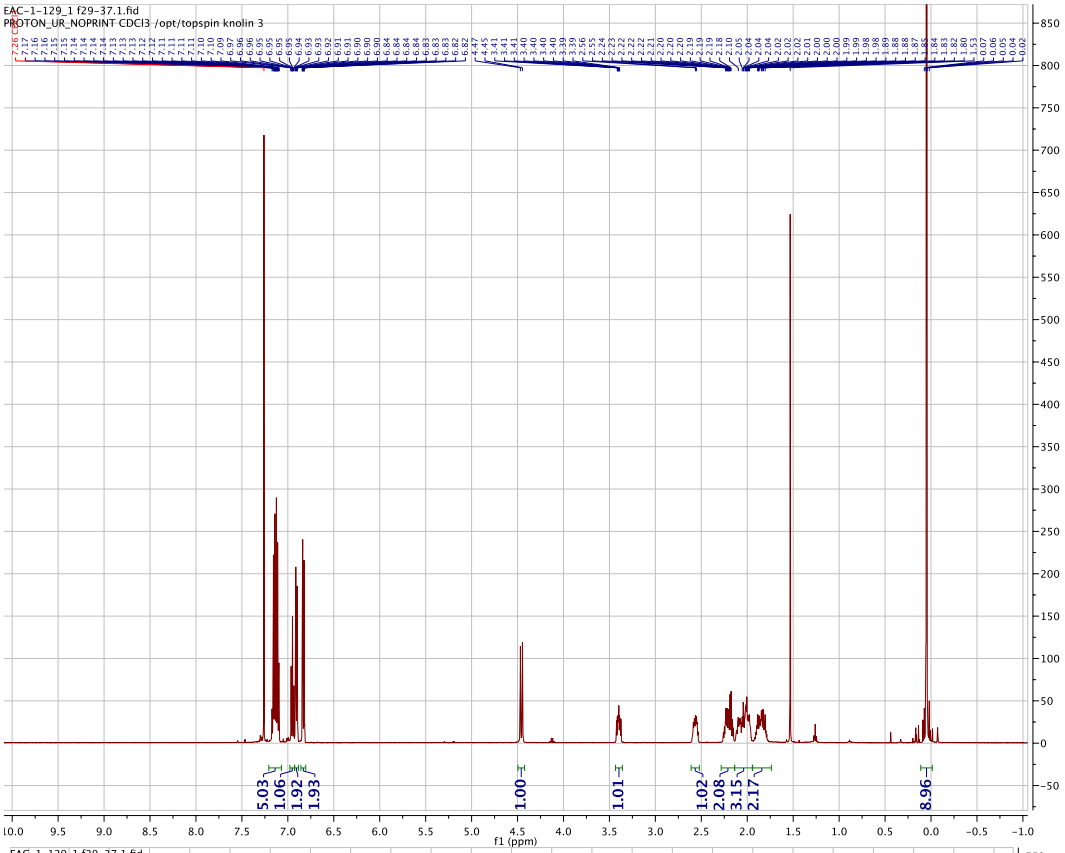
EAC-1-129_1 f29-37.1.fid
PROTON_UR_NOPRINT CDCl3 /opt/topspin knolin 3
5.03
1.06
1.92
1.93
1.00
1.01
1.02
2.08
3.15
2.17
8.96
f1 (ppm)

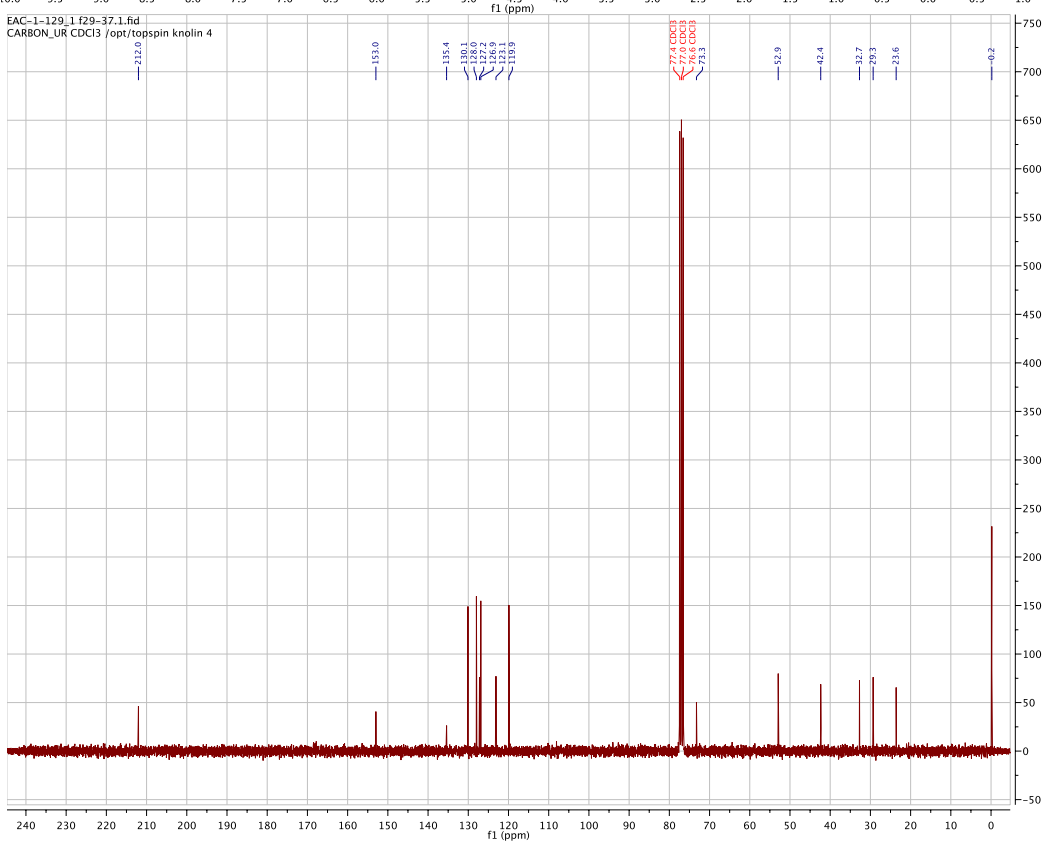
EAC-1-129_1 f29-37.1.fid
CARBON_UR CDCl3 /opt/topspin knolin 4
212.0
153.0
135.4
130.1
128.6
127.2
126.9
123.1
119.9
77.4 CDCl3
77.0 CDCl3
76.6 CDCl3
73.3
52.9
42.4
32.7
29.3
23.6
0.2
f1 (ppm)

14a

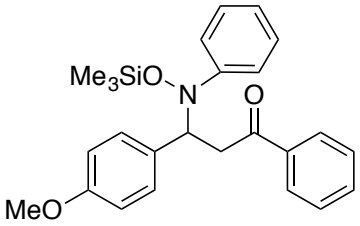
Me3SiO
N
O
MeO

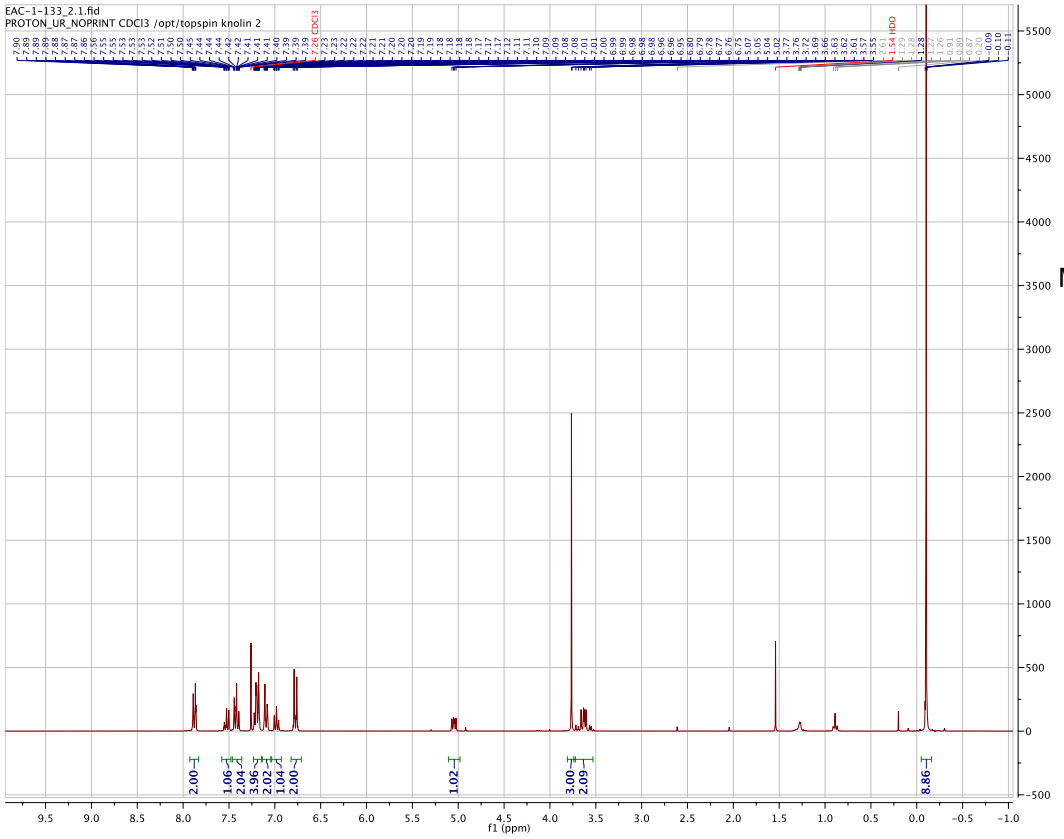
EAC-1-133_2.1.fid
PROTON_UR_NOPRINT CDCl3 /opt/topspin knolin 2
f1 (ppm)

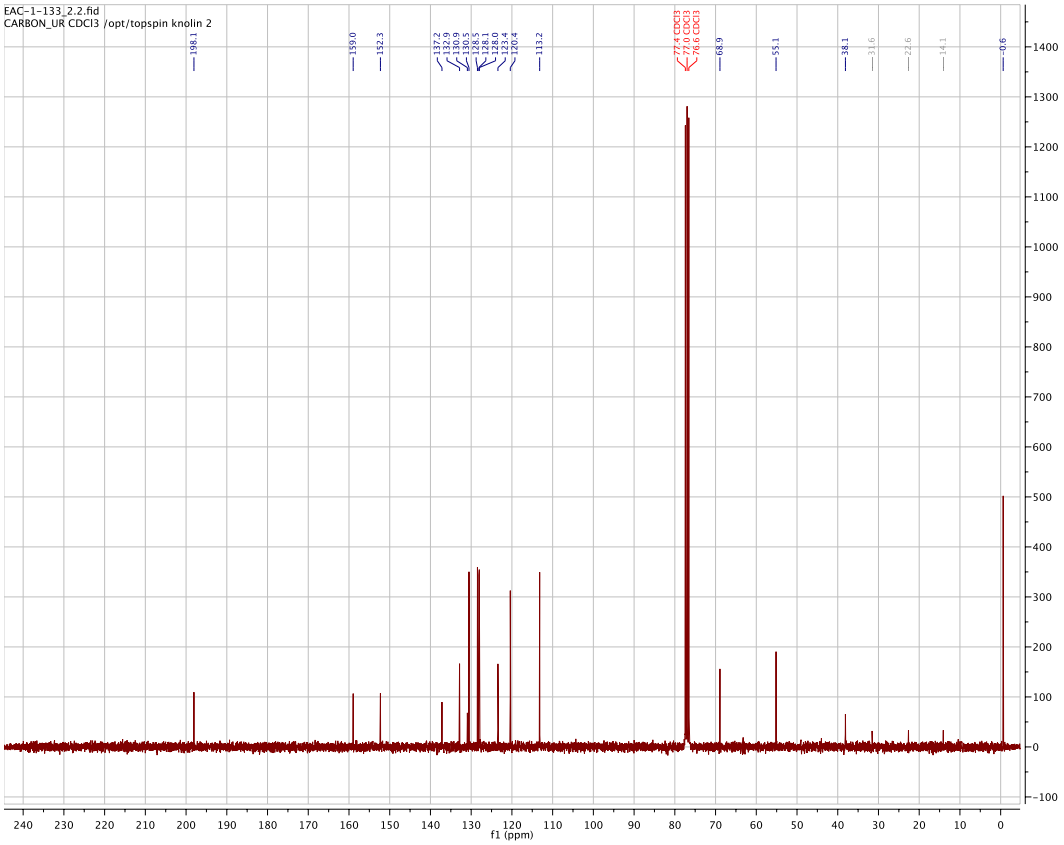
EAC-1-133_2.2.fid
CARBON_UR CDCl3 /opt/topspin knolin 2
f1 (ppm)

14b

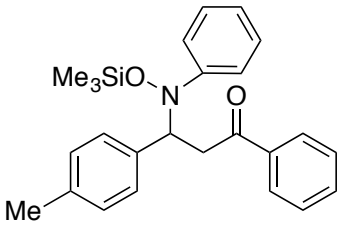
Me3SiO
N
O
Me

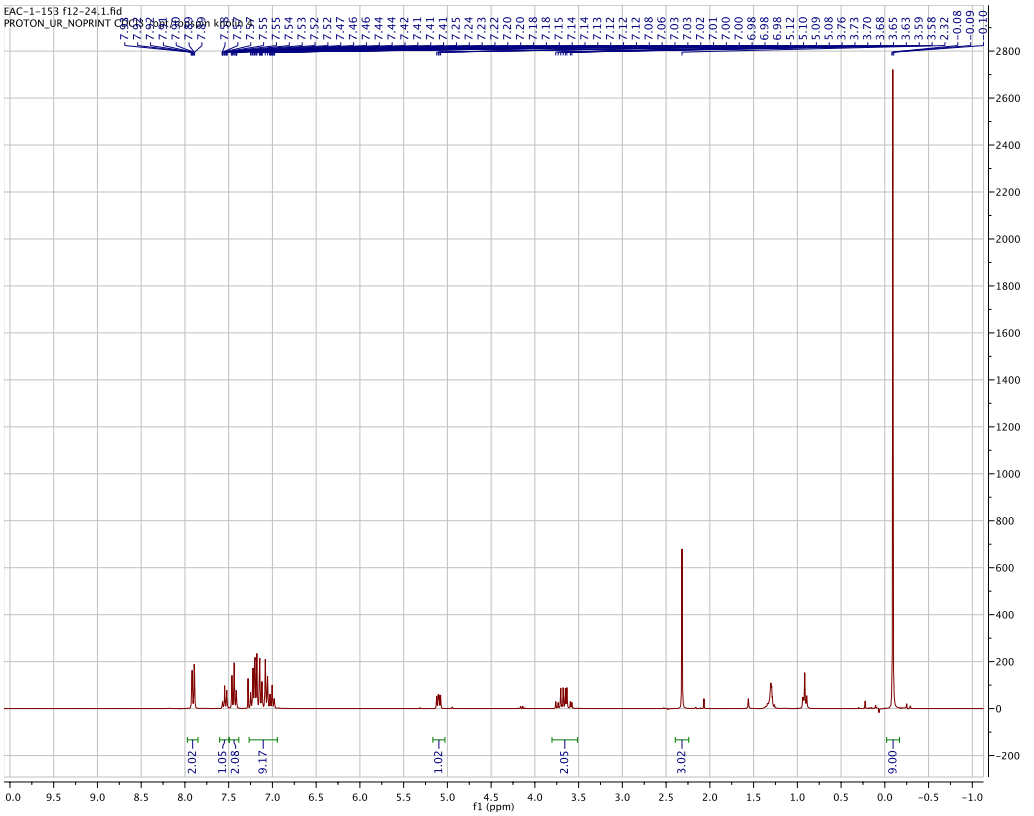
EAC-1-153 f12-24.1.fid
PROTON_UR_NOPRINT CDCl3 /opt/topspin knolln 1
2.02
1.05
2.08
9.17
1.02
2.05
3.02
9.00
f1 (ppm)

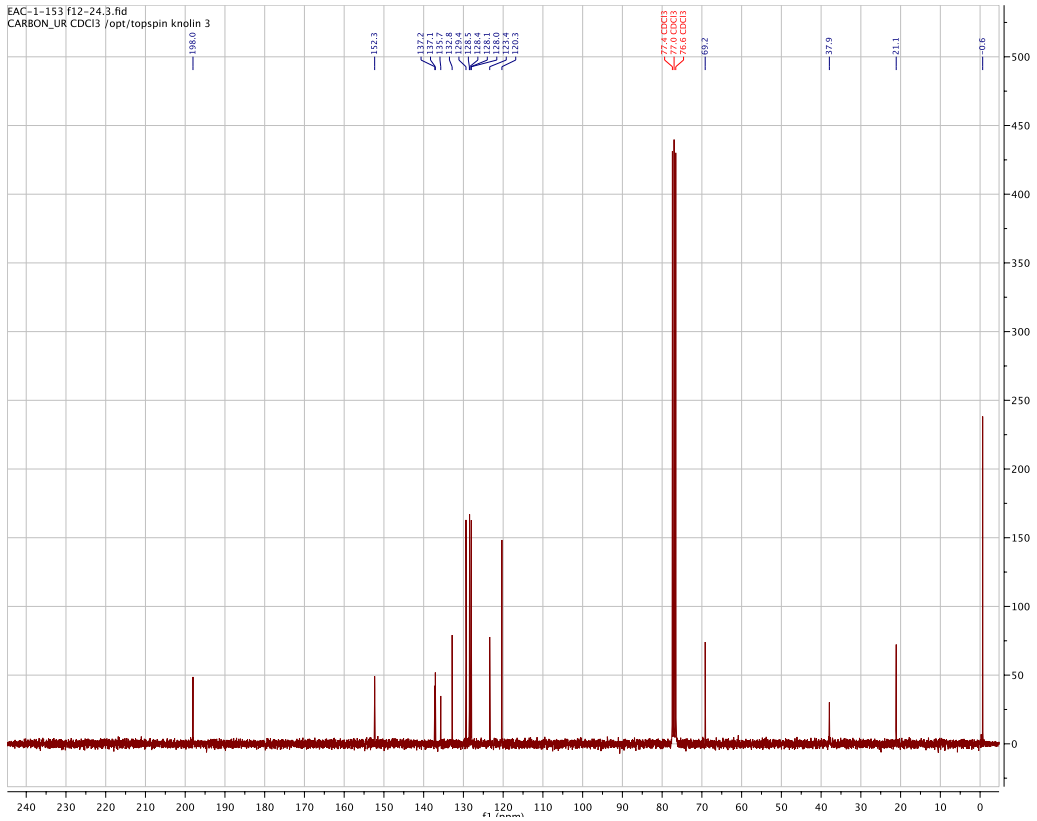
EAC-1-153 f12-24.3.fid
CARBON_UR CDCl3 /opt/topspin knolln 3
198.0
152.3
137.2
137.1
135.7
132.8
129.4
128.5
128.4
128.1
128.0
123.4
120.3
77.4 CDCl3
77.0 CDCl3
76.6 CDCl3
69.2
37.9
21.1
0.6

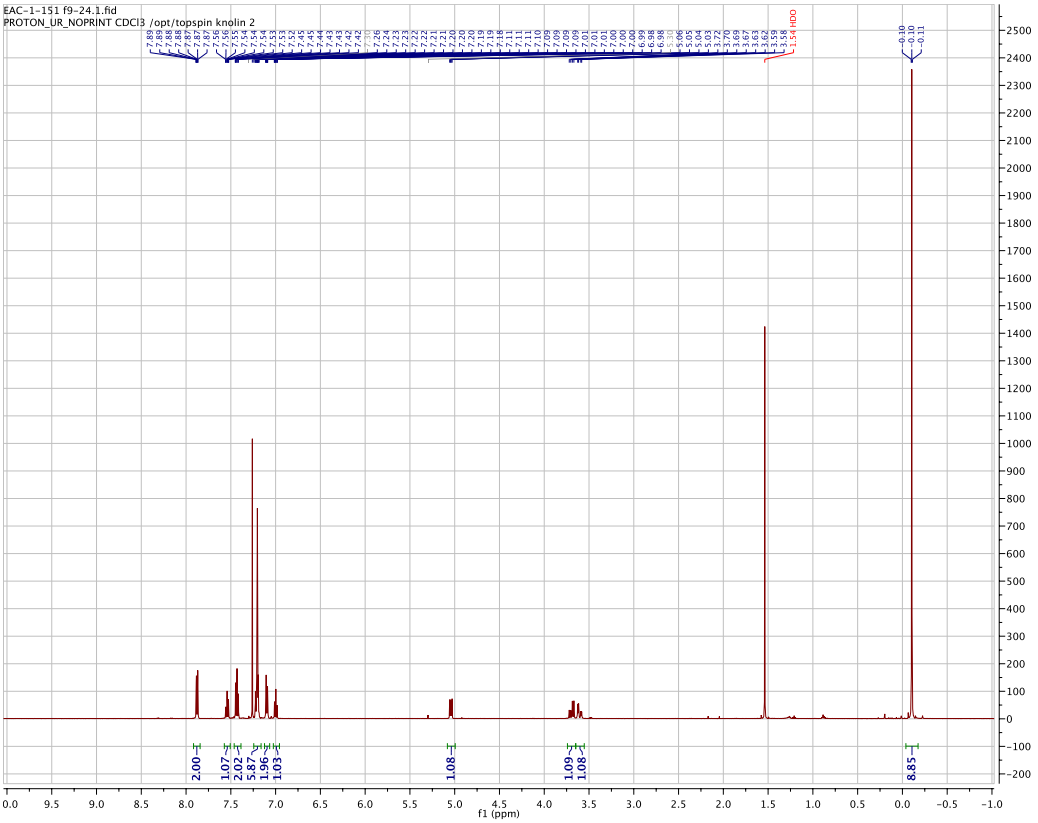
EAC-1-151 f9-24.1.fid
PROTON_UR_NOPRINT CDCl3 /opt/topspin knolin 2
2.00
1.07
2.02
5.87
1.96
1.03
1.08
1.09
1.08
8.85
f1 (ppm)

14c

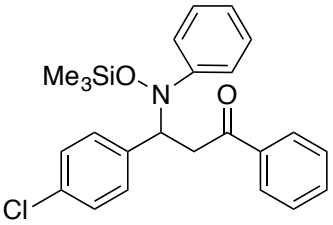
Me3SiO
N
O
Cl

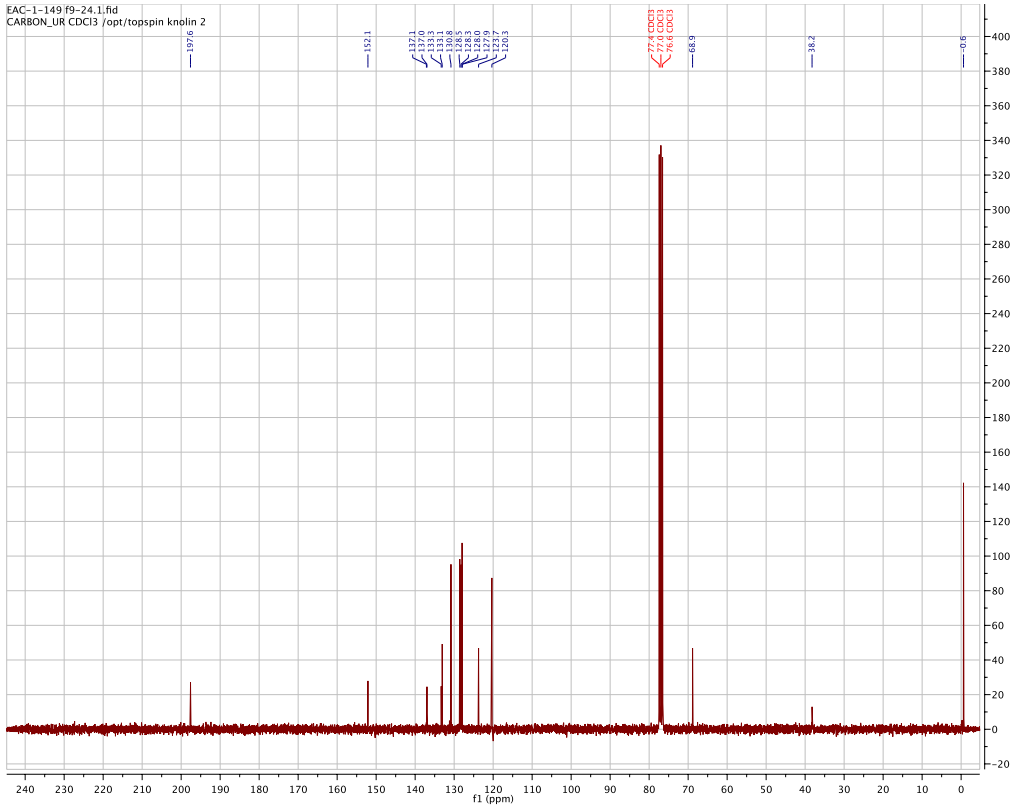
EAC-1-149 f9-24.1.fid
CARBON_UR CDCl3 /opt/topspin knolin 2
197.6
152.1
137.1
137.0
133.3
133.1
130.8
128.5
128.4
128.0
127.9
127.3
126.5
77.4 CDCl3
77.0 CDCl3
76.6 CDCl3
68.9
38.2
-0.6
f1 (ppm)

14d

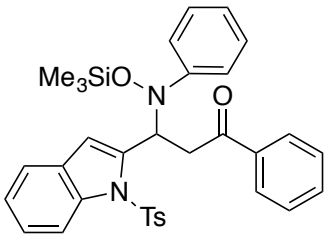
Me3SiO
N
O
N
Ts

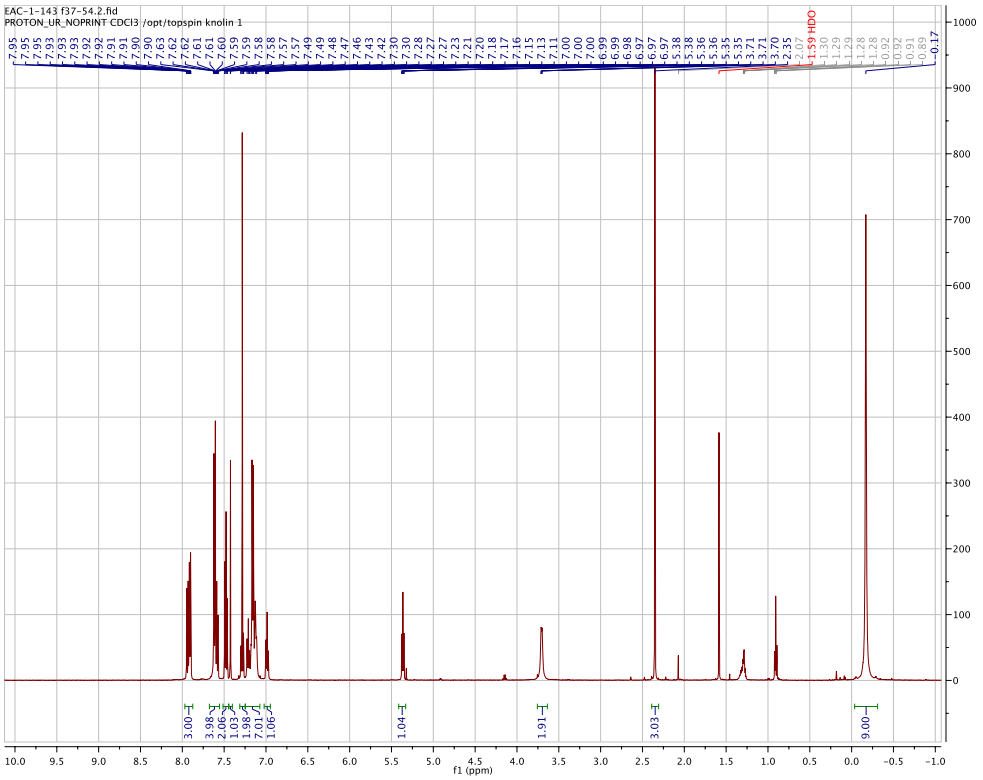
EAC-1-143 f37-54.2.fid
PROTON_UR_NOPRINT CDCl3 /opt/topspin knolin 1
f1 (ppm)

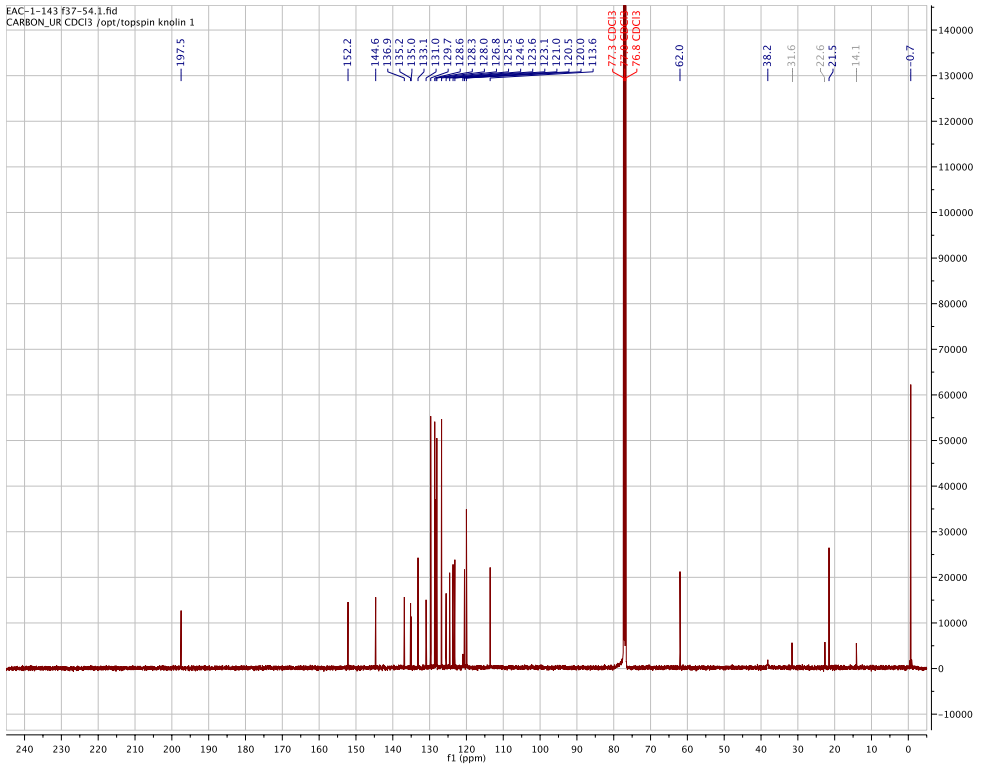
EAC-1-143 f37-54.1.fid
CARBON_UR CDCl3 /opt/topspin knolin 1
f1 (ppm)

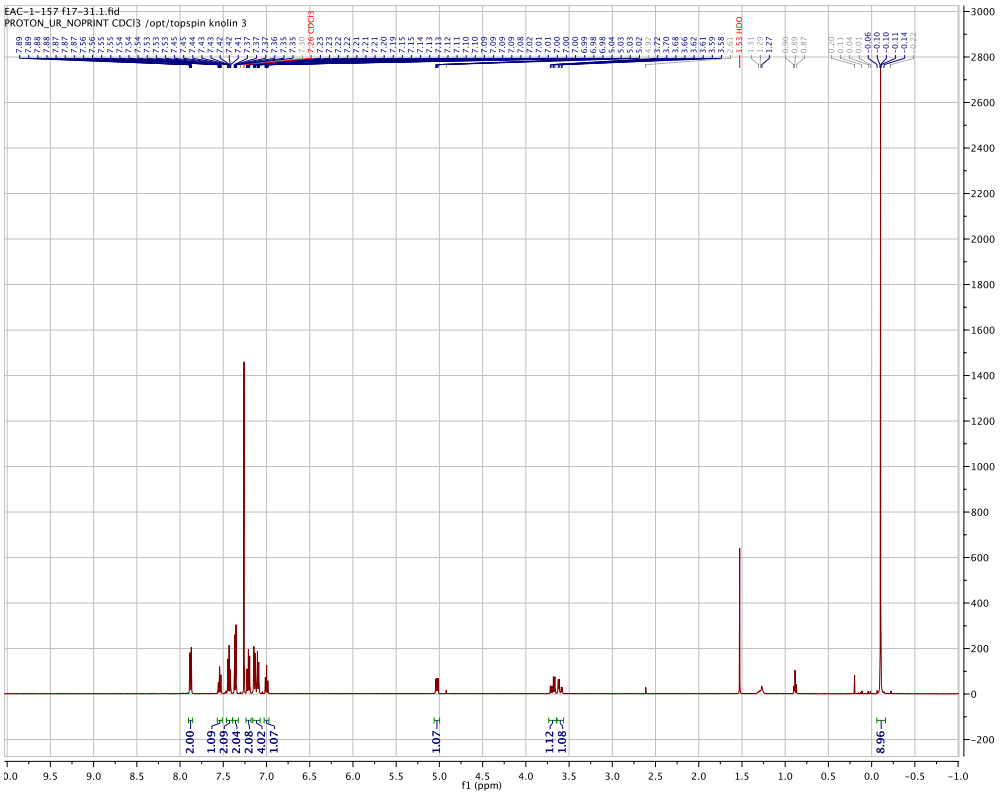
EAC-1-157 f17-31.1.fid
PROTON_UR_NOPRINT CDCl3 /opt/topspin knolin 3
f1 (ppm)

14e

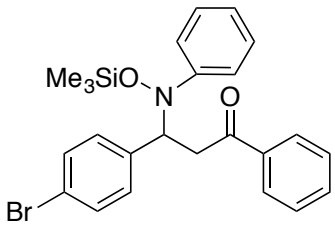
Me3SiO
N
O
Br

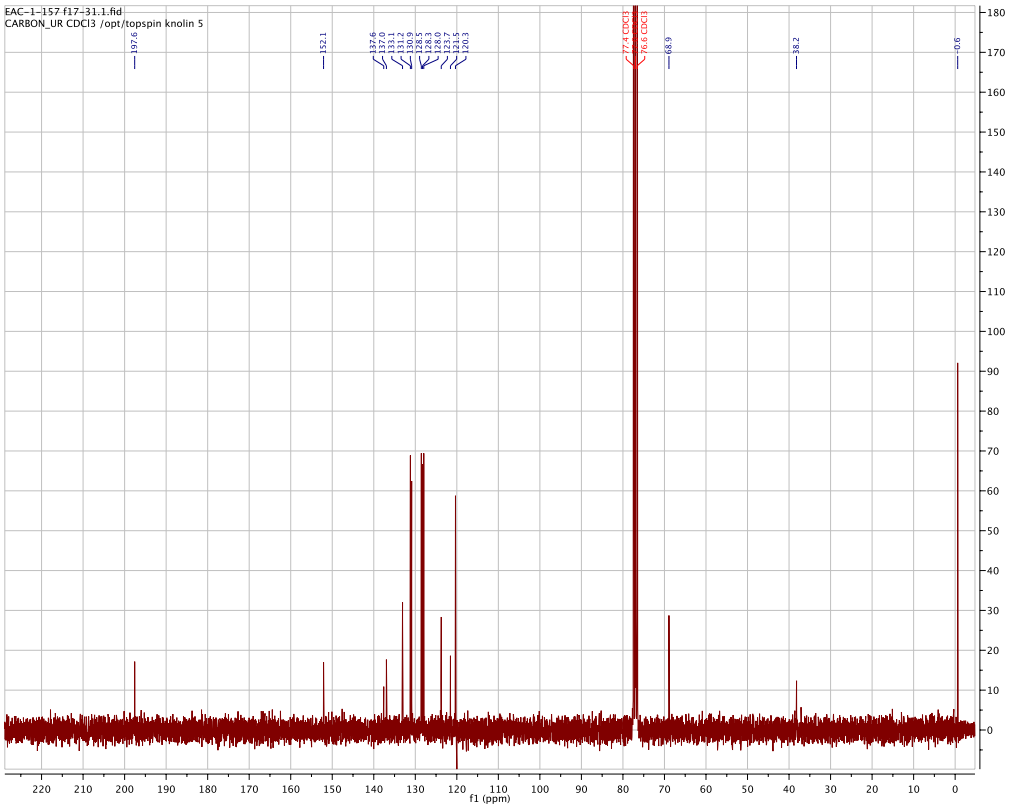
EAC-1-157 f17-31.1.fid
CARBON_UR CDCl3 /opt/topspin knolin 5
f1 (ppm)

14f

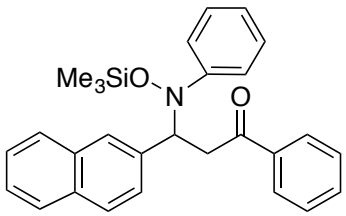
Me3SiO
N
O

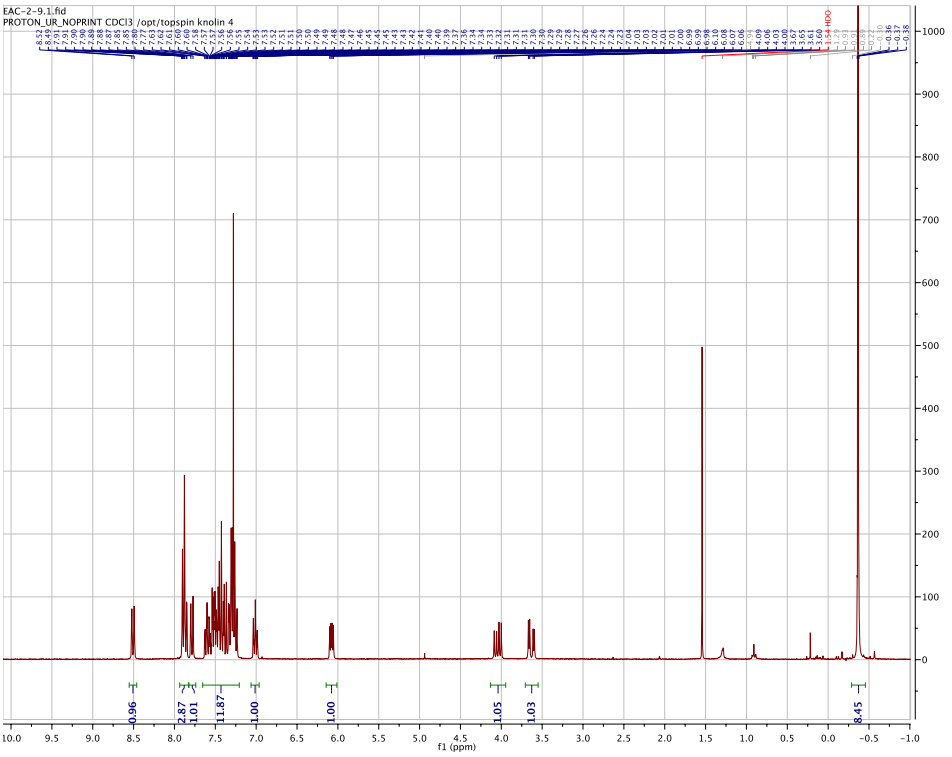
EAC-2-9-1.fid
PROTON_UR_NOPRINT CDCl3 /opt/topspin knolin 4
f1 (ppm)

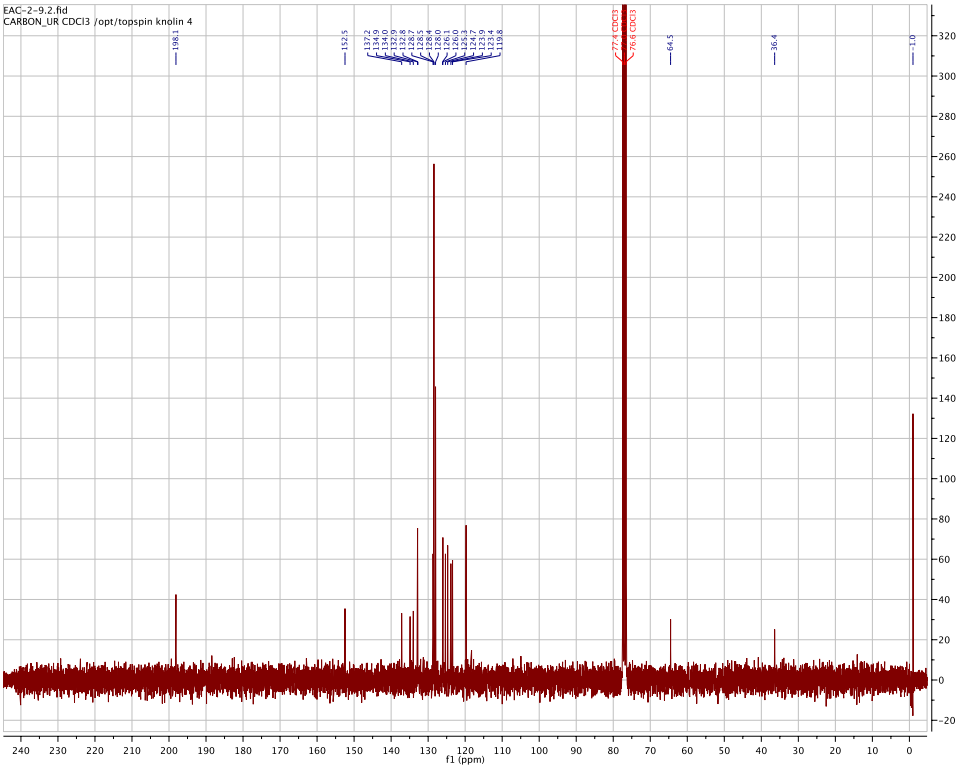
EAC-2-9-2.fid
CARBON_UR CDCl3 /opt/topspin knolin 4
f1 (ppm)

14g

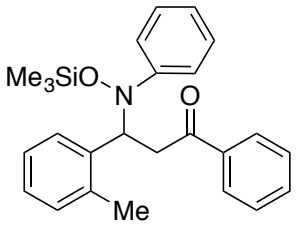
Me3SiO
N
O
Me

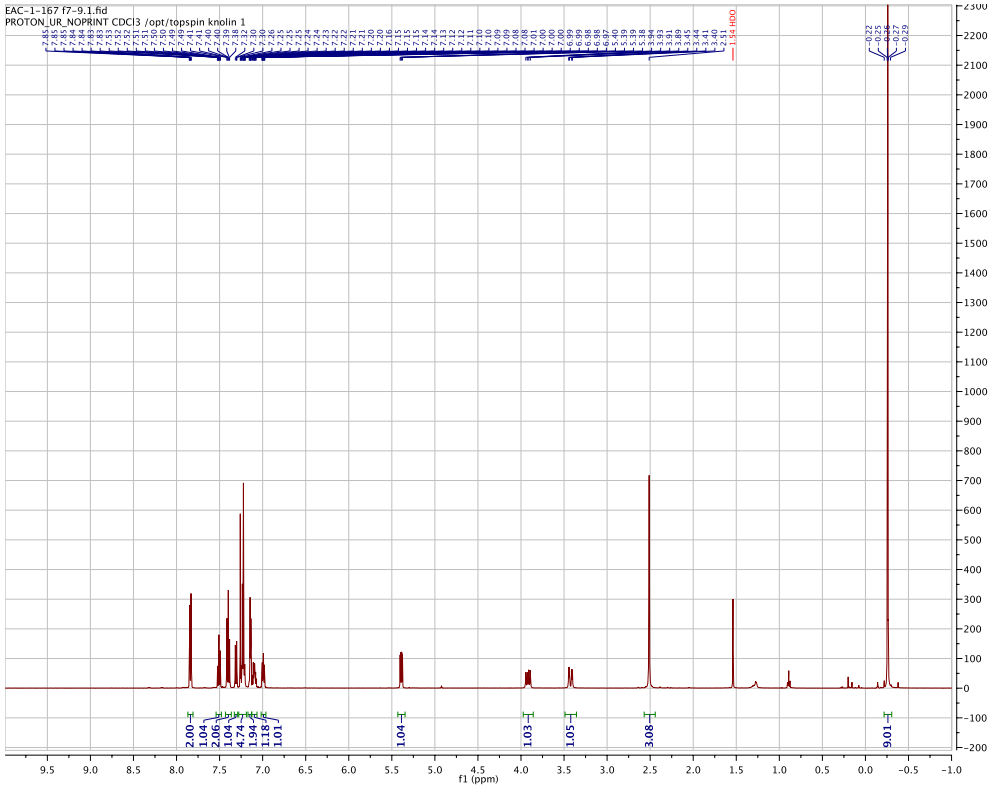
EAC-1-167 f7-9.1.fid
PROTON_UR_NOPRINT CDCl3 /opt/topspin knolin 1
f1 (ppm)

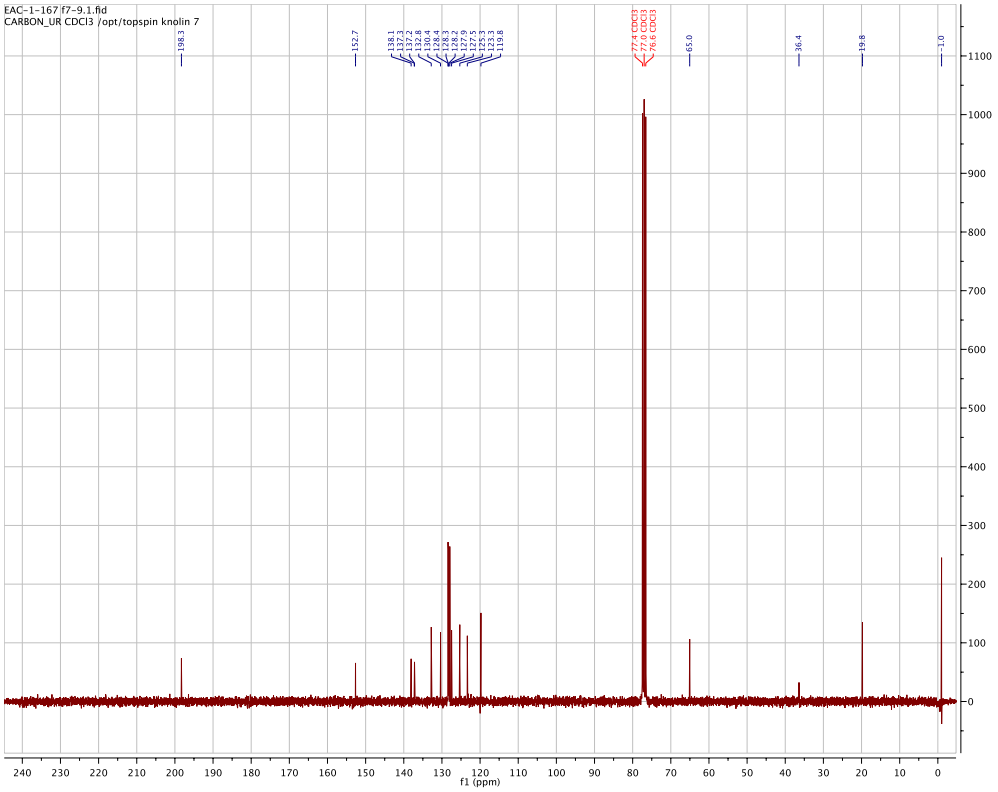
EAC-1-167 f7-9.1.fid
CARBON_UR CDCl3 /opt/topspin knolin 7
f1 (ppm)

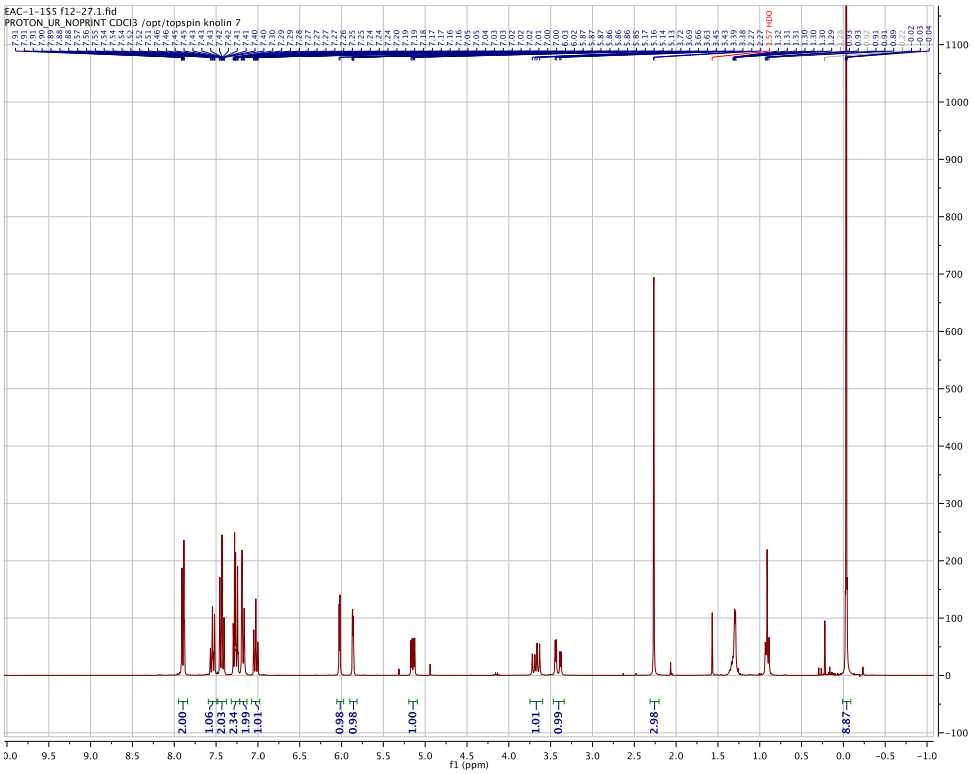
EAC-1-155 f12-27.1.fid
PROTON_UR_NOPRINT CDCl3 /opt/topspin knolin 7
2.00
1.06
2.03
2.34
1.94
1.01
0.98
0.98
1.00
1.01
0.99
2.98
8.87
f1 (ppm)

14h

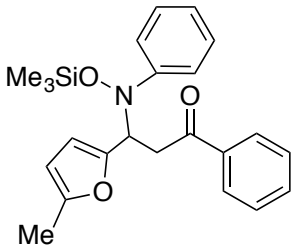
Me3SiO
N
O
O
Me

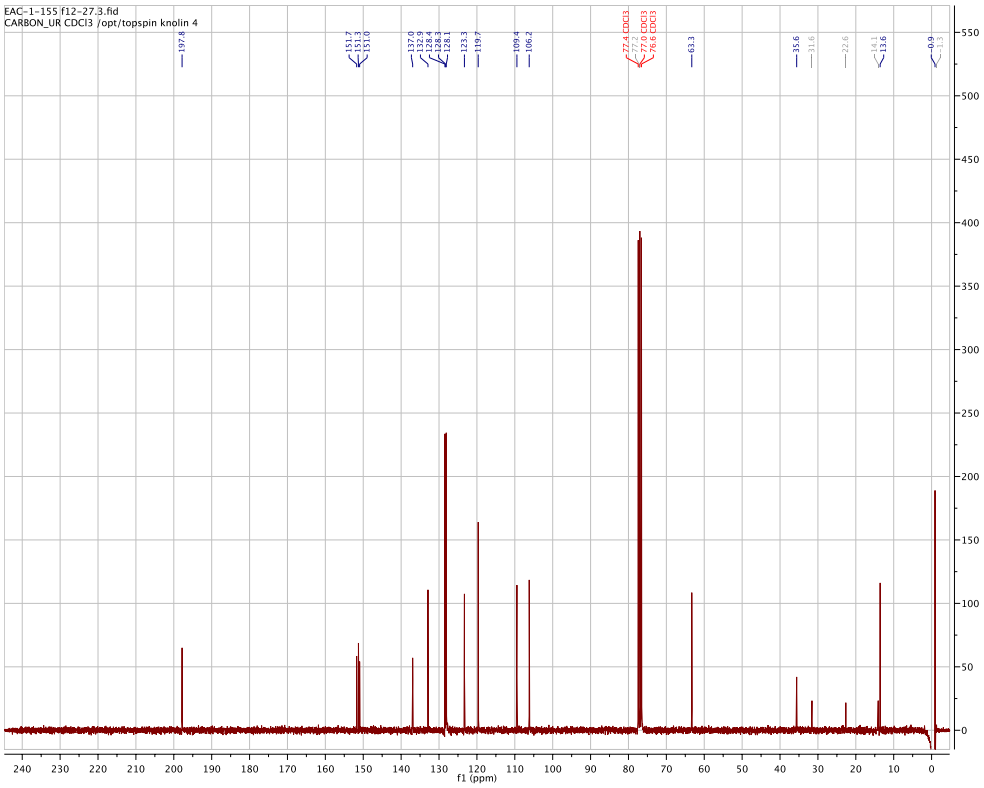
EAC-1-155 f12-27.3.fid
CARBON_UR CDCl3 /opt/topspin knolin 4
197.8
151.7
151.3
151.0
127.0
125.9
128.4
128.1
124.1
123.3
119.7
109.4
106.2
77.4 CDCl3
77.0 CDCl3
76.6 CDCl3
63.3
35.6
31.6
22.6
14.1
13.6
0.9
-1.3
f1 (ppm)

14i

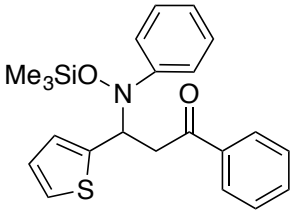
Me3SiO
N
O
S

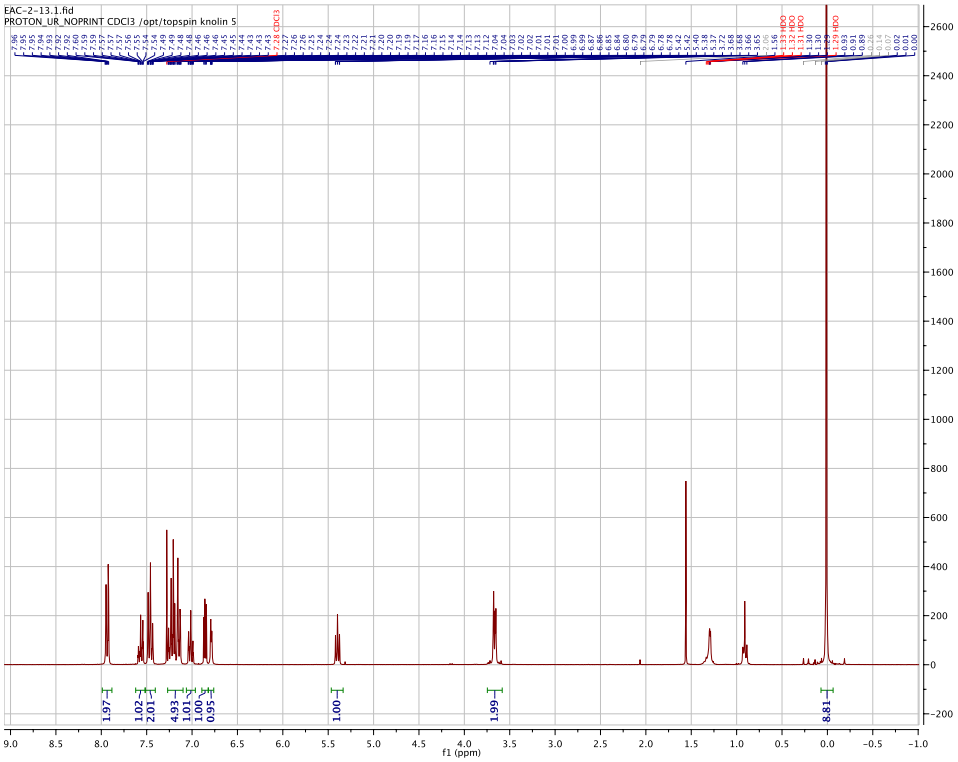
EAC-2-13.1.fid
PROTON_UR_NOPRINT CDCl3 /opt/topspin knolin 5
1.97
1.02
2.01
4.93
1.01
1.00
0.95
1.00
1.99
8.81
f1 (ppm)

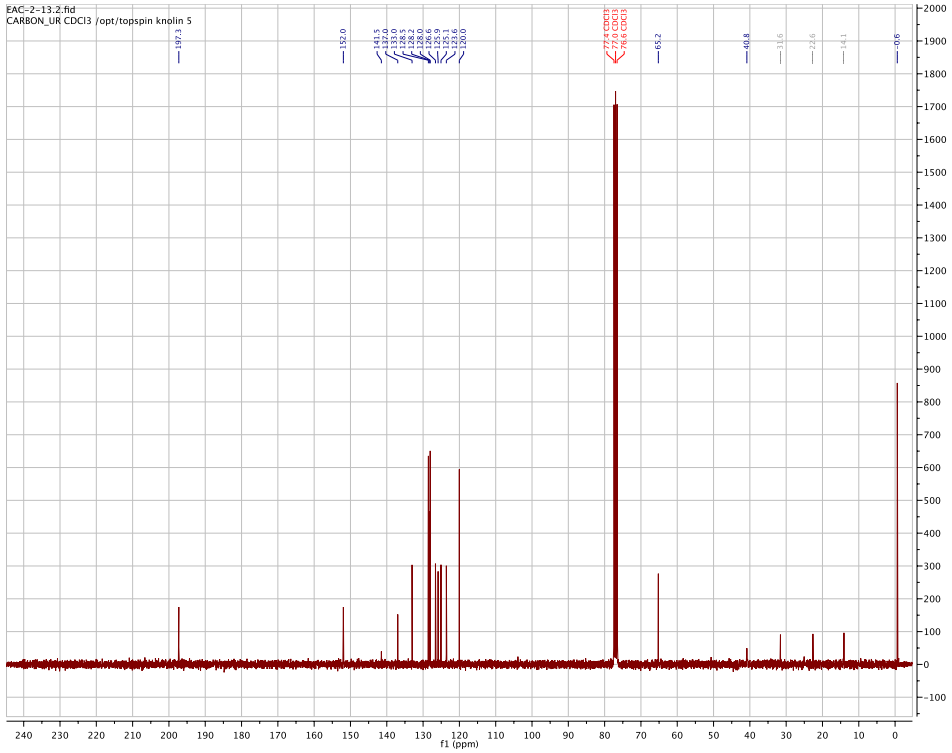
EAC-2-13.2.fid
CARBON_UR CDCl3 /opt/topspin knolin 5
197.3
152.0
141.5
137.0
133.0
128.5
128.2
128.0
126.6
125.9
125.6
123.6
120.0
77.4 CDCl3
77.0 CDCl3
76.6 CDCl3
65.2
40.8
31.6
24.6
14.1
0.6
f1 (ppm)

4. Abbreviation List

DA: Donor-Acceptor

CaI_2: Calcium Iodide

$Ca(acac)_2$: Calcium Acetylacetonate

$Ca(OMe)_2$: Calcium Methoxide

$Ca(OAc)_2$: Calcium Acetate

Ca(neodec): Calcium Neodecanoate

$Ca(OTf)_2$: Calcium Triflate

CH_3CN: Acetonitrile

$Ca(NTf_2)_2$: Calcium Triflamide